Inaugural dissertation

for

obtaining the doctoral degree

of the

Combined Faculty of Mathematics, Engineering and Natural Sciences

of the

Ruprecht - Karls - University

Heidelberg

Presented by

M. Sc. Céline Weller

Born in: Baden-Baden, Germany

Oral examination: 27th of September 2023

Inaugural dissertation

for

obtaining the doctoral degree

of the

Combined Faculty of Mathematics, Engineering and Natural Sciences

of the

Ruprecht - Karls - University

Heidelberg

Presented by

M. Sc. Céline Weller

Born in: Baden-Baden, Germany

Oral examination: 27th of September 2023

Pre-metastatic and immunological conditioning of the hepatic niche during melanoma progression

Referees:

Prof. Dr. rer. nat. Viktor Umansky

Prof. Dr. med. Cyrill Géraud

“Wir können den Wind nicht ändern,

aber die Segel anders setzen.“

Aristoteles (384 – 322 v.Chr.)

Table of content

Abstract

The approval of immune checkpoint inhibition (ICI) for advanced melanoma patients heralded a new era in melanoma therapy. ICI is approved as palliative and adjuvant treatment for stage IV and stage III patients, respectively. Neoadjuvant ICI is currently not approved but is investigated in clinical trials for stage II and stage III patients. Liver metastasis, which is detected in ~10-20% of stage IV patients, gained special attention, as it recently evolved as important indicator of treatment resistance to ICI. In this study, the pre-metastatic immunological conditioning of the murine hepatic vascular niche is characterized and compares different ICI treatment regimens (i.e. palliative, adjuvant and neoadjuvant) regarding their efficiency to prevent and treat liver metastasis formation.

Hepatic metastases in mice were induced either by intravenous or intrasplenic injection of melanoma cell lines WT31 and B16F10 to assess treatment responses among palliative, adjuvant and neoadjuvant ICI. In the neoadjuvant setting, melanoma cells were also injected intracutaneously to simulate primary cutaneous melanomas. The immune cell composition and activation was comparatively analyzed within the primary tumor, the blood and the liver with FACS, IF/IHC, *in situ* hybridization and cytokine assays.

Hepatic metastasis was similar in extent in mice with intracutaneous melanomas compared to PBS injected controls indicating that a primary melanoma did not induce a pre-metastatic niche with a strong pro- or anti-tumoral phenotype. Naïve adjuvant therapy starting on day 0 showed reduced liver metastases in comparison to late palliative therapy starting on day 9. This was accompanied by increased hepatic infiltration of $CD3^+$ $CD8^+$ T cells in the naïve adjuvant therapy. Neoadjuvant therapy in the presence of a primary cutaneous melanoma showed even less hepatic metastases in comparison to adjuvant therapy. Primary tumors showed a T cell inflamed phenotype in neoadjuvant therapy and an immune excluded phenotype in adjuvant therapy. This was paralleled by increased $CD4^+$ and $CD8^+$ T cells in the peripheral blood in the neoadjuvant therapy. Additionally, hepatic $CD4^+$ T-bet^+ T cells significantly increased in neoadjuvant therapy while $CD4^+$ $Gata3^+$ T cells decreased in comparison to adjuvant therapy.

Our data indicate that the choice of the therapeutic regimen is an important factor influencing the susceptibility of the hepatic vascular niche to liver metastasis and also therapy response to immune checkpoint inhibition. Neoadjuvant ICI was superior to adjuvant ICI regarding the prevention of liver metastasis formation. Furthermore, the liver showed a more Th1 driven immune response. Increased numbers of $CD4^+$ $Gata3^+$ T cells in the livers of mice in the adjuvant setting indicate a more Th2-driven immune response. Therefore, neoadjuvant ICI may be an excellent option for CM to prevent the spread to distant organs and to help improving the outcome of patients with distant metastases.

Zusammenfassung

Durch die Zulassung der Immuntherapie für die Therapie des fortgeschrittenen malignen Melanoms wurde eine neue Ära der Therapie des malignen Melanoms eingeleitet. Mittlerweile erhalten nicht nur Stadium IV Melanom Patienten als palliative Therapie eine Immuntherapie, sondern auch Patienten in Stadium III als adjuvante Therapie. Eine adjuvante Therapie soll das Fortschreiten in ein metastasiertes Tumorstadium verhindern. Nichtsdestotrotz entwickeln 10 -20 % der Stadium 4 Patienten im Verlauf Lebermetastasen. Diese stellen einen negativ prognostischen Faktor für diverse Therapien dar.

In meinem Mausmodell wurde die Anwesenheit eines primären Melanoms durch die intrakutane Injektion der WT31 Melanom Zellen simuliert. Die Bildung der Lebermetastasen wurde durch die intravenöse und intralienale Injektion der Tumorzellen induziert, um das Ansprechen der Lebermetastasen auf die verschiedenen Therapiemodalitäten im Detail untersuchen zu können. Die neoadjuvante, adjuvante, naiv adjuvante und palliative Therapie wurde mithilfe der unterschiedlichen Mausmodelle durchgeführt und anschließend im Detail untersucht. Anschließend wurde die Immunzellkomposition und die Aktivierung verschiedener Immunzellen im Primärtumor, dem Blut und der Leber, mittels FACS, IF, IF/IHC und Zytokin Assays näher untersucht und miteinander verglichen.

Die Anwesenheit eines Primärtumors hatte keinen Einfluss auf die Bildung der Lebermetastasen im Vergleich zu den PBS intrakutan injizierten Tieren. Die naiv adjuvante Therapie mit den Immuncheckpoint Inhibitoren schützte im Vergleich zur palliativen Therapie verstärkt vor der Bildung von Lebermetastasen. Des Weiteren zeigten die Lebern der naiv adjuvant therapierten Tiere eine erhöhte Infiltration der $CD3^+$ $CD8^+$ T Zellen im Vergleich zur spät palliativen Therapie. Die neoadjuvante Therapie mit ICI in Anwesenheit eines Primärtumors zeigte ein vielfach verstärktes Ansprechen auf die ICI im Vergleich zur adjuvanten Therapie. Außerdem konnte gezeigt werden, dass die Primärtumore der neoadjuvanten Therapie eine erhöhte Infiltration an T Zellen im Vergleich zu den Primärtumoren der adjuvanten Therapie aufweisen. Des Weiteren konnte eine erhöhte Anzahl an $CD3^+$ $CD4^+$ und $CD3^+$ $CD8^+$ T Zellen im peripheren Blut der neoadjuvant therapierten Tiere nachgewiesen werden. Durch die detaillierte Analyse der Immunzellkomposition in der Leber konnte gezeigt werden, dass die Lebern der neoadjuvant therapierten Tiere eine erhöhte Anzahl an $CD4^+$ T-bet^+ T Zellen aufweisen. Die erhöhte Anzahl an Th1 Zellen spricht für eine verstärkt Th1 induzierte Immunantwort durch die neoadjuvante Therapie mit den ICI.

Zusammengefasst, zeigen meine Daten, dass die Wahl des therapeutischen Settings die Anfälligkeit für Lebermetastasen und das Therapieansprechen im Wesentlichen beeinflussen. Die neoadjuvante Therapie mit den ICI zeigte ein erhöhtes Therapieansprechen und eine verbesserte Prävention vor der Bildung von Lebermetastasen. Deshalb könnte die

neoadjuvante Therapie einen guten Therapieansatz darstellen, um das Auftreten von Fernmetastasen effektiver zu verhindern.

Publications

Fleming V, Hu X, **Weller C**, Weber R, Groth C, Riester Z, Hüser L, Sun Q, Nagibin V, Kirschning C, Bronte V, Utikal J, Altevogt P, Umansky V. Melanoma Extracellular Vesicles Generate Immunosuppressive Myeloid Cells by Upregulating PD-L1 via TLR4 Signaling. Cancer Res. 2019 Sep 15;79(18):4715-4728.

Wohlfeil SA, Häfele V, Dietsch B, **Weller C**, Sticht C, Jauch AS, Winkler M, Schmid CD, Irkens AL, Olsavszky A, Schledzewski K, Reiners-Koch PS, Goerdt S, Géraud C. Angiogenic and molecular diversity determine hepatic melanoma metastasis and response to anti-angiogenic treatment. J Transl Med. 2022 Feb 2;20(1):62.

Roy-Luzarraga M, Reynolds LE, de Luxán-Delgado B, Maiques O, Wisniewski L, Newport E, Rajeeve V, Drake RJG, Gómez-Escudero J, Richards FM, **Weller C**, Dormann C, Meng YM, Vermeulen PB, Saur D, Sanz-Moreno V, Wong PP, Géraud C, Cutillas PR, Hodivala-Dilke K. Suppression of Endothelial Cell FAK Expression Reduces Pancreatic Ductal Adenocarcinoma Metastasis after Gemcitabine Treatment. Cancer Res. 2022 May 16;82(10):1909-1925.

Jauch AS, Wohlfeil SA, **Weller C**, Dietsch B, Häfele V, Stojanovic A, Kittel M, Nolte H, Cerwenka A, Neumaier M, Schledzewski K, Sticht C, Reiners-Koch PS, Goerdt S, Géraud C. Lyve-1 deficiency enhances the hepatic immune microenvironment entailing altered susceptibility to melanoma liver metastasis. Cancer Cell Int. 2022 Dec 10;22(1):398.

Dietsch, B., **Weller, C.**, Sticht, C., de la Torre, C., Kramer, M., Goerdt, S., Géraud C., Wohlfeil, S. A. (2023). Hepatic passaging of NRAS-mutant melanoma influences adhesive properties and metastatic pattern. *BMC cancer*, *23*(1), 1-16.

1 Introduction

1.1 Cutaneous melanoma

Cutaneous melanoma (CM) is described as a fatal form of skin cancer which develops from melanocytes. It can be located in the basal epidermis, hair follicles, mucosal surfaces and the meninges (1). In 20 – 40 % of cases, cutaneous melanoma develops from pre-existing naevi and the remaining 60 - 80 % of cases occur *de novo* (2). The number of patients diagnosed with cutaneous melanoma has been increasing dramatically, currently reaching about 160.000 new cases per year and 48.000 deaths in 2014 (3). A few years ago, cutaneous melanoma was still considered a rare disease. However, in 2018 CM became number four (women) and number five (men) of the most common solid tumors in Germany respectively (4).The increased incidence can in part be explained by higher levels of UV exposure, changes in the diagnostic approach towards skin lesions and higher diagnosis rates due to increased awareness and economic development (5). In addition, CM accounts for 90 % of skin cancer related deaths (6). Therefore, early detection of melanoma without metastatic spread is highly important. First, melanoma is typically diagnosed by visual inspection including the dermatoscopy. Melanocytic lesions can be interpreted by its shape, definition of the border, color, size and its evolution (“ABCDE”) (7). For patients with a large amount of atypical naevi, total-body photography is used. Furthermore, epiluminescence microscopy and dermatoscopy allow the magnified and rapid *in vivo* observation of skin lesions (8).Then suspicious lesions are completely excised including a margin of a few millimeters and a subsequent histological analysis of the lesion by a derma pathologist is performed. Factors such as melanocytic maturation, thickness, ulceration and mitotic index are of a high importance for the correct diagnosis of CM (9) (Table 1-Table 4).

Table 1 T classification of cutaneous melanoma.

Information taken and modified from (10)

Tumor (T) classification

T1 **T1a** **T1b**	≤ 1.00 mm Without ulceration With ulceration
T2 **T2a** **T2b**	1.01 – 2.00 mm Without ulceration With ulceration
T3 **T3a** **T3b**	2.01 – 4.00 mm Without ulceration With ulceration
T4 **T4a** **T4b**	>4.00 mm Without ulceration With ulceration

Table 2 N classification of cutaneous melanoma.

Information taken and modified from (10)

Node (N) classification

N1 **N1a** **N1b**	One lymph node Micrometastases Macrometastases
N2 **N2a** **N2b** **N2c**	Two or three lymph nodes Micrometastases Macrometastases In-transit met(s) /satellite(s) with metastatic lymph node (s)
N3	Four or more lymph nodes or in-transit met(s) /satellite(s) with metastatic lymph node (s)

Table 3 M classification of cutaneous melanoma.

Information taken and modified from (10)

Metastasis (M) classification

M1a	Metastases in skin, subcutaneous or lymph node
M1b	Lung metastases
M1c	Distant metastases

The tumor stage is mainly defined by the histologic analysis of the primary tumor (tumor thickness and/or ulceration), detection of lymph node metastases or distant metastases. Patients diagnosed with CM can be separated into four groups (Stage I-IV) (Table 4) (10). Stage I is defined as low-risk primary melanomas and compromises patients that show no regional or distant metastases. Stage II patients have high-risk primary tumors which do not

show evidence for lymphatic disease or distant metastases and can be subdivided into three subgroups (Stage IIA, IIB and IIC), depending on thickness and ulceration of the primary tumor. Stage III is classified as patients with involvement of regional lymph nodes or patients with in-transit or satellite metastases. These patients can be further divided into three subgroups (Stage IIIA, IIIB and IIIC), dependent on the number of lymph nodes involved. Stage IV is classified by the presence of distant metastases and the three subgroups are dependent on the location of distant metastases (10).

Furthermore, melanomas show the highest mutational load among all cancer types with high amounts of a C > T transitions mainly caused by ultraviolet radiation (11, 12). Melanomas caused by non-ultraviolet radiation most commonly occur at non-cutaneous sites such as eyes, mucosal surfaces and acral sites (hands and feets) (11). In a whole genome sequencing study of cutaneous, acral and mucosal subtypes of melanoma, Hayward *et al.* showed that the most commonly mutated genes in cutaneous melanoma are *BRAF*, *CDKN2A*, *NRAS* and *TP53* whereas *NF1*, *BRAF*, *NRAS* and *SF3B1* are most commonly affected in acral and mucosal melanomas (13).

Table 4 Stage groups for cutaneous melanoma

Information taken and modified from (10)

Stage	**Clinical stage**		
I	T1a -1b	N0	M0
II	T2b-T4b	N0	M0
III	T1-4 (any)	N1-3	M0
IV	Any T	Any N	M1

In general, metastases are the main cause of death in patients diagnosed with cancer (14). Cutaneous melanoma most frequently metastasizes in an organotypic fashion and the most common sides of metastases are the skin, the lymph nodes, the lung, the liver and the brain (15).

1.3 Hallmarks of cancer

Human tumor pathogenesis and metastasis formation is a multistep process in which normal cells acquire a succession of hallmark capabilities to become a neoplastic cell. These biological capabilities were first postulated as Hallmarks of cancer by Douglas Hanahan and Robert Weinberg in 2000 (16). The Hallmarks of cancer were expanded in 2011 with further characteristics, tumor-promoting inflammation and genome instability and mutation (Figure 1, indicated in red). Moreover, two new emerging hallmark capabilities, deregulating cellular energetics and avoiding immune destruction (indicated in green), were added to the model in 2011 (17). The hallmarks of cancer are shown in (Figure 1). Douglas and Hanahan claim that most human cancer types combine these six capabilities (16). In the following chapter, the six hallmarks of cancer will be discussed in relation to the cutaneous melanoma.

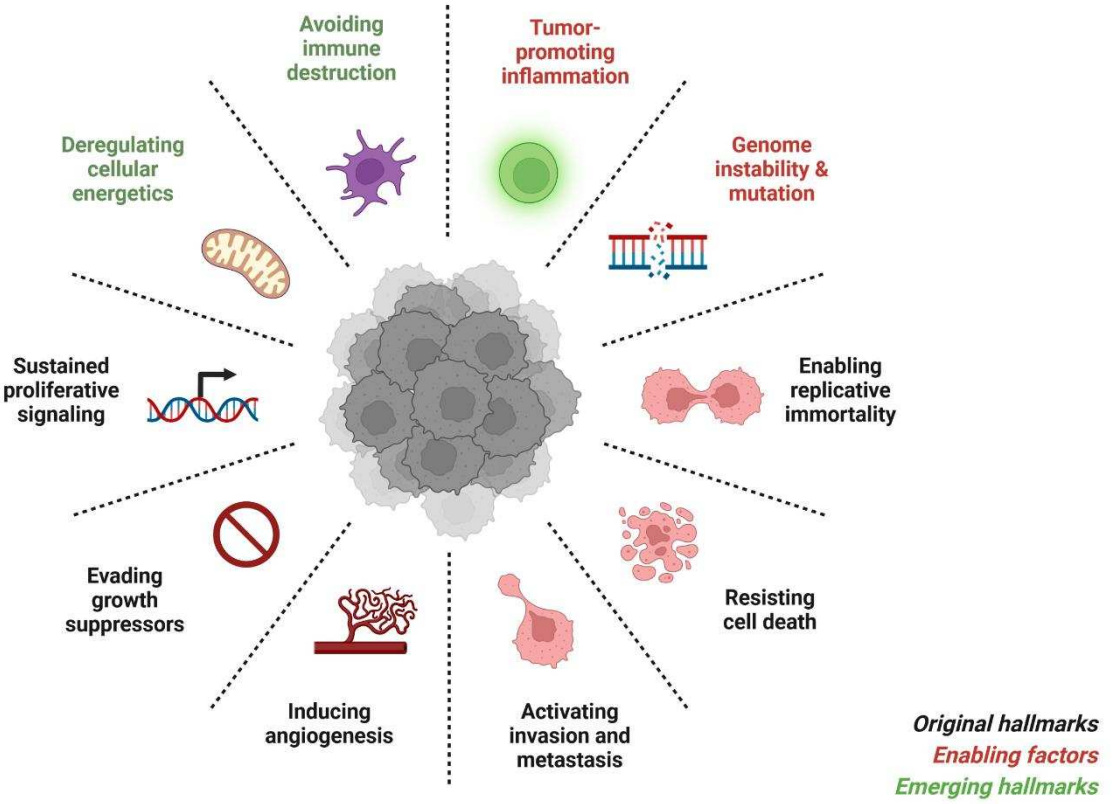

Figure 1: The Hallmarks of cancer with the two emerging hallmarks and the two enabling factors.

Illustration showing the six hallmarks of cancer (indicated in black), the two enabling factors which are illustrated in red and the two new emerging hallmarks of cancer (indicated in green). Adapted from (17). Illustration was created using Biorender.com.

Enabling replicative immortality

Neoplastic cells acquire the ability of unlimited replicative potential whereas most normal cell lineages only pass through limited cell cycles before undergoing senescence, a viable but non-proliferative cell state followed by apoptosis (17). Telomeres consisting of repetitive DNA and associated proteins are defined as the ends of linear chromosomes and are mainly involved in acquiring the capability of unlimited proliferation (18, 19). In addition, the specialized DNA polymerase which is responsible for the elongation of the telomeres is present in all cell types. This DNA polymerase, called Telomerase, is responsible to counteract the telomere shortening occurring during normal DNA replication. It is present in cell types that undergo continuous cell division such as germ cells, hematopoietic cells and stem cells. It rarely occurs in non-immortalized cell types. However, telomerase is highly expressed in about 90 % of immortalized cells such as human cancer cells (17, 20). The activity of the telomerase is mainly regulated by the *TERT* gene (21). Mutations in the *TERT* gene are commonly found in human tumors such as glioblastoma, melanoma and hepatocellular carcinoma (22). Mutations in the *TERT* promoter region leads to the increased expression of *TERT* and is associated with the restoration of the telomerase activity (23, 24).

In cutaneous melanoma, mutations in the *TERT* promotor region are the most common mutations in non-coding regulatory regions (22). They are associated with high telomerase activity and poor prognosis (25). Further, Nagore *et al.* showed in 2016 that the amount of *TERT* promotor mutations was twice as high in fast-growing melanomas as in slow-growing melanomas (26).

Resisting cell death

Besides replicative immortality, cancer cells acquire the ability to inactivate programmed cell death or apoptosis (16). Apoptosis and the programmed cell death are mechanisms which are highly important to protect the cells from genomic instability caused by DNA damage, telomere dysfunction or the loss of cell-cycle checkpoints (16). The mechanism of apoptosis can be separated into two pathways, the intrinsic (mitochondrial) and the extrinsic pathway. On the extrinsic pathway, the cell receives death-inducing signals from the outside of the cell, for example the binding of the Fas Ligand (FasL) to the Fas Receptor (FasR). On the intrinsic pathway, the cell receives and integrates signals of intracellular origin such as hypoxia and DNA damage. The intrinsic pathway mainly works through the release of cytochrome c from the mitochondria and the activation of different caspases (27). Another important player within the mechanism of apoptosis is the protein p53, which is mutated in about 50 % of human cancers (28). The protein p53 is a transcription factor, with a short half-life existing in low levels in unstressed cells (29). After sensing cellular stresses, the cellular level of p53 increases and p53 activates target genes involved in apoptosis, DNA repair or cell-cycle arrest (30).

One gene which is commonly mutated in hereditary melanoma is *CDKN2A*, a tumor suppressor gene encoding for two tumor suppressor proteins namely P16INK4a and P14ARF. Tumor suppressor proteins are proteins which are responsible for the inhibition of cell proliferation and tumor development (31).The two tumor suppressor proteins lead in a mutated form to the inhibition of RB1 and p53, stimulating the entry of a cell into the cell cycle and enabling the resistance of the cell to undergo apoptosis (32).

Evading growth suppressors

In line with the finding that cancer cells acquire the ability to resist cell death, cancer cells have to evade programs that negatively regulate cell proliferation, which primarily depends on so-called tumor suppressor genes (17). Two major tumor suppressor proteins are RB (retinoblastoma-associated) and the above-mentioned p53 protein. The RB protein enhances the integration of intra- and extracellular signals, thereby leading the cell either into proliferation or apoptosis. Mutations in the RB1 gene predispose to familial cutaneous melanoma and retinoblastoma. Defects in the RB pathway led to the loss of a critical gatekeeper and the persistence of cell proliferation (33-35).

Sustained proliferative signaling

Sustained proliferative signaling is another hallmark of cancer and one of the most important traits of cancer cells. In non-cancerous cells, cell growth and division cycle are carefully controlled by the production and release of promoting or inhibitory signals. In cancer cells there are many alternative ways to sustain proliferative signaling such as the production of own growth factor ligands, stimulation of normal cells within the tumor-associated stroma to produce growth factors or the constitutive activation of cell proliferation associated signaling pathways such as the MAP kinase (MAPK) pathway or the PI3 kinase (PI3K) pathway (17).

More than 40 % of cutaneous melanomas harbor an activating mutation of the BRAF gene (36) leading to the constitutive activation of the MAP kinase pathway (36). Further, in about 20 – 40 % of cutaneous melanomas a *PTEN* loss of function mutation can be found (3) leading to the constitutive activation of the PI3K pathway (3). The activation of both the MAPK pathway and the PI3K pathway leads to the sustained proliferative signaling and the continuously activated proliferation of cancer cells (3).

Activating invasion and metastasis

The dissemination of malignant cells is the main cause of cancer-related deaths. Metastasis formation is a multistep process which can lead to secondary tumors and can also be described as the invasion-metastasis cascade (37, 38). The local invasion of the tumor cells into the surrounding tissue is the first step of the metastatic cascade. To obtain an invasive phenotype, the cells develop changes in their shape and the ability to attach to other cells or the extracellular matrix (39, 40). The next step in metastases formation is the intravasation, in which tumor cells enter blood and lymphatic vessels followed by the escape of the tumor cells from the blood and lymph into secondary organs (extravasation). The initial step within the secondary organ is the survival of tumor cells surrounded by the foreign microenvironment, thereby forming small nodules (micrometastases). The multistep process of invasion and metastases formation ends with the outgrowth of micrometastatic lesions into macroscopic tumors and is called “colonization” (17, 41).

The origin of the malignant melanoma are skin melanocytes which are defined as melanin-producing cells located in the basal layer of the epidermis and the hair follicles (42, 43). Epidermal keratinocytes control the homeostasis of melanocytes. The switch of melanocytes into cancerogenic cells is based on several genetic and environmental factors including the loss of adhesion molecules and mutations of growth regulatory genes. This loss allows the melanocytes to interact with stromal cells from the dermis including fibroblasts and endothelial cells and to circumvent the control by keratinocytes. This event is mainly driven by the loss of E-cadherin and the gain to express N-cadherin and is a crucial step in the metastasis formation of the cutaneous melanoma (44).

Inducing angiogenesis

Another Hallmark of cancer which was postulated by Hanahan and Weinberg is the induction of angiogenesis (16). For their growth and survival mammalian cells need oxygen and nutrients which can be taken up from blood vessels (45). The main components of blood vessels are endothelial cells forming tubes and thereby maintain the blood flow and tissue perfusion. During tumor development, an angiogenic switch leads to the activation of the usually quiescent vasculature and promotes development of new blood vessels. Newly derived blood vessels then support the outgrowth of neoplastic cells (46). Two well-described drivers of angiogenesis, are the two growth factors named Vascular endothelial growth factor (VEGF) and Fibroblast growth factor (FGF). In transformed melanocytes VEGF is produced in high amounts (47-49). Furthermore, in blood vessels of human cutaneous melanoma high amounts of FGF were found in the extracellular matrix and basement membrane of newly developed blood vessels (50). In addition, it was shown that matrix bound FGF, which is released by the

digestion of the extracellular matrix through matrix metalloproteinases leads to endothelial cell proliferation and vascular vessel formation in cutaneous melanoma (51, 52).

Avoiding immune destructions

Already in the 1900s, Paul Ehrlich postulated that the immune system is capable of suppressing the outgrowth of an “overwhelming frequency” of carcinomas (53). The hypothesis of “immunosurveillance” was strengthened by Macfarlane Burnet and Lewis Thomas (54) who also postulated that lymphocytes are able to eliminate nascent and transformed cells but at that time no convincing evidence could be detected (55). The hypothesis of immunosurveillance was supported and renewed by two key findings. First, it was shown that endogenously produced Interferon γ (IFNγ) protects the host against the outgrowth of transplantable tumors (56). Second, perforin knockout (KO) mice (Perforin $^{-/-}$) develop more tumors after the treatment with the carcinogen methylcholanthrene (MCA) than the control mice. Perforin is known to be a component of the cytolytic granules released by cytotoxic T cells and NK cells (57-59). Yet, the strongest evidence supporting the hypothesis of immunosurveillance is that tumors occur in much higher frequency and develop faster in *Rag1* and *Rag2* knockout mice (54). The two recombination activating genes (RAG) are exclusively expressed in the lymphoid compartment and are involved in the repair of double strand breaks. The KO of *Rag1* and *Rag2* leads to the missing rearrangement of antigen receptors. Therefore, the knockout of these genes induces a complete lack of natural killer cells (NK cells), T and B cells in these mice (60). Further investigations supporting the hypothesis of immunosurveillance were carried out in immunocompromised patients, showing that these have a much higher risk of developing tumors than patients which are not immunocompromised (61). Interestingly, it was also shown that in the absence of an intact immune system the formed tumors are more immunogenic compared to tumors which developed in immunocompetent hosts. This suggests that the hosts immune system can protect against tumor formation but can also edit tumor immunogenicity (62). Altogether, these findings led to the formulation of the immunoediting hypothesis as a refinement of the cancer immunosurveillance hypothesis (54).

Cancer immunoediting which in part describes the avoidance of immune destructions as a hallmark of cancer can be divided in three different phases termed “elimination”, “equilibration” and “escape” (55) and is illustrated in (Figure 2).

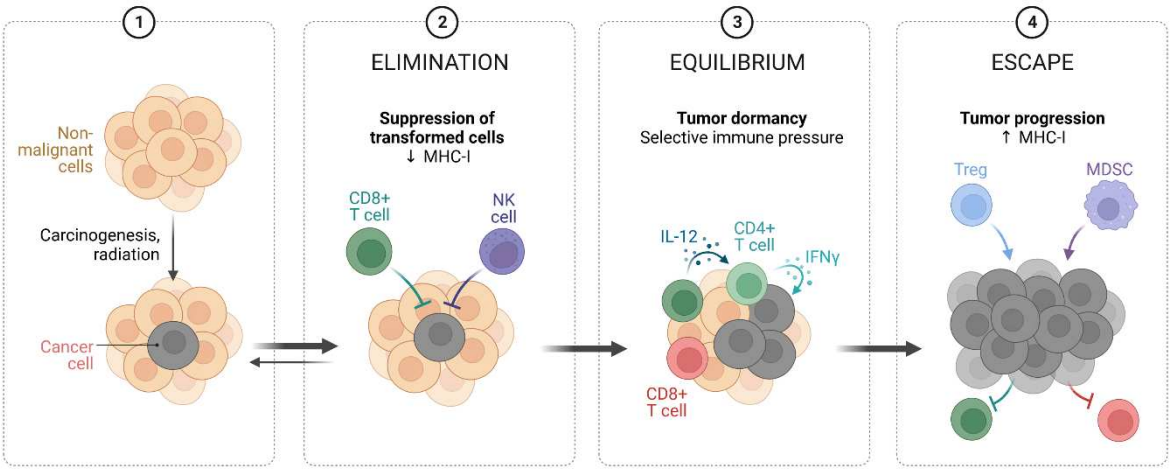

Figure 2: The concept of cancer immunoediting.

The concept of cancer immunoediting can be divided into four phases. During the first phase a non-malignant cell transforms into a cancer cell by carcinogenesis, radiation, chronic inflammation or mutations. During the elimination phase different cell types of the host´s innate and adaptive immune system, such as CD8⁺ T cells or NK cells, attack cancer cells. Cancer cells that survived may enter into the equilibrium phase. This phase is characterized by dormancy of the cancer cells and continuous immunoselection. This selection pressure leads to the emergence of cancer cells which are no longer recognized by the immune system. These can than enter the escape phase and are no longer recognized by the immune system. Information was taken from (63) and Illustration was created using Biorender.com.

Elimination

The first phase of cancer immunoediting is the elimination phase in which transformed cells are detected by the adaptive and innate immune system before they become clinically apparent. If complete destruction of the tumor cells is achieved, the elimination phase would be the endpoint of cancer immunoediting (63).

Equilibrium

The equilibrium phase is the longest phase of the cancer immunoediting process and involves cells which survived the elimination phase. During this phase, the immune system holds residual tumor cells in a functional state of dormancy, where these cells can reside in a patient for decades until resuming growth either as a primary tumor or distant metastases (64). During the equilibrium phase the original escape variants of the tumor can be destroyed, however due to the inherent genetic and chromosomal instability of the malignant cells, new variants of transformed cells can develop, which are even more resistant against the attacks of the hosts immune system (54, 55).

Escape

In the escape phase, tumor cells acquire traits to circumvent the recognition by the immune system. This can be achieved through different mechanisms such as:

I. The loss of major histocompatibility complex (MHC) presenting antigens to tumor specific T cells (54, 65).
II. The loss of antigen processing functions (54, 65) e.g. KO of *Rag1* and *Rag2*, the appearance of tumor cells lacking the expression of strong antigens, e.g. melanoma cells express GP100 which can be recognized by the immune system (54, 65).
III. Facilitating the formation of an immunosuppressive microenvironment e.g. by the expression of negative co-stimulatory molecules such as cytotoxic T-lymphocyte associated protein 4 (CTLA-4) and programmed cell death ligand 1 (PD-L1) or the recruitment of immunosuppressive cell types including regulatory T cells (T_{regs}), tumor-associated macrophages (TAMs) or myeloid derived suppressor cells (MDSCs) (62, 63).

Melanoma cells are known to be highly immunogenic and capable of expressing high amounts of antigens (66). The permanent exposure of the immune system to melanoma antigens induces the functional exhaustion of the immune system (immunosurveillance) and the strong expression of inhibitory molecules such as PD-1, PD-L1 and CTLA-4 making cytotoxic T cells ineffective (67, 68). Furthermore, it is known that the melanoma microenvironment is associated with the enrichment of immunosuppressive cell types including T_{regs}, TAMs and MDSCs which can also be responsible for the ineffectiveness of e.g. cytotoxic T cells. In addition, it was shown by several publications that the CM directly leads to the ineffectiveness of the immune system to kill malignant cells by the overproduction of negative modulators of immune cells (69) such as adenosine, tumor necrosis factor-β (TGF-β), vascular endothelial growth factor (VEGF) and indoleamine 2,3-dioxygenase (IDO) (70, 71).

Deregulating cellular energetics

The deregulation of energy metabolism was already observed by Otto Warburg in 1930. He described that cancer cells have an anomalous cell energy metabolism which is mostly switched to “glycolysis” (72, 73). In a glycolytic metabolic state metabolic intermediates supply pathways that support the generation of nucleotides and amino acids and facilitate bio mass production (74, 75). However, the deregulation of cellular energetics is mostly dependent on factors already included in the six core hallmarks of cancer such as sustained proliferative signaling and is therefore designated as an emerging hallmark which on the one hand highlights its importance, but on the other hand implies its dependency on other core hallmarks of cancer (17). Melanoma cells can produce adenosine triphosphate (ATP) and carbon precursors which are used for cell growth and proliferation, without oxygen and mainly through lactic fermentation and glycolysis (“Warburg effect”) (76). A master regulator of glycolysis and hypoxia-inducible genes, called hypoxia-inducible factor 1α (HIF-1α) is highly upregulated in melanoma cells also under normoxic conditions (normal levels of oxygen) (77, 78). Besides, it was shown that melanoma cells are able to stabilize HIF-1α through mTOR and melanoma antigen-11 (MAGE11) (77). MAGE-11 is able to inhibit the prolyl hydroxylase domain protein 2 (PHD2) which is a negative regulator of HIF-1α (79). The increased amounts and the protein stabilization of HIF-1α leads to the induction of glycolysis in the presence and absence of oxygen, thereby supporting the development and progression of melanoma (77, 80).

1.4 The liver

The liver is one of the largest internal organs located in the upper abdomen (81) and accounts for 2 – 3 % of the average body weight (82). The liver is involved in numerous physiological processes, including the metabolism of macronutrients, regulating the blood volume, supporting the immune system, controlling different growth signaling pathways in an endocrine manner, the homeostasis of lipids and cholesterol and the conversion of xenobiotic compounds (drugs) (83).

1.4.1 Anatomy of the liver

The liver can be divided into so-called liver lobes. The human liver consists of four liver lobes namely the left lobe, the right lobe, the caudate lobe and the quadrate lobe (84). The vasculature of the liver is quite unique due to the fact that the liver is supplied by arterial as well as venous blood. Blood rich in oxygen comes from the hepatic artery (30 %) and nutrient-rich blood comes from the portal vein. The blood merges and flows along the liver sinusoids which are lined by liver sinusoidal endothelial cells (LSECs) to the central vein (85, 86). The portal triad is formed by branches of the portal vein, the hepatic artery and the bile duct (83). Bile is a fluid produced by the liver which is mainly involved in the digestion of lipids and is stored and concentrated in the gall bladder (87).

1.4.2 Cellular anatomy of the liver

Liver sinusoidal endothelial cells (LSECs)

Liver sinusoidal endothelial cells (LSECs) line the liver sinusoids and account for 15 -20 % of total liver cells. LSECs are endothelial cells lacking a continuous basement membrane and diaphragm. LSECs contain open pores called fenestrae allowing the transfer of nutrients, ions, fluids and metabolites to the space of disse (85, 86, 88). LSECs are therefore the direct contact to other non-parenchymal cells (Hepatic stellate cells (HSC)) and parenchymal cells (Hepatocytes) of the liver (89).

Stellate cells

Hepatic stellate cells (commonly known as perisinusoidal cells or Ito cells) are pericytes which are mainly found in the space of disse. In a healthy liver, stellate cells are mainly quiescent and show a low proliferation state. Furthermore, in a healthy liver stellate cells contain Vitamin A rich lipid droplets and under developed organelles. But, under a chronic liver disease stellate cells can switch to an “activated phenotype” with a high proliferative capacity and a decreased number of Vitamin A containing lipid droplets (90).

Hepatocytes

Hepatocytes are parenchymal cells, accounting for 85 % of the liver mass and are involved in a wide range of cellular functions including the metabolism of carbohydrates, lipids and proteins, detoxification and the activation of immune cells (91).

Kupffer cells

Kupffer cells are defined as the resident macrophages within the liver and account for the largest population of resident macrophages throughout the body. Kupffer cells play a major role in the innate immune response through phagocytosis of pathogens entering the liver by the portal or arterial circulation. Also, Kupffer cells are involved in the first line of defence against immunoreactive compounds entering the liver from the gastrointestinal tract through the portal circulation (92).

1.4.3 The liver as a pre-metastatic niche

The local microenvironment of distant organs can be prepared by the primary tumor even before the arrival of circulating tumor cells (CTCs). This phenomenon is referred to as the formation of a pre-metastatic niche. Stephan Paget first postulated in his “seed and soil” hypothesis that metastatic tumor cells (“seeds”) are prone to colonize specific organ sites (“soils”) (93). Several publications have shown that the liver can be prepared for the uptake of CTCs by the primary tumor. In this regard, Peinado *et al.* suggest that extracellular vesicles (EVs) induce vascular leakiness and inflammation during the formation of a pre-metastatic niche and that specific integrins expressed on EVs mediate the adhesion of tumor cells to specific cell types as well as the extracellular matrix and therefore increase liver metastases (94, 95). In a pancreatic ductal adenocarcinoma (PDAC) mouse model it was demonstrated that PDAC-derived exosomes can induce the formation of a pre-metastatic niche thereby increasing the hepatic metastatic burden. The PDAC-derived exosomes are taken up by Kupffer cells leading to the secretion of TGF β and the upregulation of fibronectin production by hepatic stellate cells. This fibrotic microenvironment in turn leads to the recruitment of bone-marrow derived macrophages (and neutrophils) to the liver which provides a beneficial metastatic niche (96).

1.4.4 The liver as a metastatic side

The liver is one of the major target sites for metastases of several malignancies such as colorectal carcinoma, pancreatic cancer, breast cancer (97) and cutaneous melanoma (98). Macrometastases in the liver are often not diagnosed in the first place, although it is very likely that the liver harbors micrometastases from early on. Already the special architecture of the liver makes it susceptible for circulating disseminated tumor cells (DTCs). One of these architectural features is the liver-specific microcirculation with low blood pressure and its

unique liver sinusoidal endothelial cells representing the first barrier encountered by CTCs (99-101).

LSECs can mediate the formation of liver metastases by either adhesive or angiocrine mechanisms. It was shown in several cancer entities that intracellular adhesion molecule 1 (ICAM1) exerts a role in the formation of liver metastases (102). In addition, it was shown that C-type lectin 4G (Clec4G), an endothelial lectin mediates the hepatic colonization of colorectal metastases (103). In addition, LSECs are prone of releasing inflammatory cytokines including Interleukin 1 (IL-1) (104), MIF and Cxcl12 (105) which mediate liver metastases formation (106).

The liver is also known to be an immunological organ able to balance the continuous exposure to gut-derived microbial and food antigens. LSECs are the first barrier encountered by circulating antigens. Therefore, LSECs have to exhibit innate and adaptive immunological functions including the presentation of antigens and the elimination of invading pathogens (107). Moreover, LSECs have to prevent damaging immune responses against harmless antigens due to the fact that the liver is continuously exposed to different antigens. LSECs have to be able to maintain the balance between tolerance and effector immune reponses. It is known, that LSECs express low levels of costimulatory molecules and are able to produce IL-10 and TGF-β (107, 108), thus making LSECs unable to function as professional antigen presenting cells (APCs) and to induce a more Th1 driven immune response. Additionally, LSECs are defined as B7-H1^{high} CD86/80^{low} cells (109, 110). These imbalances between stimulatory and inhibitory signals induce the tolerance of CD8^{+} T cells and provide a more immunotolerant environment (107).

The immunological tolerance of the liver was targeted using mellitin nanoparticles (α-mellitin-NPs) which are taken up by LSECs. The α-mellitin NPs activate LSECs leading to the activation of the immunological state of the liver by changing the chemokine/cytokine milieu which in turn leads to a reduced metastatic burden within the liver and increased survival rates in a spontaneous mouse model of liver metastases (111).

1.5 Therapeutic strategies

The strategy for the treatment of cutaneous melanoma is highly dependent on different features of the primary tumor namely the stage and the genetic profile (112).

1.5.1 Surgical resection

Patients diagnosed with cutaneous melanoma, which means a primary tumor and lymph node involvement (see 1.1 and Table 4), receive surgery as the primary treatment. Already in 1970, W. Handley stated in *The Lancet* that the primary tumor of cutaneous melanoma had to be excised with a safety margin. At that time, the recommended safety margin was 5 cm independently of the thickness of the primary tumor (113). Nowadays, the standard of care is a safety margin of 0.5 cm for *in situ* melanomas, 1 cm for melanomas with a Breslow thickness ≤ 2 mm and 2 cm for melanomas with a tumor thickness ≥ 2 cm (114). Several trials compared different safety margins and demonstrated no significant advantages between safety margins of 5 cm compared to 2 cm (115). However, patients with a high-risk melanoma and a safety margin of 1 cm display an increased local recurrence and a trend towards reduced survival rates suggesting that the safety margin cannot be excluded (116).

Further, it is known that cutaneous melanoma predominantly metastasizes via the lymphatic and hematogenous stream. Therefore Morton *et al.* introduced the sentinel lymph node biopsy in order to detect early lymph node metastases. For the detection of micrometastases the peritumoral intradermal injection of ^{99}techneticum antimony trisulphide colloid is used. This colloid can be detected by the lymphoscintigraphy and gamma ray probe detection in order to find the first node receiving lymph from the primary tumor (117, 118). This method is characterized by a high level of accuracy, detecting about 97 % of positive sentinel lymph nodes (119). A sentinel lymph node biopsy is recommended in the german guideline for patients with primary tumors thicker than 1 mm (120) or with a tumor thickness between 0.75 and 1 mm and additional risk factors such as young age or high rate of mitoses. The result of the lymph node biopsy correlates with the outcome and prognosis of patients with cutaneous melanoma and is nowadays accepted as valuable diagnostic tool and helps to further define future treatment strategies (121).

1.5.2 Chemotherapy

In the past, the main treatment option for advanced melanoma was chemotherapy. But chemotherapy only improves the clinical response and not the overall survival of patients (112). Dacarbazine has been approved by the Food and Drug Administration (FDA) in 1974 and is the only approved alkylating agent and cytotoxic drug for the treatment of metastatic melanoma (122). Though several studies have found that the response rate of Dacarbazine ranges from 6- 20 % and that less than 5 % achieved a complete response and less than 2 % of patients survived more than 5 years (123, 124). However, the treatment of metastatic melanoma with

dacarbazine as single agent or in combination with targeted therapies (TTs) and immunotherapies was further investigated in several clinical trials (125). The combination of chemo- and immunotherapy was named biochemotherapy (BCT). A combination of Dacarbazine and Interleukin 2 (IL-2) showed higher response rates but could not improve the overall survival of patients. Furthermore, the combination therapy of chemo – and immunotherapy was associated with severe side effects (126).

1.5.3 Targeted therapy

TTs describe therapies interfering with important signaling pathways which are involved in cell growth, cell division and migration spread of these cells (127). As already mentioned in section 1.3, for cutaneous melanoma the MAPK or the PI3K pathway are relevant (128).

BRAF inhibitors

About 50 % of patients with metastatic melanoma harbor a *BRAF* mutation (129) leading to activation of the MAPK signaling pathway and enhanced proliferation of cells (130). The most common mutation of the *BRAF* gene is a missense mutation found at the codon 600 which leads to an exchange of the amino acid valine to glutamic acid (BRAFV600E) (131). This BRAFV600E mutation constitutively activates the BRAF kinase (132) resulting in an activation of the downstream MEK/ERK pathway leading to the evasion of senescence and apoptosis and uncontrolled proliferation of cells (133).

In 2011, Vemurafenib a selective BRAF inhibitor (BRAFi) was approved by the FDA for the treatment of unresectable or metastatic melanoma with a BRAFV600E mutation (134). Furthermore, Dabrafenib another BRAFi was approved in 2013 by the FDA. In contrast to the chemotherapy (see section 1.5.2) both BRAF inhibitors improved the clinical outcomes of patients diagnosed with cutaneous melanoma (130, 135). In 2018, the FDA approved Encorafenib (BRAFi) in combination with binimetinib (MEKi) for the treatment of patients with unresectable or metastatic melanoma showing a BRAF V600E and V600K mutation (136).

MEK inhibitors

MEK is a tyrosine kinase acting downstream of BRAF. In 2013, the MEK inhibitor Trametinib was approved by the FDA and EMA for the treatment of unresectable and metastatic melanoma (137). In contrast to the BRAF inhibitors, Trametinib showed activity in patients with a *BRAF* mutation as well as in patients with a *NRAS* mutation (138). Moreover, MEKi improved the progression free survival (PFS), overall survival (OS) and the clinical outcome of patients with unresectable and metastatic melanoma harboring a *BRAF* mutation (139). Cobimetinib and Binimetinib, two MEKi are approved for the combination therapy with BRAFi for the treatment of metastatic melanoma (136).

Yet, the clinical benefit of BRAF and MEK inhibitors remains restricted because cancer cells rapidly develop resistance mechanisms (140) and only one third of patients show a controlled or stabilized disease (141).

New therapeutic options focusing on the immune system in the emergence of a tumor have been investigated and led to the development and approval of different immunotherapies.

1.5.4 Immunotherapy

The fact that there is a strong correlation between the presence of tumor-infiltrating lymphocytes within the primary tumor and the clinical outcome of patients (142) and the finding that cutaneous melanoma is highly immunogenic (143) makes the cutaneous melanoma highly susceptible for the treatment with immunological modalities. In addition, it is known that melanoma cells are highly immunogenic due to the expression of different tumor-associated antigens including neo-antigens such as the carcinoembryonic antigen (CEA) (144), melanoma associated antigens (MAGEs) and the cancer/testis antigen (NY-ESO1). The expression of these antigens is an important factor regarding immunosurveillance and cancer progression (145).

1.5.4.1 Vaccines

Efforts have been made to test the use of different vaccines for the treatment of cutaneous melanoma involving $CD4^+$ or $CD8^+$ T cells to get activated by the presentation of different antigens via major histocompatibility complex (MHCI or MHCII) restricted processes. Therefore, the idea was to use such antigens to trigger a therapeutic immune response (146, 147).

One of the most studied cancer vaccines which was tested in a phase II study for the treatment of metastatic melanoma is CancerVax®, a vaccine consisting of three melanoma cell lines which are viable and irradiated (148). This vaccine consists of at least 11 melanoma specific tumor-associated antigens such as Mart-1/Melan-A, gp100, gp75 and MAGE-1 and MAGE-3 (149, 150). Patients treated with CancerVax® showed a median survival of 23 months compared to 7.5 months which was seen in historical controls. In addition, patients treated with CancerVax® showed a 5-year survival of 40 % compared to 13 % in the control group (151). Another vaccine named Melacine® consisting of two different melanoma cell lines and DETOX®, an immunological adjuvant consisting of the cell wall cytoskeleton from *Mycobacterium phlei* and an endotoxin from *Salmonella minnesota* showed promising results in stage IV melanoma patients (152). Several other vaccines have been investigated for the treatment of cutaneous melanoma including dendritic cell vaccines, peptide vaccines, ganglioside vaccines or DNA vaccines. However, in these cases no randomized, large prospective trial could show a survival benefit so far (147). The use of vaccines based on tumor-associated antigens (TAAs) which are highly expressed on melanoma cells were mostly

ineffective in the generation of a clinical effective antitumor immune response due to the fact that the TAA-specific T cells can lead to a central and/or peripheral tolerance (153). Furthermore, TAAs are also present on non-malignant cells causing a risk of vaccine-induced autoimmune toxicities (153). Melanom FixVac (BNT111), a liposomal RNA vaccine, targets four different non-mutated, tumor-associated antigens such as New York oesophageal squamous cell carcinoma 1 (NY-ESO1), melanoma associated antigen A3 (MAGE-A3) and trans-membrane phosphatase with tensin homology (TPTE). These antigens show a normal tissue expression, but are highly abundant and immunogenic in melanomas. BNT11 is tested in a phase I clinical trial (Lipo-MERIT, NCT02410733). Melanoma FixVac showed durable objective responses either as single agent or in combination with a PD-1 inhibitor in unresectable melanoma patients which are already ICI experienced (154). Neoantigens or neoepitopes, which are referred to be novel epitopes or self-antigens developing from mutations in tumor cells can be used for the development of personalized cancer vaccines (155). Personalized cancer vaccines have several advantages including the prevention of “off-target” damage and the circumvention of T cell tolerance caused by self epitopes (155). The individualized mRNA cancer vaccine BNT122 (BioNTech SE and Genentech) targeting personalized neoantigens of cancer patients is tested in a Phase II clinical trial for the treatment of untreated advanced melanoma (GO40558 Study; NCT03815058) (156). Additionally, the cancer vaccine mRNA-4157/V940 from Moderna in combination with Pembrolizumab (Merck) showed in a Phase IIb clinical trial (Keynote 942) an improved recurrence-free survival in comparison to Pembrolizumab alone. After 18 months the cancer vaccine in combination with the ICI Pembrolizumab decreased the risk of disease recurrence by 44 %. Taken together, cancer vaccines might further improve the clinical outcome of melanoma patients (157).

1.5.4.2 Oncolytic virus therapy

Over the last decade, oncolytic viruses have become promising tools to treat cancer. In 2015, the FDA approved the first oncolytic virus for the treatment of surgically unresectable skin and lymph node lesions of patients with advanced melanoma (158). Talimogene laherparepvec (T-VEC) is a genetically modified herpes simplex virus type I which is directly injected into a metastatic lesion. The virus selectively replicates in cancer cells leading to the lysis of the cells, thereby releasing GM-CSF and specific tumor antigens which in turn activates the patients´ own adaptive immune response by recruiting and activating e.g. antigen-presenting cells (159).

A Phase III clinical study of patients with stage IV or unresectable stage III melanomas (OPTiM trial) showed that the intralesional injection of T-VEC was superior to the subcutaneous injection of GM-CSF regarding durable response rates, overall response rates and the median overall survival which was 23.3 months compared to 18.9 months. Furthermore, the oncolytic virus therapy with T-VEC was associated with very few AEs (adverse events) defining a good safety profile (160). Another oncolytic virus, the Coxsackievirus A21 or CAVATAK was tested

in a Phase II study in patients with unresectable stage IIIC or stage IV melanoma (161) and several clinical trials are ongoing investigating the combination of oncolytic viruses with other immunotherapies (162). However, the combination of T-VEC with neoadjuvant Nivolumab showed no clinical benefit (163).

1.5.4.3 Interleukins and Interferons

Interleukins (ILs) and interferons (IFNs) are secreted signaling proteins regulating both the innate and adaptive immune system in an autocrine or paracrine manner (164).

IL-2 is a naturally occurring cytokine which has several immunological functions such as the proliferation and differentiation of T lymphocytes. IL-2 is capable to exhibit its anti-cancer effects by the amplification of the hosts immune response already directed against the cancer cells (165). High-dose (HD) interleukin 2 was the first immunotherapy approved by the US FDA for the treatment of advanced melanoma (166). However, the overall response rate of the high-dose IL-2 therapy was less than 20 % and the complete response rate was reported to range from 0 – 10 %. Further, the treatment with HD IL-2 was associated with numerous AEs. Therefore, a lower dosage of IL-2 is investigated in combination with other therapies to possibly generate a better overall clinical efficacy (165). The systemic use of IL-2 was associated with severe side effects and complete responses of patients were achieved in only 10 % of cases (167). In order to reduce severe side effects IL-2 was applied intralesional and complete responses lasting for more than 6 months were achieved in 70 % of cases (168).

IFNs are molecules which are involved in anti-proliferative, pro-apoptotic and antitumor mechanisms (169). Due to its involvement in antitumor activities, the FDA approved high-dose IFN-α-2b in 1995 for the treatment of resected stage IIB-IIID melanoma in an adjuvant setting. IFN-α shows an inhibitory effect on the proliferation of melanoma cells with a dose-dependent pro-apoptotic effect (170). A meta-analysis published by Ives *et al.* points to an improved survival of melanoma patients and a reduced risk of recurrence (171). However, very few patients respond to the treatment with IFN-α and it was shown that the therapy response to the treatment was highly dependent on the ulceration of the primary tumor (172).

1.5.4.4 Adoptive T cell therapy

A relatively new treatment strategy involving the hosts immune system is the adoptive cell transfer (ACT). It is based on the fact that an effective immunotherapy is dependent on the presence of high numbers of tumor infiltrating lymphocytes (TILs) with appropriate homing and effector functions, which can effectively destroy cancer cells *in vivo* (173). This treatment approach starts with the identification of anti-tumor lymphocytes, which can then be expanded *ex vivo*. After the expansion, lymphocytes are reinfused into the cancer patients (173). The *ex vivo* expansion of the lymphocytes allows to test the specificity of lymphocytes prior to the reinfusion (174). In metastatic melanoma, ACT is associated with complete and durable

responses and a prolonged stabilization of the disease. This is important to note since ACT of TILs is mainly applied to patients with an advanced disease and multiple metastatic sides, for whom other therapies were not effective. In addition, several clinical trials demonstrated that most of the patients showing a complete response stayed disease-free for many years, highlighting the curative potential of the adoptive T cell transfer (175-177).

Another immunotherapeutic approach is the chimeric antigen receptor T cell (CAR T cell) therapy which already showed good results in the therapy of hematological malignancies (178-180). CAR T cells consist of a single chain variable fragment (scFv) from a monoclonal antibody able to target a specific antigen of the cancer cell. Furthermore, CAR T cells consist of a signaling domain from the T cell receptor, commonly the zeta subunit of the CD3 complex and some co-stimulatory motifs such as CD28 (181, 182). The clinical use is similar to the adoptive T cell transfer except the fact that the CAR T cells get genetically transduced *ex vivo* with the above-mentioned CAR construct. Several clinical trials targeting the ganglioside GD2 which is highly expressed in melanoma cells (NCT02107963) or CAR T cells against VEGFR2 (NCT01218867) were performed.

1.5.4.5 Immune checkpoint inhibitors

Key immune cells for the killing of tumor cells are cytotoxic $CD8^+$ T cells. Naïve $CD8^+$ T cells are primed by dendritic cells that present tumor antigens via MHC molecules and its co-stimulatory receptors CD80/CD86. After priming, $CD8^+$ T cells are activated effector T cells and are able to kill cancer cells via the release of Perforin, Granzyme B or the release of different cytokines such as IFNγ or TNFα (Figure 3) (183, 184).

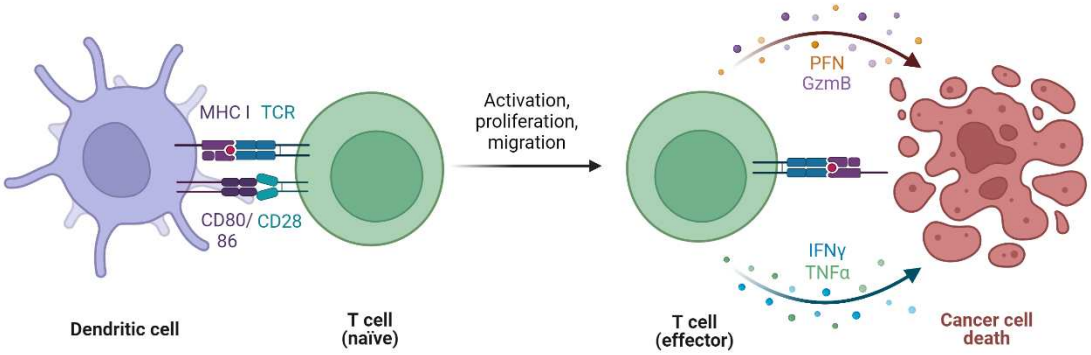

Figure 3: Mechanism of T cell activation and killing of cancer cells.

Activation of T cells requires the binding of an antigen to the T cell receptor via MHC mediated processes and the co-stimulatory signaling by CD80/CD86 and CD28. After the binding of the naïve T cell to the dendritic cell, the T cell gets activated leading to the proliferation and migration to the tumor microenvironment. The effector T cell recognizes the tumor antigen leading to the cancer cell death via the release of different molecules (184). Illustration was created using BioRender.com.

One important trait of cancer cells is the immune evasion described as the immunosurveillance hypothesis of cancer cells (see Section 1.3) in which cancer cells acquire traits making them able to circumvent the evasion of the host's immune system. One way in which this can occur are the expression of immune checkpoint molecules on the surface of either the cancer cell or the immune cell. Well known immune checkpoint inhibitors (ICIs) are CTLA-4, PD-1, V-domain immunoglobulin suppressor of T cell activation (VISTA), T cell immunoglobulin and mucin domain-containing protein 3 (TIM-3), B and T lymphocyte attenuator (BTLA) and the lymphocyte activation gene (LAG-3) (185). Tim-3 interacts with many different ligands such as Galectin 9 (Gal9), phosphatidylserine (Ptdser), high mobility group box1 (HMGB1) and the carcinoembryonic antigen-related cell adhesion molecule (CEACAM1). TIM-3 is expressed on many different immune cells including T helper cells (Th1 and Th17), dendritic cells, regulatory T cells, exhausted cytotoxic T cells and natural killer cells (NK cells). Targeting TIM-3 antibodies is intensively studied for the treatment of several advanced solid tumors (185). In addition, LAG-3 which is similar to PD-1 and CTLA-4, not expressed on naïve T cells but abundant on exhausted $CD4^+$ and $CD8^+$ T cells upon antigen stimulation, is extensively

researched for the therapeutic application in cutaneous melanoma (186, 187). Until now, none of these antibodies have been approved yet for the treatment of the cutaneous melanoma.

CTLA-4 is expressed on T cells and binds to the CD80/CD86 molecule commonly expressed on tumor cells. The binding of CTLA-4 to CD80/CD86 and PD-1 to PD -L1 leads to the inactivation of the T cell. PD-1 can bind to its ligand PD-L1, which is commonly expressed on tumor cells. Through the binding of PD-1 to PD-L1, the T cell gets exhausted (Figure 4, left side). Both signals cause the reduction of T cell function supporting the proliferation and outgrowth of cancer cells (188). Different antibodies targeting the immune checkpoint molecules CTLA-4, PD-1 and PD-L1 have been developed and revolutionized the treatment of about 50 cancer types (189). The antibodies against PD-1, PD-L1 and CTLA-4 bind to the immune checkpoint molecules, thereby blocking the negative signaling cascade resulting in activation of the T cells (Figure 4, right side) (188).

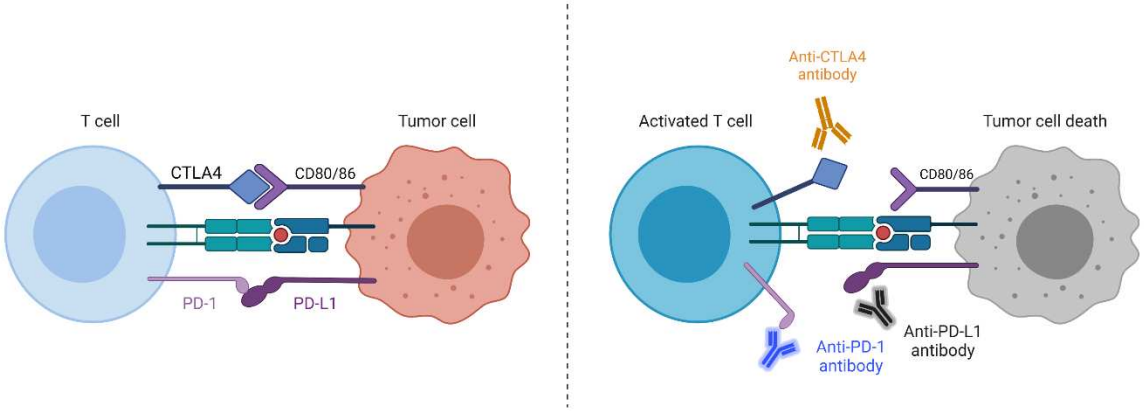

Figure 4: Activation of T cells by anti PD-1, anti CTLA-4 and anti PD-L1.

Left side: *The T cell can bind to the tumor cell via MHC molecules and the immune checkpoint molecules PD-1 and CTLA-4. This binding causes the activation of an inhibitory signaling cascade causing the exhaustion or inactivation of the T cell.* ***Right side:*** *Antibodies against CTLA-4, PD-1 and PD-L1 prevent the binding of the T cell to the tumor cell which in turn causes the activation of the T cell. The activated T cell can than lead to the death of the tumor cell. Illustration was created using BioRender.com.*

In 2011, Ipilimumab an antibody against CTLA-4 was approved by the FDA for the treatment of advanced (unresectable or metastatic) melanoma patients (190, 191). The approval of Ipilimumab was rapidly followed by the development of other ICIs such as Pembrolizumab and Nivolumab targeting PD-1 (190).

Ipilimumab was the first drug which significantly improved the OS of patients diagnosed with advanced malignant melanoma with a Phase III clinical trial, showing that Ipilimumab was superior to the chemotherapeutic agent Dacarbazine (192) regarding OS. The median OS of

patients receiving the combination therapy including Dacarbazine plus Ipilimumab was 11.2 months compared to 9.1 months in the group receiving Dacarbazine plus placebo (192, 193).

Pembrolizumab and Nivolumab, two ICIs targeting PD-1 showed a superior efficacy in phase III clinical trials in therapy naïve patients compared to Ipilimumab. The 5-year overall survival was 43 % for Pembrolizumab treated patients, 44 % for Nivolumab treated patients and 26 % for Ipilimumab treated patients (194-196). The combination of Ipilimumab and Nivolumab was tested in a Phase I clinical study showing higher response rates compared to the therapy with a single agent (197). The CheckMate-067 study found in an exploratory analysis that the combination therapy of Ipilimumab and Nivolumab significantly improved the efficacy regarding the progression-free survival and overall survival of patients compared to the monotherapy with Nivolumab (195, 198). Due to the fact that patients showed improved therapeutic responses after the palliative therapy with the ICI, additional clinical trials were carried out and investigated the adjuvant therapy with the ICIs. Adjuvant therapy is used for the treatment of high risk melanoma patients after the resection of the primary cutaneous melanoma and involved sentinel lymph nodes in order to prevent the formation of distant metastases (190). The adjuvant therapy with Ipilimumab (199), Nivolumab (200) and Pembrolizumab (201) showed improved efficacy in Stage III melanoma patients. Hence, adjuvant ICI was approved for the treatment of stage III CM with locoregional disease (200, 202, 203) and is nowadays frequently used in the clinic.

1.5.5 Therapy resistance against ICI

With the approval of new therapeutic options, such as ICI or TT, the prognosis of patients diagnosed with advanced cutaneous melanoma has dramatically improved (141, 195). However, metastases at several distant sites show reduced responses and require improved therapeutic strategies. Likewise, the duration of the overall response and the progression-free survival is significantly reduced in patients with brain metastases after the treatment with BRAFi/MEKi (204). Furthermore, several publications proclaim that liver metastases are associated with a reduced response to ICI (205). The reduced response to ICI can in part be explained by the recruitment of $CD11b^+$ $F4/80^+$ $FasL^+$ monocyte-derived macrophages by liver metastases causing the local and systemic apoptosis of cytotoxic $CD8^+$ T cells (206). In addition, Lee *et al.* show that the presence of liver metastases is associated with the activation of regulatory T cells and the recruitment of $CD11b^+$ monocytes to the subcutaneous (s.c.) tumor in an MC38 and melanoma tumor model leading to a systemic immunosuppression (207). In addition, liver metastases are also associated with a reduced therapy response to TTs, as Hauschild *et al.* found out that patients without liver metastases show the longest median OS after the treatment with BRAF and/or MEK inhibitors (208).

The adjuvant therapy with ICI has significantly improved the outcome of patients with CM and the adjuvant therapy for stage III melanoma patients has already become standard of care (209). After the adjuvant therapy with anti PD-1, around 25-30 % of patients show recurrence within one year and suffer from cancer progression (210). Owen *et al.* showed that the most common side for recurrence are the lung, the liver and the brain (210).

One relatively new therapeutic approach for the treatment of cutaneous melanoma that has already been tested in several clinical trials is the neoadjuvant therapy (211).

In 2016 Liu and colleagues demonstrated that the therapeutic efficacy and the eradication of distant metastases of the neoadjuvant therapy is significantly increased when compared to the adjuvant therapy in two preclinical models of TNBC (Triple negative breast cancer). This finding is in line with the finding that tumor-specific $CD8^+$ T cells were significantly increased in the blood and organs of mice receiving the neoadjuvant therapy. Moreover, it has been shown that the therapeutic efficacy of the neoadjuvant therapy is restricted to therapies targeting T cell antitumor immunity since the comparison of neoadjuvant chemotherapy (Paclitaxel) with the adjuvant chemotherapy using Paclitaxel does not improve the overall long-term survival of patients (212).

The mechanism underlying the improved response to ICI after neoadjuvant therapy might be the activation of different immune cells including cytotoxic T cells (212), T helper cells and APCs which mostly depends on the exposure to different antigens (Figure 5). These different cell types might activate T cells via T cell receptor (TCR) signaling. Thus, the hypothesis is that the ICI in the presence of the primary tumor may be more effective due to the higher amount of present antigens in comparison to the adjuvant therapy, where the tumor is already completely resected (211) (Figure 5).

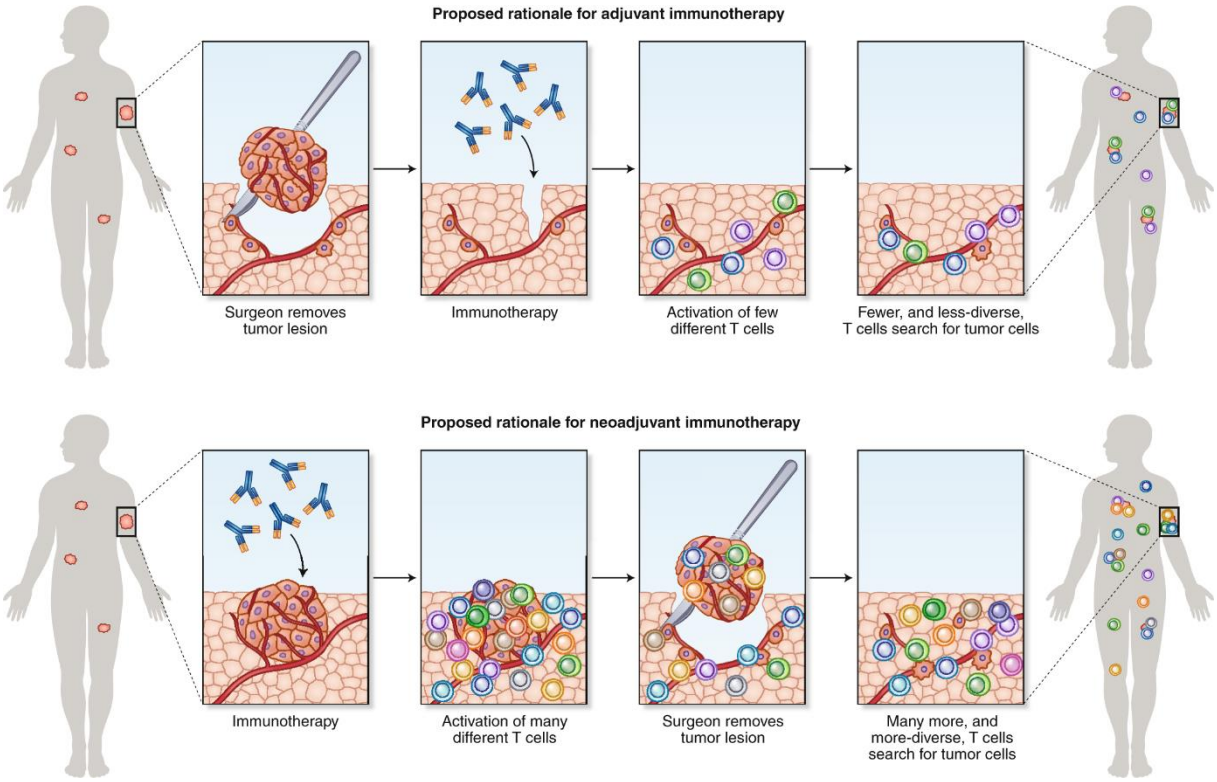

Figure 5: Comparison of proposed mechanisms underlying the adjuvant versus the neoadjuvant ICI.

Adjuvant immunotherapy: *Immunotherapy is applied after the surgical resection of the tumor lesion, resulting in the activation of few different T cells (above).* ***Neoadjuvant immunotherapy:*** *Immunotherapy is applied in the presence of the tumor lesion leading to the activation of more diverse T cell subsets. Illustration is taken from (211). Reproduced with permission from Springer Nature.*

The neoadjuvant chemotherapy and radiotherapy became already standard of care for the treatment of locally advanced rectal carcinoma (213, 214). Furthermore, the neoadjuvant therapy showed an improved protection against distant metastases in breast cancer patients when compared to the adjuvant therapy (212).

The traditional management of operable colon cancer (Stage I – III) was surgery followed by the adjuvant chemotherapy. To improve the local control ahead of surgery the neoadjuvant radiotherapy and chemotherapy are used in rectal cancer (215). The use of the immunotherapy for patients with operable colon cancer has been tested in the NICHE phase I and II clinical trial with promising results (216). Further, the neoadjuvant therapy with pembrolizumab in combination with paclitaxel and carboplatin was tested in a phase 3 clinical trial for the treatment of untreated stage II and III triple-negative breast cancer patients. Patients receiving the neoadjuvant chemotherapy with pembrolizumab have shown increased percentages of pathological complete responses in comparison to patients receiving the neoadjuvant chemotherapy plus placebo (217).

Regarding the treatment of CM, already phase II studies investigating the neoadjuvant therapy with ICI were carried out showing promising results. Most of the studies included Stage III melanoma patients (218-224). Two of these studies included Stage III as well as Stage IV melanoma patients (218, 222). One first phase III clinical trial (NADINA trial) investigating the neoadjuvant therapy with Nivolumab and Ipilimumab is currently ongoing (225). Possibly, the neoadjuvant therapy of melanoma patients with ICI could improve the therapeutic response of patients with distant metastases including liver metastases.

2 Aim of the study

Since 2018, the cutaneous melanoma became number four (women) and number five (men) of the most common solid tumors in Germany respectively (4). The CM accounts for 90 % of skin cancer related deaths (6). The treatment options of patients with cutaneous melanoma and a metastatic disease was limited. In this, the approval of the TT and the ICI for the treatment of CM has significantly improved the outcome of CM patients (226).

The liver is one of the most common target sites for metastases of the CM (15). In addition, patients with liver metastases show a reduced therapeutic response to the ICI and TT when compared to patients without liver metastases (205, 208). Different features of the liver make the organ susceptible for the uptake of CTCs. Furthermore, the liver as a secondary organ can be prepared for the uptake of CTCs by the primary tumor which is referred to the formation of a pre-metastatic niche (95, 96).

The first aim of this project was the investigation of the formation of a pre-metastatic niche in order to identify new target structures supporting the susceptibility of the liver for the uptake of CTCs. Therefore, the intracutaneous injection of tumor cells were performed in order to simulate the presence of a primary tumor. Liver metastases formation was analyzed after the intralienal injection of the tumor cells in order to investigate if a primary tumor influences the hepatic colonization of melanoma cells.

Due to the lack of therapeutic options for the treatment of melanoma patients with a metastatic disease and the low predictability of liver metastases for the therapeutic response to ICI, the second aim of this project was to study different time points of ICI to prevent the colonization of the liver by CTCs and to further investigate the hepatic resistance mechanisms developing after the treatment with the ICIs. Therefore, different therapeutic regimens (palliative, adjuvant and neoadjuvant) were comparatively analyzed in different mouse models of melanoma metastases formation. Afterwards, the aim was to comparatively analyze the composition and activation of different immune cells within the primary tumor, the blood and the liver.

The overall aim of this part of the project was to investigate how the different timing of the ICI can improve the therapeutic response of liver metastases and to discover new therapeutic options for the treatment or better prevention of liver metastases in order to improve the clinical outcome of melanoma patients.

3 Material and Methods

3.1 Materials

3.1.1 Devices

Table 5 Devices

Device	Name	Manufacturer
Anesthesia machine	Tragbares Tischnarkosegerät	Dr. Wilfried Müller GmbH
Cell culture hood	Safety cabinet Herasafe KS class II	Thermo Fisher Scientific
Cell culture Incubator	HERAcell® 150i	Thermo Fisher Scientific
Centrifuges	Centrifuge 5417 R Centrifuge 5810 R Centrifuge 6K15 Refrigerated	Eppendorf Eppendorf Sigma Aldrich
Cryostat	Cryostat CM3050S	Leica
Flow cytometer	BD FACS Canto II	BD Biosciences
Gas anaesthesia system	XGI-8	Caliper Life Sciences
IVIS	IVIS200 charge-coupled device imaging system	Caliper Life Science
Microplate reader	Tecan Infinite M200	Tecan
Microscope	Eclipse Ni-E motorized upright microscope	Nikon Instruments
Microtome	Rotary Microtome 3006EM	Pfm medical
OP table (heatable)	Kleintier OP Tisch (ME12511)	Fa. MEDAX
Sterilizer	Dual Clasping stainless steel sterilization container	Fine Science Tool (FST)
Vortexer	Vortex Genie™	Scientific Industries
Water baths	Water bath TW8 Water bath pura22 Water bath 1000	Julabo Julabo Pfm medical
Fluorescence microscope	Nikon Eclipse NI	Nikon
Slide scanner	Axio Scan Z1	Zeiss

3.1.2 Consumables

Table 6 Consumables

Consumable	Manufacturer	Catalog No.
Cell culture flask T75	Greiner Bio-One	658175
Cell culture flask T175	Greiner Bio-One	660175
Cell strainer, 100 µm	neoLab Migge	352360
Compensation Beads	Life Technologies	01-2222-42
Cryo tubes, 2 ml	Greiner Bio-One	122263
Cryomold, 15 x 15 x 15 cm	Weckert	4566
Dako Pen	Agilent Technologies	S200230
Disposable Scalpel	Carl Roth	T998.1
Microscopy slides Super Frost Plus	Langenbrinck	03-0060
Microtome Blades, S35	Pfm medical	207500000
Needle, 26 G $^{1}/_{2}$	BD	303800
Needle 30 G$^{1}/_{2}$	BD	304000
Parafin embedding cassettes	neoLab Migge	60001580
Parafilm® M	Merck	P7793
Pipette filter tips, 10 µl	Biozym	VT0200
Pipette filter tips, 100 µl	Biozym	VT0230
Pipette filter tips, 200 µl	Biozym	VT0240
Pipette filter tips, 1250 µl	Biozym	VT0270
Pipette tips, 10 µl	Biozym	VT0104
Pipette tips, 200 µl	Biozym	VT0144
Pipette tips, 1250 µl	Biozym	VT0174
Polystrene Round-bottom tube, 5 ml	Falcon	352052
Precellys® 2 ml Ceramic kit 1,4/2,8 mm	VWR	431-0170
Reaction tubes Safe-Lock, 1,5 ml	Eppendorf	30120086
Reaction tubes Safe-Lock Biopur, 1,5 ml	Eppendorf	30121589
Reaction tubes Safe-Lock, 2 ml	Eppendorf	30120094
Reaction tubes Safe-Lock, 5 ml	Eppendorf	30119401
Serological Pipette, 5 ml	Greiner Bio-One	606180
Serological Pipette, 10 ml	Greiner Bio-One	607180
Serological Pipette, 25 ml	Greiner Bio-One	760180
Syringe, 1 ml	B.Braun	9161502
Syringe, 20 ml	B.Braun	4606205V
Tissue-Tek® optimum cutting temperature (O.C.T) Compound	Weckert	600001
Conical tube, 15 ml	Falcon	352096
Conical tube, 50 ml	Falcon	352070
96- Well plate, U-bottom	Greiner Bio-One	650180
Neubauer Chamber	Brand	718606
Humidity chamber	NeoLab	2-1878
Vicryl coated Polyglactin 910, 6-0, 70 cm	Ethicon, J&J	V991H
Surgical pad, 40 x 60 cm	NeoLab	1-1964
Mulkompressen 5 x 5 cm steril 12fach, 50 x 2 Stück	Henry Schein medical	20002093-B
Trucount Absolute Counting tubes	BD Biosciences	663028
RBC Lysis Buffer (10x)	Biolegend	420301

3.1.3 Chemicals

Table 7 Chemicals

Chemical	Manufacturer	Catalog No.
4 % formaldehyde solution ROTI Histofix	Carl Roth	P087.3
4',6-Diamidino-2-phenylindol (DAPI)	Thermo Fisher Scientific	D1306
BD Pharm Lyse 10x	Becton Dickinson (BD)	555889
Bovine Serum Albumin (BSA)	VWR	J642-1ml
cOMPLETE Ethylenediaminetetraacetic acid (EDTA) free Protease Inhibitor	Sigma-Aldrich	11873580001
Dako Antibody Diluent	Agilent Technologies	S080983-2
Dako aqueous mounting media	Agilent Technologies	S302580-2
Dako fluorescence mounting media	Agilent Technologies	S202386-2
D-Luciferin Potassium	Hölzel	AGSC-L_1207-1g
Dulbecco's Phosphate Buffered Saline w/o. Magnesium and Calcium	Gibco™	14190144
Dulbecco's Phosphate Buffered Saline with Magnesium and Calcium	Gibco™	14040133
Fc receptor blocking reagent, mouse	Miltenyi Biotec	130-092-575
Fetal bovine serum (FBS)	Life Technologies	10270106
Heat Induced Epitope Retrieval (HIER) Citrate Buffer pH=6, 10 x	Zytomed Systems	ZUC028-500
Heat Induced Epitope Retrieval (HIER) Citrate Buffer pH=9, 10 x	Zytomed Systems	ZUC029-500
Isoflurane	WDT	21311
NaCl 0.9 % Injektionslösung Mini-Plasco connect 8	B. Braun	REF2350748
Normal donkey serum	Dianova	017-000-121
Paraformaldehyde (PFA)	Carl Roth	0335.3
Penicillin-Streptomycin , 10000 U/ml	Thermo Fisher Scientific	15140122
Radioimmunprecipitation assay (RIPA) buffer	Sigma-Aldrich	R0278
Trypan blue solution	Sigma-Aldrich	T8154
Trypsin-EDTA, 10 x	Sigma-Aldrich	59418C
UltraComp eBeads™ Compensation Beads	Thermo Fisher Scientific	01-2222-42

3.1.4 Solutions, buffers and media

Table 8 Solutions, buffers and media

Buffer/medium	Composition
4 % PFA pH 7.2	40 g PFA powder 100 ml 10 x PBS 900 ml dH_2O
Cell culture media	500 ml RPMI Medium 10 % FBS 1 % P/S
FACS Buffer	1 x PBS 1 % FBS 2mM EDTA

3.1.5 Primary antibodies

Table 9 Unconjugated antibodies

Target	Specificity	Host	Clone	Manufacturer	Catalog No.	Application	Dilution
CD11b	Mouse	Rat	M1/70	Biolegend	101202	IF (FF)	1:100
CD178	Mouse	Arm.Hamster	MFL3	Biozol	106602	IF (FF)	1:100
CD3	Mouse	Rabbit	SP7	abcam	ab16669	IF (FFPE)	1:100
CD3	Mouse	Rat	CD3-12	abcam	ab11089	IF (FFPE)	1:100
CD4	Mouse	Rat	GK1.5	Biolegend	100402	IF (FF)	1:200
CD4	Mouse	Rabbit	ERP19514	abcam	ab183685	IF (FFPE)	1:2000
CD45	Mouse	Rabbit	Polyclonal	abcam	ab10558	IF (FF)	1:100
CD8	Mouse	Rabbit	ERP21769	abcam	ab217344	IF (FFPE)	1:1000
CD8a	Mouse	Rat	5H10-1	Biolegend	100802	IF (FF)	1:500
F4/80	Mouse	Rabbit	SP115	abcam	ab111101	IF (FF)	1:100
Gata3	Mouse	Rabbit	D13C9	Cell Signaling	5852S	IF (FF)	1:100
IFNγ	Mouse	Rat	XMG1.2	Invitrogen	MM700	IF (FF)	1:100
Ly6C	Mouse	Rat	ER-MP20	abcam	ab15627	IF (FF)	1:100
Ly6G	Mouse	Rat	RB6-8C5	abcam	ab25377	IF (FF)	1:100
T-bet/TBX21	Mouse	Rabbit	E412K	Cell Signaling	97135S	IF (FF)	1:100

3.1.6 Secondary antibodies

Table 10 Secondary antibodies

Specificity	Conjugate	Clonality	Manufacturer	Catalog No.	Application	Dilution
Armenian Hamster IgG	AF488	Polyclonal	Dianova	127-545-160	IF	1:400
Goat IgG	AF488	Polyclonal	Dianova	705-545-147	IF	1:400
Goat IgG	AF647	Polyclonal	Dianova	705-605-147	IF	1:400
Goat IgG	Cy3	Polyclonal	Dianova	705-165-147	IF	1:400
Rabbit IgG	AF488	Polyclonal	Dianova	711-545-152	IF	1:400
Rabbit IgG	AF647	Polyclonal	Dianova	711-605-152	IF	1:400
Rabbit IgG	Cy3	Polyclonal	Dianova	711-165-152	IF	1:400
Rat IgG	AF488	Polyclonal	Dianova	712-545-153	IF	1:400
Rat IgG	AF647	Polyclonal	Dianova	712-605-153	IF	1:400
Rat IgG	Cy3	Polyclonal	Dianova	712-165-153	IF	1:400

3.1.7 Antibodies for flow cytometry

Table 11 Antibodies for flow cytometry

Target	Conjugate	Specificity	Host	Clone	Manufacturer	Order No.	Dilution
CD25	BV510™	Mouse	Rat	PC61	Biolegend	102042	1:100
CD3	PeCy7	Mouse	Rat	17A2	Biolegend	100219	1:400
CD4	APC Cy7	Mouse	Rat	RM4-5	Biolegend	100525	1:100
CD45	FITC	Mouse	Rat	30-F11	Biolegend	103108	1:400
CD8	PE	Mouse	Rat	53-6.7	Biolegend	100708	1:200
Fixable/Viability Stain	eFluor™ 450	Mouse	--	--	Invitrogen	65-0863-14	1:8000
FoxP3	AF647	Mouse	Rat	150D	Biolegend	320014	1:100
PD-1	PerCP Cy5.5	Mouse	Rat	29F.1A12	Biolegend	135208	1:100

3.1.8 *In vivo* antibodies

Table 12 *In vivo* antibodies

Target	Specificity	Host	Clone	Manufacturer	Order No.	Concentration
PD-1 (CD279)	Mouse	Rat	RMP1-14	Bio X Cell	BE0146-50 MG	12.5 mg/kg
IgG2a	--	Rat	2A3	Bio X Cell	BE0089-50MG	12.5 mg/kg
CTLA-4	Mouse	Rat	9D9	Bio X Cell	BE0164-50MG	5 mg/kg
IgG2b	--	Mouse	MPC-11	Bio X Cell	BE0086-50MG	5 mg/kg

3.1.9 Fluorescence in situ hybridization probes

Table 13 *Fluorescence in situ hybridization* probes

Target	Manufacturer	Order No.
CD3e-C2	ACD Biotechne	314721-C2
CD4-C2	ACD Biotechne	406841-C2
IFNγ	ACD Biotechne	311391
IL4	ACD Biotechne	312741
TNFα	ACD Biotechne	311081

3.1.10 Commercial kits

Table 14 Commercial kits

Name	Manufacturer	Catalog No.
FoxP3 Transcription Factor Fixation/Permeabilization Concentrate and Diluent	eBiosciences	00-5521-00
Milliplex Mouse Cytokine Magnetic Kit	Merck Millipore	MCYTOMAG-70K-09
RNA scope Multiplex Fluorescent Kit v2	Bio Techne	323100

3.1.11 Cell lines

Table 15 Cell lines

Name	Species	Tissue	Disease	Reference
B16F10 *luc2*	Mus musculus	Skin	Melanoma	
WT31	Mus musculus	Skin	Melanoma	(227)

3.1.12 Mouse models

For this project, female C57Bl/6 wildtype mice were used and purchased from Janvier.

All animals received human care in compliance with the Guide for the Care and Use of Laboratory Animals published by the National Academy of Sciences and all experiments were approved by the animal ethics committee of Baden-Württemberg (Regierungspräsidium Karlsruhe).

3.1.13 Software

Table 16 Software

Software	Version	Manufacturer
Fiji ImageJ	2.0.0	National Institutes of Health
FlowJo	V10.1	FlowJo, LLC
Graph Pad Prism 9	9.5.0	Graph Pad Sofware
BD FACS Diva™ Software	9	BD Biosciences
Imaris	9.9	Oxford Instruments
Biorender (Premium)	---	BioRender

3.2 Methods

3.2.1 *In vivo* studies

3.2.1.1 Animals

Female wildtype C57Bl/6 mice were purchased from Janvier and used at the age of at least 12 weeks. All animals were hosted in single ventilated cages in a 12 h/12 h day and night cycle under specific-pathogen free conditions and fed ad libitum with a standard rodent diet. All animals received human care in compliance with the Guide for the Care and Use of Laboratory Animals published by the National Academy of Sciences and all experiments were approved by the animal ethics committee of Baden-Württemberg (Regierungspräsidium Karlsruhe).

3.2.1.2 Intrasplenic injection of tumor cells

Before the intrasplenic injections of tumor cells, mice received Buprenorphin as analgetics [0.1 mg/kg] and were anaesthetized with isoflurane. The skin and the peritoneum were cut with a scissor. Then the spleen was taken out the peritoneum with a cotton stick and either 1.5 x 10^5 B16F10 *luc2* or 1.5 x 10^4 Wt31 melanoma cells in 60 µl of sterile PBS were carefully injected into the spleen. To avoid the growth of an intrasplenic tumor, a splenectomy was performed after 15 min. Then the peritoneum and skin were closed by a suture. For rehydration, mice received 0.9 % NaCl subcutaneously. Buprenorphin was used as analgetics and mice were monitored carefully every day (106, 228).

3.2.1.3 Intravenous injection of tumor cells

Mice were anaesthetized with isoflurane. Then 1.25 x 10^6 Wt31 melanoma cells in 100 µl of sterile PBS were slowly injected into the tail vein.

3.2.1.4 Cutaneous injection of tumor cells

For the cutaneous injection of 5 x 10^5 Wt31 or B16F10 *luc2* melanoma cells in 20 µl of sterile PBS, mice were anesthetized with isoflurane and hair was removed at the back and left flank of the mice. At indicated time points, melanoma cells were injected cutaneously. Mice were monitored rigorously and the tumor development was measured every second day.

3.2.1.5 Bioluminescence imaging

To perform *in vivo* bioluminescence imaging (BLI), mice were intraperitoneally injected with luciferin and imaged using an IVIS200 charge-coupled imaging system with an exposure time of 45 sec. For the performance of the *ex vivo* BLI, animals were sacrificed 10 mins after luciferin injection and livers and lungs were excised and imaged using an exposure time of 15 and 45 secs.

3.2.1.6 Retrobulbar blood collection

Before sacrificing the mice by cervical dislocation, blood samples were taken at indicated time points. Therefore, mice were anesthetized by isoflurane and blood samples were taken by

punctuating the retrobulbar venous plexus. The blood was collected either in lithium heparin tubes (Plasma and FACS analysis) or in EDTA tubes (Multiplex assay).

For plasma collection, blood was separated by centrifugation at 7000 x g for 7 min. Afterwards, the plasma was transferred to 1.5 ml reaction tubes and stored at – 20 °C.

3.2.1.7 Application of antibodies

For immune checkpoint blockade, a combination of 12.5 mg/kg anti-PD-1 and 5 mg/kg CTLA-4 or the respective isotype control antibodies, anti-IgG2a and anti- IgG2b (Table 12) were injected intraperitoneally (i.p.) at indicated time points. Mice received at least 3 doses of ICI.

3.2.1.8 Tissue sample preparation

After the removal of the lung and the liver, the organs were weighed and pictures were taken. Subsequently, the organs were transferred to a petri dish, the macroscopic number of metastases were analyzed and the organs were dissected.

For histological analysis, sectioned organs were either fixed in 4 % formaldehyde solution at RT for one to seven days and rehydrated according to standard protocol or snap-frozen in liquid nitrogen using cryomolds and optimal cutting temperature compound.

For molecular and biochemical analysis, sectioned organs were snap-frozen in liquid nitrogen and stored at – 80 °C.

3.2.2 Cell culture methods

3.2.2.1 Cell cultivation

B16F10 *luc2* melanoma cells were cultured in T75 flasks, whereas Wt31 melanoma cells were cultured in T175 flasks in the appropriate cell culture media (see Table 8). To detach cells, 2 ml (T75 flask) or 4 ml (T175 flask) of 1 x Trypsin/EDTA was used and added to the cells. Afterwards, the cells were incubated 3 – 5 mins at 37 °C allowing the cells to detach. To stop the reaction, 10 ml of the respective cell culture media was added to the cells and transferred to a 50 ml Falcon. After centrifugation, for 5 min at 300 x g the supernatant was removed and the cell pellet was resuspended in 10 ml of the respective cell culture media. Subsequently, cells were either split 1:3, 1:5 or seeded for the *in vivo* experiment.

For *in vivo* experiments, the tumor cells were seeded in a predefined density one day prior to the experiment. B16F10 *luc2* cells were seeded in a density of 2.5 x 10^6 cells/T175 flask and the Wt31 melanoma cells were seeded in a density of 4 - 4.5 x 10^6 cells/T175 flask. Tumor cells are then harvested at sub-confluency and used for the tumor experiments.

3.2.2.2 Cell counting

For manual cell counting, cell suspensions were centrifuged for 5 min at 300 x g and pellets were resuspended in 10 ml of their respective cell culture media. Afterwards, 20 µl of the cell suspension was mixed with 20 µl of Trypan blue in a 96 well-plate. Cells were counted using 10 µl in a Neubauer counting chamber. Since, Trypan blue cannot cross intact membranes, only dead cells are stained which allows the quantification of vital cells. Stained cells were excluded from counting.

The predefined amount of cells for seeding was calculated with the following formula:

$$X = \frac{A}{B} \times C \times 10000$$

X = Cells/ ml

A = Counted cells in 4 squares of the Neubauer counting chamber

B = Number of counted squares

C = Dilution factor

10000 = Factor of the Neubauer counting chamber

3.2.2.3 Cell harvesting

For the above-described *in vivo* experiments, cells were harvested in advance. For the detachment of the cells, 4 ml of enzyme free dissociation buffer was transferred to the cells and cells were incubated for 15 min at 37 °C. To stop the reaction, 10 ml of sterile PBS was added to the cells and transferred to a 50 ml Falcon followed by the centrifugation for 5 mins at 300 x g. Cell pellet was resuspended in 10 ml of sterile PBS and cells were counted as described in section 3.2.2.2. After counting, cells were again centrifuged for 5 min at 300 x g and resuspended in sterile PBS with Ca^{+} and Mg^{+}. Cell suspension was transferred to a 1.5 ml reaction tube and stored at 4 °C until usage.

3.2.3 Histological methods

3.2.3.1 Immunofluorescence staining of paraffin embedded tissue (FFPE)

Paraffin embedded organs were cut in 3 µm sections and dried over night at 60 °C. Afterwards, sections were deparaffinized. First, sections were put three times in 100 % of Xylene for 5 mins. Second, sections were put two times in 100 % of ethanol for 3 mins. Subsequently, sections were put in 90 %, 80 % and 70 % of ethanol for 3 mins each. Then, sections were rinsed in PBS and dH_2O for 3 mins. For antigen retrieval, sections were incubated in 1 x HIER Citrate Buffer (pH depending on the first antibody) for 45 min at 95 °C in the water bath. The antigen retrieval slides were cooled down at RT for 20 min and transferred to dH_2O. After re-immersion for 5 mins in PBS, a hydrophobic ring was drawn around the sections and sections were again washed in PBS for 5 mins. Afterwards, the first antibody was diluted in Dako antibody diluent and incubated over night at 4 °C using a humidity chamber. On the next day, sections were washed three times in PBS for 5 mins and the secondary antibody with DAPI was incubated for 1 h at RT in a humidity chamber protected from light. For reducing the autofluorescence of the erythrocytes within the cutaneous tumor, sections were incubated for 5 mins with Reagent B (Post-conditioner) of the MaxBlock Autofluorescence Reducing Reagent Kit. After incubating the secondary antibody, sections were again washed three times for 5 mins and rinsed in dH_2O. After rinsing, sections were mounted by using Dako fluorescence mounting medium.

3.2.3.2 Immunofluorescence staining of fresh frozen tissue (FF)

For immunofluorescence stainings of fresh frozen tissue, organs were cut in 8 µm thick sections using the cryotome. Afterwards, sections were air-dried for 1 h at RT. Then sections were fixed for 10 mins using 4 % of PFA and washed for 5 mins in PBS. Afterwards, sections were blocked using 5 % of normal donkey serum in PBS for 30 mins at RT. Next, the first antibody was incubated in 20 % of blocking buffer in PBS over night at 4 °C in a humidity chamber. On the next day, sections were washed three times for 5 mins in PBS. The secondary antibody with DAPI was then incubated in 20 % of blocking buffer in PBS for 1 h at RT in a humidity chamber protected from light. After incubation with the secondary antibodies, sections were washed three times for 5 mins in PBS and mounted using DAKO Fluorescence mounting media.

3.2.3.3 H&E staining

H&E stainings were performed using an automatic stainer by technicians of the ZMF according to standard protocols.

Table 17 H&E staining procedure

Staining step	Time
Xylol	3 x 2 min
100 % ethanol	1 min
96 % ethanol	1 min
80 % ethanol	1 min
70 % ethanol	1 min
Running tap water	1 min
Hematoxylin	4 mins
Running tap water	10 mins
Eosin	2 mins
Tap water	30 secs
80 % ethanol	30 secs
96 % ethanol	1 mins
100 % ethanol	2 x 1 min
Xylol	2 x 1 min

3.2.3.4 Fluorescence *in situ* hybridization (FISH)

Fluorescence *in situ* hybridization of paraffin-embedded sections were performed using the RNAscope ® Fluorescence Multiplex Reagent Kit v1 according to the protocol of the manufacturer (ACD Bio).

3.2.3.5 Image adjustment and quantification

Representative images of the stainings were captured using Nikon Eclipse NI microscope and the NIS-Elements Advanced Research (Ar) version 5.02. The microscope is equipped with a Nikon Intensilight Epifluorescence Illuminator and Nikon CFI Materials and Methods - 56 - Plan Apochromat Lambda series objectives from 4-fold to 100-fold. For microscopy DAPI, SpGreen, SpOrange, Cy5 and FITC filters were used. Images were adjusted and analyzed with Fiji ImageJ 2.0.0 software.

Immunofluorescence stainings of immune cells were scanned with an automated slide scanner Axio Scan.Z1. Whole liver sections were analyzed by Imaris 9.9. The analysis of the whole liver sections and the quantification of the immune cells was performed by Verena Häfele. Briefly, the whole liver tissue was analyzed as DAPI positive area by calculating a surface. Double-positive immune cells were detected by a threshold-based spot calculation. Thresholds were set for two immune cell markers and the DAPI signal. The number of positive spots was counted in the peritumoral liver tissue.

3.2.4 Proteinbiochemical methods

3.2.4.1 Protein isolation and determination

For protein isolation, Milliplex lysis buffer was supplemented with EDTA free protease inhibitor. Murine liver tissue (snap frozen) was homogenized in homogenizing CKMix tubes (1.4/2.8 mm) containing 200 µl of lysis buffer using the Precellys Evolution Homogenizer for 20 secs at 5000 rpm. Afterwards, samples were centrifuged for 5 mins at 13000 x g at 4 °C. The supernatant containing the proteins was transferred in a new 1.5 ml reaction tube and stored at – 20 °C.

3.2.4.2 BCA Assay

The protein concentration was measured using a colorimetric DC Protein assay based on the Lowry Assay. For measuring the protein concentration, a bovine serum albumin (BSA) dilution series was prepared by diluting BSA with the milliplex lysis buffer to final concentrations of 10 mg/ml, 5 mg/ml, 2.5 mg/ml, 1.25 mg/ml, 0.625 mg/ml, 0.3125 mg/ml and 0.15625 mg/ml. For protein determination, Reagent S was diluted 1: 50 in Reagent A and 25 µl of the mixture was pipetted in each well of a 96 well plate (Number of well depends on the number of samples). Afterwards, 5 µl of each sample and BSA standard series was pipetted in duplicates to the well containing the A/S mixture. Then, 200 µl of Reagent B was added to each well and the plate was incubated for 10 mins at RT. The absorbance at 655 nm was measured using the Tecan Infinite M200 Pro Microplate Reader. Protein concentration was calculated using the BSA standard curve.

3.2.4.3 Multiplex assay

For quantification of cytokines and chemokine in mouse liver tissue and plasma, a Milliplex Mouse Cytokine Magnetic Kit from Merck Millipore was performed according to the protocol of the manufacturer.

3.2.5 Flow cytometry

3.2.5.1 Blood preparation for flow cytometry

For flow cytometric analysis of blood, blood samples were taken at indicated time points in lithium heparin tubes. 120 µl of blood was transferred in 1.5 ml reaction tube and 1 ml of 1 x BD Pharm lyse was added, samples were vortexed for 1 min and incubated at RT for 15 mins protected from light. After incubation, samples were centrifuged for 5 min at 300 x g. After centrifugation, the supernatant was discarded, the cell pellet was resuspended in 1 ml of FACS buffer and centrifuged for 5 min at 300 x g. Cells were seeded in a 96 well plate and stored at 4 °C until performing flow cytometry staining indicated in 3.2.5.

3.2.5.2 Flow cytometry

The analysis of cells by flow cytometry is accomplished by means of a specialized microfluidic based system. It allows the analysis of the cell size (forward-scatter (FSC)) and the granularity of cells (side-scatter (SSC)) from a heterogeneous cell population by light scattering whereas fluorescent signals emitted from each cell allow the analysis of the protein expression (229)

3.2.5.2.1 Extracellular staining

The cells seeded as indicated in 3.2.5.1 were washed by adding 150 µl of PBS and centrifugation for 5 min at 300 x g. The supernatant was discarded and 50 µl of Fc-Block (clone 2.4g2), 1:50 diluted in FACS buffer, was added to the cells. As a next step, the cells were incubated for 10 min at 4 °C in the dark. Then, the cells were washed using 150 µl of PBS. Subsequently, 50 µl of the extracellular staining mastermix was added to the cells and the cells were again incubated for 30 min at 4 °C in the dark. Afterwards, the cells were washed using 150 µl PBS and centrifuged for 5 min at 300 x g. The cell pellet was resuspended in 150 µl of FACS buffer and stored at 4 °C in the dark until performing flow cytometry analysis or intracellular staining indicated in section 3.2.5.2.2.

3.2.5.2.2 Intracellular staining

After the performance of the extracellular staining, the cells were washed twice by adding 150 µl of PBS to the cells and centrifugation at 300 x g for 5 mins. Then, the supernatant was aspirated and 50 µl of the FoxP3 Transcription Factor Fixation/Permeabilization Concentrate and Diluent (mixed 1:4) was added and incubated for 15 min at 4 °C under dark conditions. The cells were again washed using 150 µl of Permeabilization/Washing Buffer. After washing, 50 µl of intracellular staining master mix was added to the cells followed by incubation for 30 mins at 4 °C under dark conditions. Afterwards, the cells were again washed with 150 µl of Permeabilization/Washing Buffer and centrifuged for 5 mins at 300 x g. Then, the cell pellet was resuspended in 150 µl Permeabilization/Washing Buffer and stored at 4 °C under dark conditions until performing flow cytometry analysis. Flow cytometric analysis was performed by a BD FACS Canto II and data was analyzed using FlowJo.

3.2.6 Statistical analysis

The statistical analysis was performed with GraphPad Prism. A Shapiro Wilk test was used to test for normal distribution of the data. A F test was used for testing equal variances of the data. For the statistical analysis of two groups, a two-tailed students t-test or Welsh's t-test was used assuming normal distribution of the data. For not normally distributed data, the Mann Whitney U test was used. For the statistical analysis of more than two groups with one independent variable, a one-way ANOVA (Bonferroni post hoc test) was used. For the statistical analysis of two or more groups with more than one variable a two way ANOVA (Tukey's post hoc test) was used. For the statistical analysis of the clinical response either a Fisher's exact test or the Cochran-Armitage Trend test was used. P values < 0.05 were assumed as statistically significant when * < 0.05, ** < 0.01, *** < 0.0001; ns= not significant.

4 Results

4.1 Pre-metastatic activation of the hepatic niche

To investigate neoadjuvant ICI and its influence on the formation of hepatic metastases, one has to study the effects of a single primary cutaneous melanoma on the hepatic microenvironment (pre-metastatic activation). In order to investigate a possible pre-metastatic activation of the hepatic niche, the WT31 melanoma cell line was injected intracutaneously and the primary tumor was resected on day 18 followed by the intralienal injection of the WT31 melanoma cell line. The control group only received intracutaneous injections with PBS on day 0. After 21 days, mice were sacrificed, and the number of hepatic metastases was analyzed (Figure 6A). The number of hepatic melanoma metastases did not differ between mice that developed an cutaneous tumor and the control group. (Figure 6B).

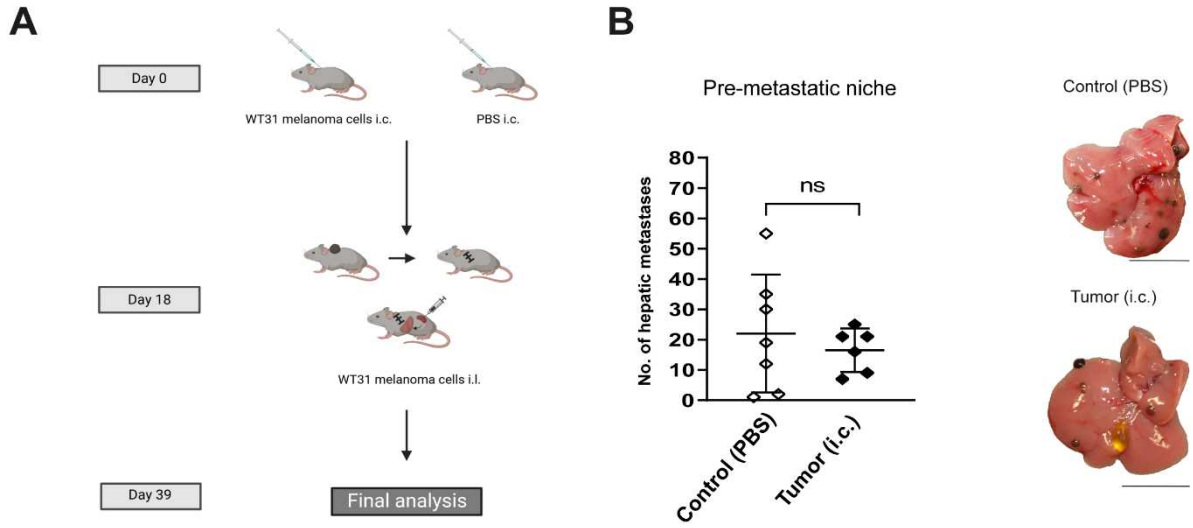

Figure 6: A primary dermal tumor does not change the amount of hepatic metastases.

A: *The WT31 melanoma cell line or sterile PBS (Ctrl.) was injected intracutaneously. After 18 days the primary tumor was resected and WT31 melanoma cells were injected intrasplenically. On day 39 the mice were sacrificed. Illustration was created using BioRender.com.* ***B:*** *The number of macroscopically visible liver metastases were analysed in mice with a primary tumor (n=6) and the corresponding controls (n=6); P=0.8059. Representative images of livers of each group are shown. Scale: 1 cm. P values < 0.05 were assumed as statistically significant when * < 0.05, ** < 0.01, *** < 0.0001; ns= not significant. The WT31 melanoma cell line was used.*

4.2 Immune checkpoint inhibition of liver metastases

4.2.1 Palliative ICI of liver metastases

To study the timing of hepatic resistance mechanisms to ICI, the WT31 or B16F10 *luc2* melanoma cell lines were injected intravenously or intrasplenicaly. The intravenous injection of the WT31 melanoma cell line leads to the formation of hepatic and pulmonary metastases (228). The palliative setting mimicks the clinical setting of a stage IV melanoma patient with distant metastases after the resection of the primary tumor (Figure 7A). The WT31 melanoma cell line was injected intravenously and the ICI with anti PD-1 and anti CTLA-4 was initiated either on day 6 (early palliative therapy) or on day 9 (late palliative therapy) (Figure 7B). Early palliative ICI starting on day 6 leads to a significant reduction of hepatic metastases (P = 0.0402). On the contrary, late palliative ICI starting on day 9 only led to a trend towards a numeric reduction of hepatic metastases (P = 0.1266).

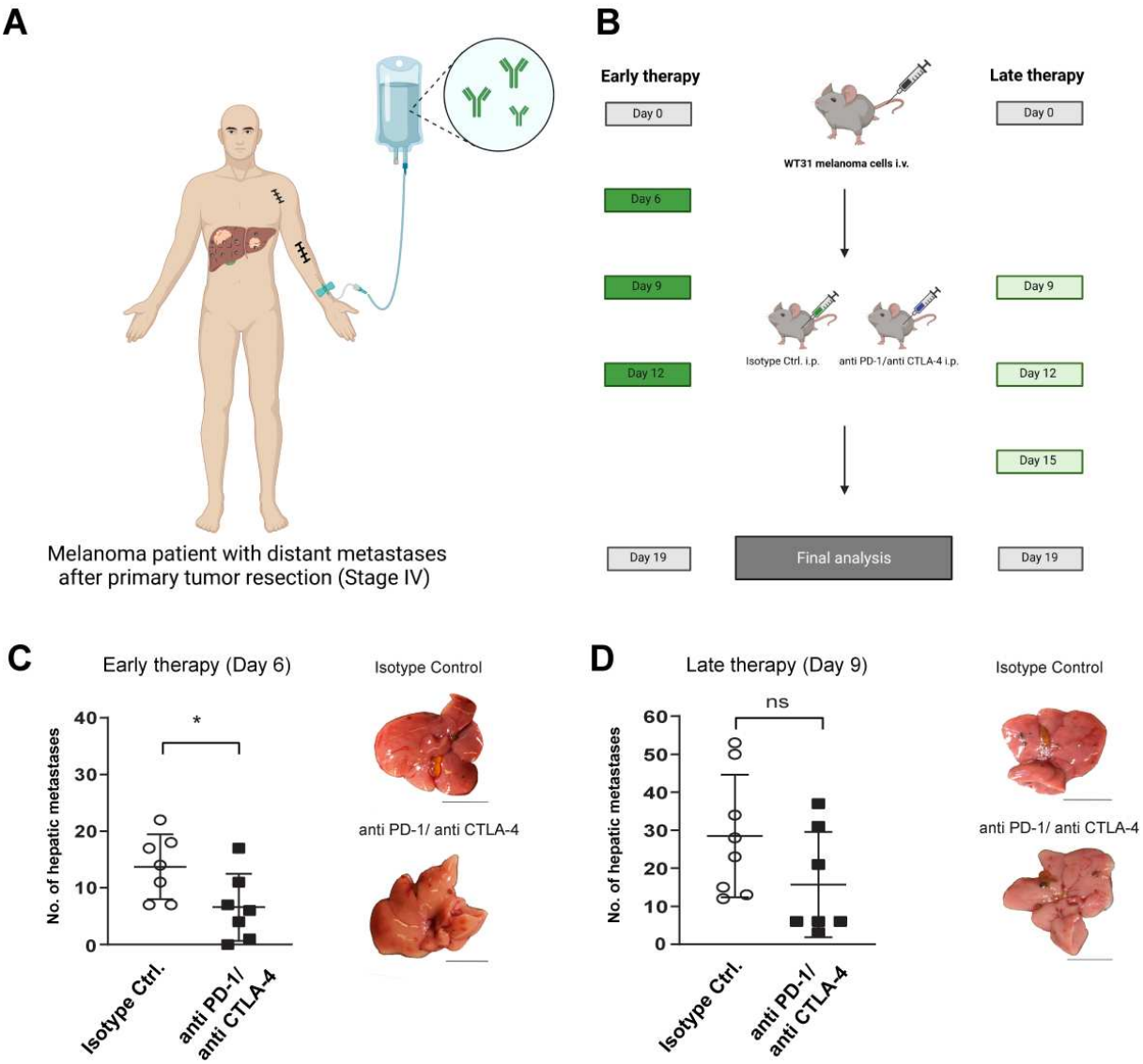

Figure 7: Early therapy with ICI significantly reduced the number of hepatic metastases.

A: *Scheme of a stage IV melanoma patient with distant metastases after the excision of the primary tumor and regional lymph node metastases. Illustration was created using BioRender.com.* ***B:*** *Illustration presenting our early and late palliative mouse model. WT31 melanoma cells were intravenously injected on day 0. After establishment of liver metastases, mice received either αPD-1/αCTLA-4 or the corresponding isotype controls on day 6, 9, 12 (early palliative ICI (dark green) or on day 9, 12 and 15 (late palliative ICI (light green)). Illustration was created using BioRender.com.* ***C:*** *The number of macroscopic liver metastases were analysed for mice receiving αPD-1/αCTLA-4 or the corresponding isotype controls in the early therapy setting. Numbers per group: 7; (P=0.0361). Representative images of livers are shown for each group. Scale: 1 cm.* ***D:*** *The number of macroscopic liver metastases were analysed for mice receiving αPD-1/αCTLA-4 (n=8) or the corresponding isotype controls (n=7) in the late therapy regimen; (P=0.1189). Representative images of livers are shown for each group. Scale: 1 cm. P values < 0.05 were assumed as statistically significant when * < 0.05, ** < 0.01, *** < 0.0001; ns= not significant. The WT31 melanoma cell line was used.*

4.2.2 Naïve adjuvant ICI of liver metastases

In addition, stage III melanoma patients with locoregional disease receive adjuvant ICI to prevent metastatic spread (Figure 8A). To study the effects of adjuvant ICI on hepatic melanoma metastasis, tumor naïve wildtype mice received three doses of ICI (αPD-1/αCTLA-4) or the corresponding isotype controls 6 days prior to the i.v. injection of the WT31 melanoma cells (Figure 8B). Naïve adjuvant ICI led to a significant reduction of hepatic metastases compared to the isotype control group (P= 0.0017) (Figure 8C).

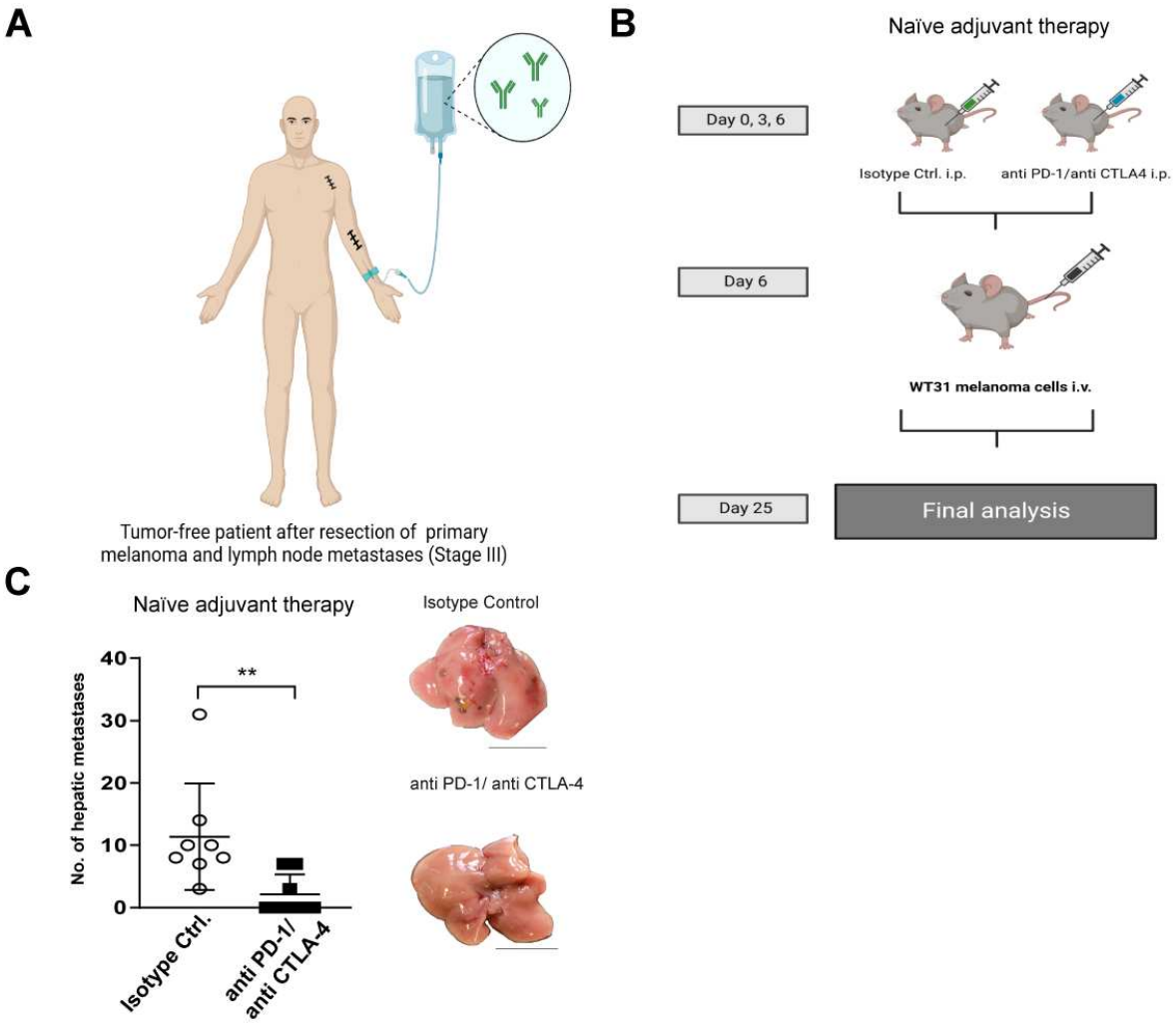

Figure 8: Naïve adjuvant immune checkpoint inhibition protects from hepatic melanoma metastases.

A: *Illustration of a stage III melanoma patient after the resection of the primary tumor and regional lymph node (s). Illustration was created using BioRender.com.* ***B:*** *Time line presenting our naïve adjuvant mouse model. Mice were injected with either αPD-1/αCTLA-4 or the corresponding isotype control antibodies on day 0, 3 and 6 followed by the intravenous injection of the WT31 melanoma cells. Mice were sacrificed on day 25. Illustration was created using BioRender.com.* ***C:*** *The number of macroscopic liver metastases were analysed for mice receiving αPD-1/αCTLA-4 or the corresponding isotype controls in the adjuvant therapy setting. Number of mice per group: 8; (P= 0.0017). Representative images of livers are shown for each group. Scale: 1 cm. P values < 0.05 were assumed as statistically significant when * < 0.05, ** < 0.01, *** < 0.0001; ns= not significant. The WT31 melanoma cell line was used.*

To compare the effectiveness of ICI in a naïve adjuvant, early and late palliative regimen, the tumor burden reduction and the clinical response were calculated. To calculate the clinical response rate, the number of metastases treated with ICI was set in relation to the mean number of metastases of all isotype controls. Naïve adjuvant ICI showed an almost two-fold stronger reduction of the tumor burden as compared to palliative ICI starting on day 9 (Figure 9A). Furthermore, about 60 % of mice showed a complete response, defined as no visible

metastases detected (Number of metastases = 0) in the naïve adjuvant therapy setting as compared to 14.3 % in the early palliative setting. In addition, in the late palliative ICI all mice developed liver metastases (Figure 9B).

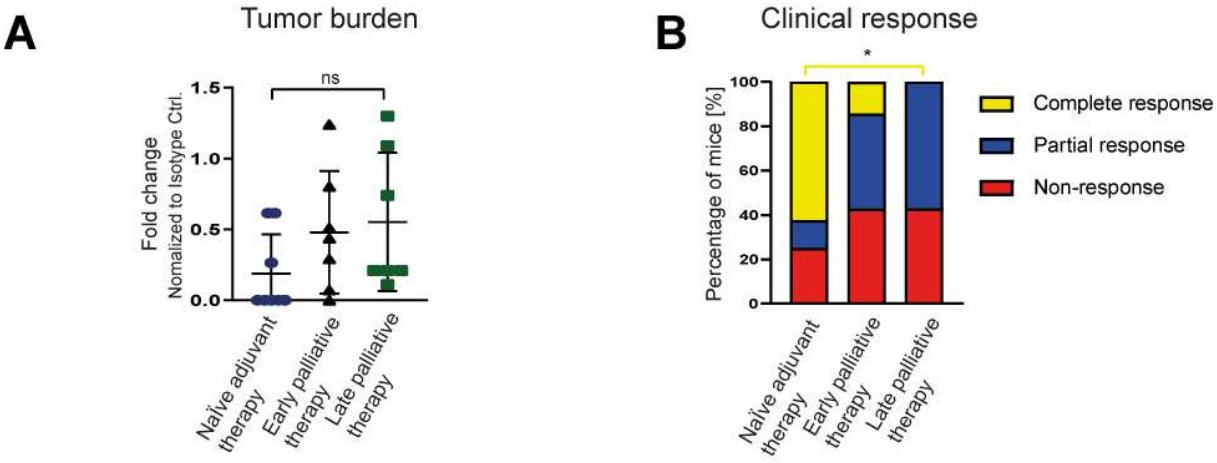

Figure 9: Naïve adjuvant ICI protects best from melanoma metastases compared to early and late palliative therapy in the WT31 melanoma metastases model.

A: *The tumor burden reduction of the mice treated with αPD-1/αCTLA-4 in the respective therapy regimen (adjuvant, early and late ICI) was calculated in relation to the corresponding isotype controls. Comparison of naïve adjuvant therapy with late therapy (day 9); Numbers of hepatic metastases of the therapy group was normalized to the mean of the corresponding isotype controls (Fold change); (P=0.1887).* ***B:*** *The clinical response of the mice that received αPD-1/αCTLA-4 was divided into non-responders, partial responders and complete responders based on the corresponding isotype controls (P=0.0195). P values < 0.05 were assumed as statistically significant when * < 0.05, ** < 0.01, *** < 0.0001; ns= not significant. The WT31 melanoma cell line was used.*

In a second mouse model with spleen injections of B16F10 *luc2* melanoma, this data was confirmed. In the palliative therapy regimen, mice received intrasplenic injections of the B16F10 *luc2* cells on day 0, followed by three doses of ICI or the corresponding isotype controls on day 6, 9, 12 (Figure 10A). In the palliative setting, no differences in the macroscopic numbers of hepatic metastases were observed by comparing the therapy group with the isotype control group (P= 0.7586) (Figure 10C). Furthermore, the naïve adjuvant therapy with ICI was applied in the B16F10 *luc2* mouse model. Mice received three doses of ICI on day 0, 3 and 6 prior to the intrasplenic injection. The comparison between the therapy group and the isotype control group showed no significant difference (P = 0.0875) (Figure 10D).

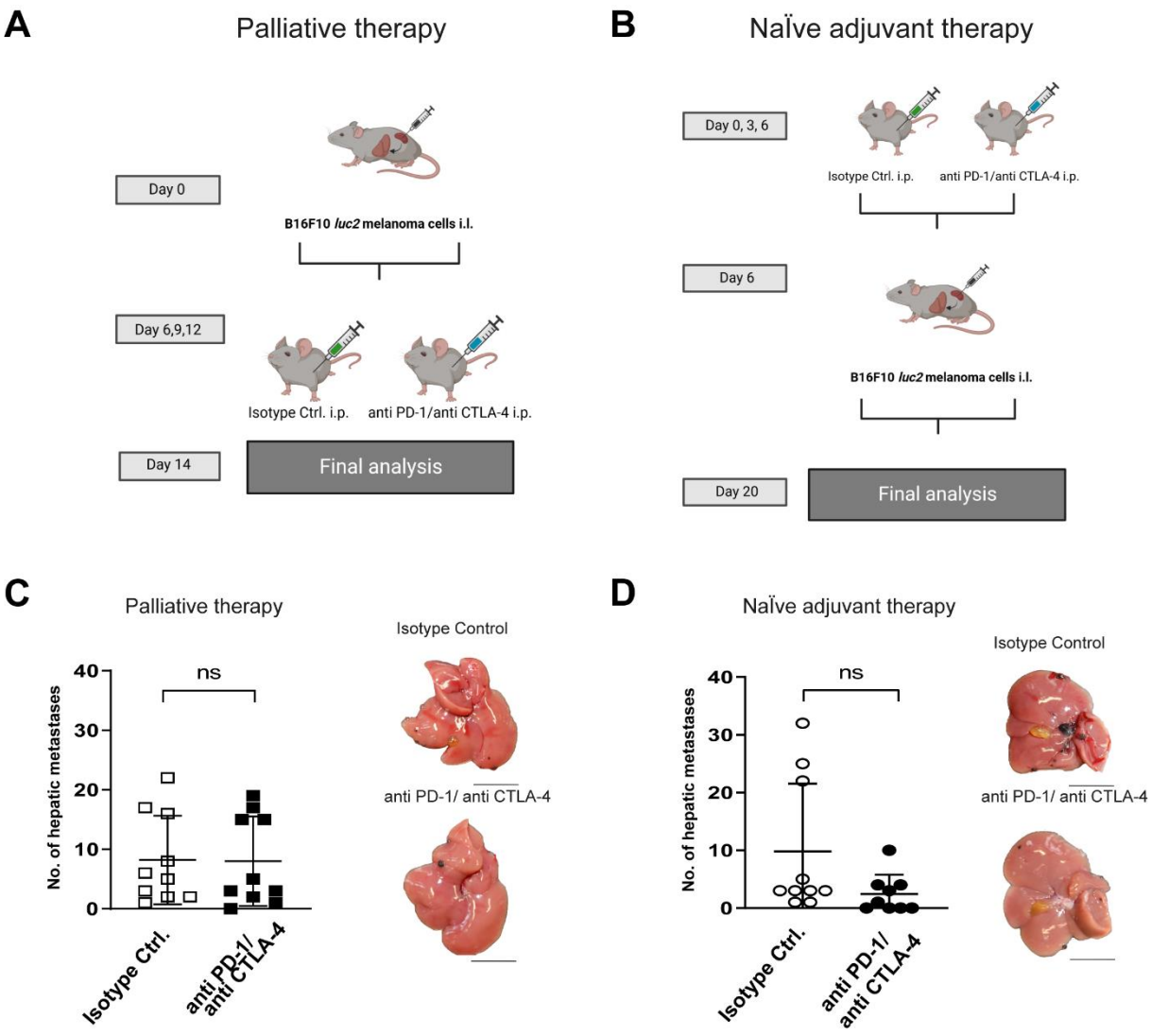

Figure 10: Naïve adjuvant therapy protects from melanoma liver metastases in the B16F10 *luc2* melanoma mouse model.

A: *Time line presenting the application of palliative ICI in the B16F10 luc2 melanoma mouse model. B16F10 luc2 melanoma cells were intrasplenically injected on day 0. After the establishment of liver metastases, mice received the combination therapy αPD-1/αCTLA-4 or the corresponding isotype controls on day 6,9 and 12. Illustration was created using BioRender.com.* ***B:*** *Time line presenting our naïve adjuvant mouse model using the B16F10 luc2 melanoma cell line. Mice were injected with either αPD-1/αCTLA-4 or the corresponding isotype control antibodies on day 0, 3 and 6 followed by the intrasplenic injection of the B16F10 luc2 melanoma cells. Mice were sacrificed on day 20. Illustration was created using BioRender.com.* ***C:*** *The number of macroscopic liver metastases were analysed for mice receiving αPD-1/αCTLA-4 or the corresponding isotype controls in the palliative therapy setting. Number of mice per group: 10; (P=0.7586). Representative images of livers are shown for each group. Scale: 1 cm.* ***D:*** *The number of macroscopic liver metastases were analysed for mice receiving αPD-1/αCTLA-4 or the corresponding isotype controls in the adjuvant therapy setting. Numbers per group: 10; (P=0.0875). Representative images of livers are shown for each group. Scale: 1 cm. P values < 0.05 were assumed as statistically significant when * < 0.05, ** < 0.01, *** < 0.0001; ns= not significant. The B16F10 luc2 melanoma cell line was used.*

The tumor burden of mice with B16F10 *luc2* melanoma was significantly reduced by naïve adjuvant ICI as compared to palliative ICI (Figure 11A). Furthermore, about 40 % of mice in the naïve adjuvant therapy group showed a complete response whereas around 50 % of mice were classified as non-responders in the palliative therapy regimen (Figure 11B).

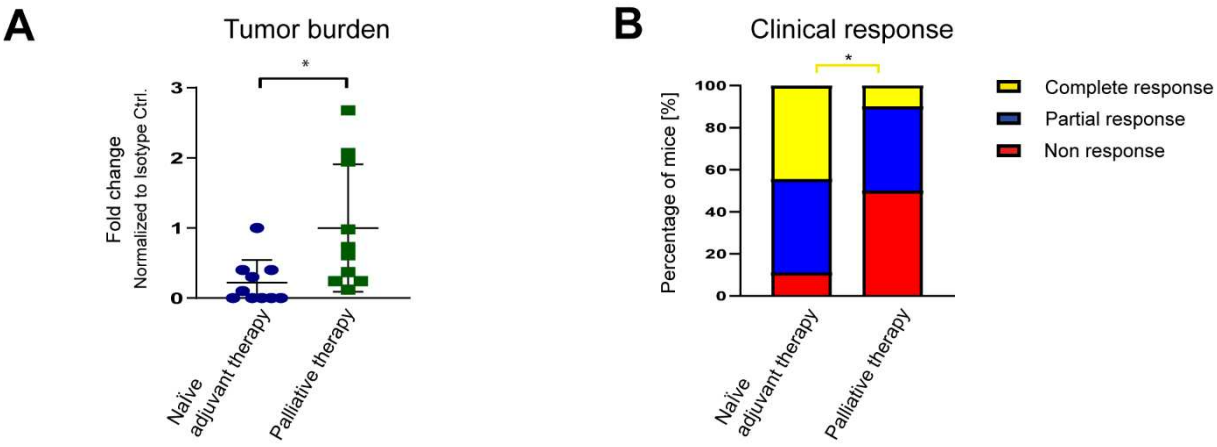

Figure 11: Naïve adjuvant therapy protects best from melanoma liver metastases in the B16F10 *luc2* model.

A: *The tumor burden reduction of the mice treated with αPD-1/αCTLA-4 in the respective therapy regimen (naïve adjuvant and palliative ICI) was calculated in relation to the corresponding isotype controls. Number of animals per group: 10; Number of hepatic metastases of the therapy group was normalized to the mean of the corresponding isotype controls (Fold change); (P=0.0085).* ***B:*** *The clinical response of the mice that received αPD-1/αCTLA-4 was divided into non-responders, partial responders and complete responders based on the corresponding isotype controls (P=0.0131). P values < 0.05 were assumed as statistically significant when * < 0.05, ** < 0.01, *** < 0.0001; ns= not significant. The B16F10 luc2 melanoma cell line was used.*

To understand the mediation between these different therapy regimens, melanoma liver metastases were analyzed by histology (Figure 12A). However, no differences in neither the growth pattern, necrotic areas nor the size of hepatic metastases were observed (Late palliative therapy: P = 0.5435; Early palliative therapy: P = 0.5087; Naïve adjuvant therapy: P = 0.7167) (Figure 12B).

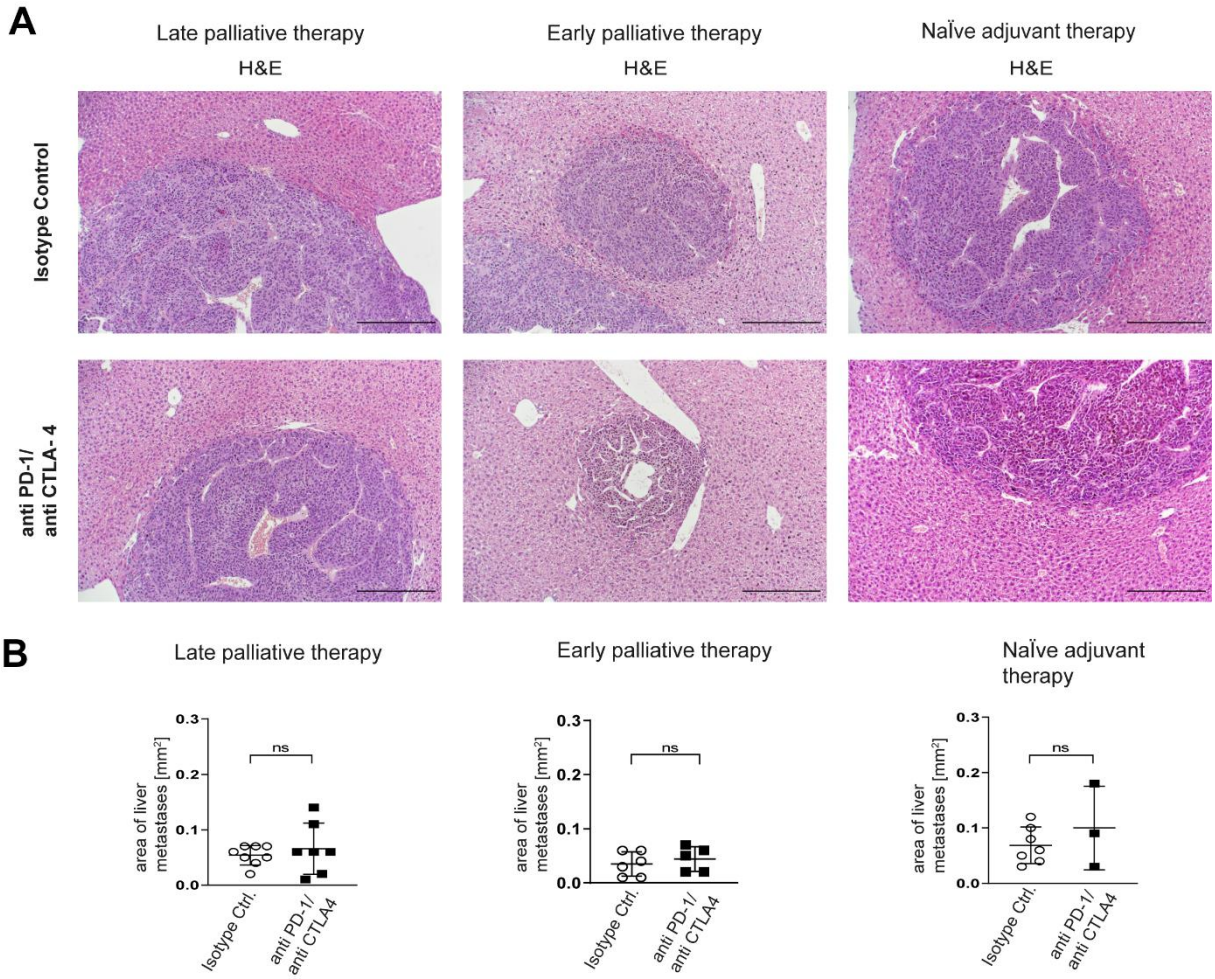

Figure 12: Palliative and naïve adjuvant ICI does not change the morphology and size of liver metastases.

A: *Pictures of livers stained by routine histochemical staining (H&E) of the respective therapy regimen (Late palliative (Day 9), Early palliative (Day 6) and naïve adjuvant ICI). Scale bars: 100 µm.* ***B:*** *Late palliative therapy (Day 9): Size of liver metastases are shown (Isotype: n=8; anti PD-1/anti CTLA-4: n=7; P=0.8435).Early palliative therapy (Day 6): Size of liver metastases are shown (Isotype: n=6; anti PD-1/anti CTLA-4: n=5; P=0.5087). Naïve adjuvant therapy: Area of liver metastases are shown (Isotype: n=7; anti-PD-1/anti-CTLA-4: n=3; P = 0.7167). P values < 0.05 were assumed as statistically significant when * < 0.05, ** < 0.01, *** < 0.0001; ns= not significant.*

To further analyze how the timing of ICI might alter the therapy response of the different therapy regimens (naïve adjuvant and late palliative therapy), the immune cell infiltration in the livers were analyzed by immunofluorescence stainings. Indeed, the numbers of $CD3^+$ $CD8^+$ T cells were significantly increased (P = 0.0296) (Figure 13A), while a significant decrease in the numbers of $CD3^+$ $CD4^+$ T cells was found when comparing naïve adjuvant therapy to late palliative ICI (P = 0.0243) (Figure 13B).

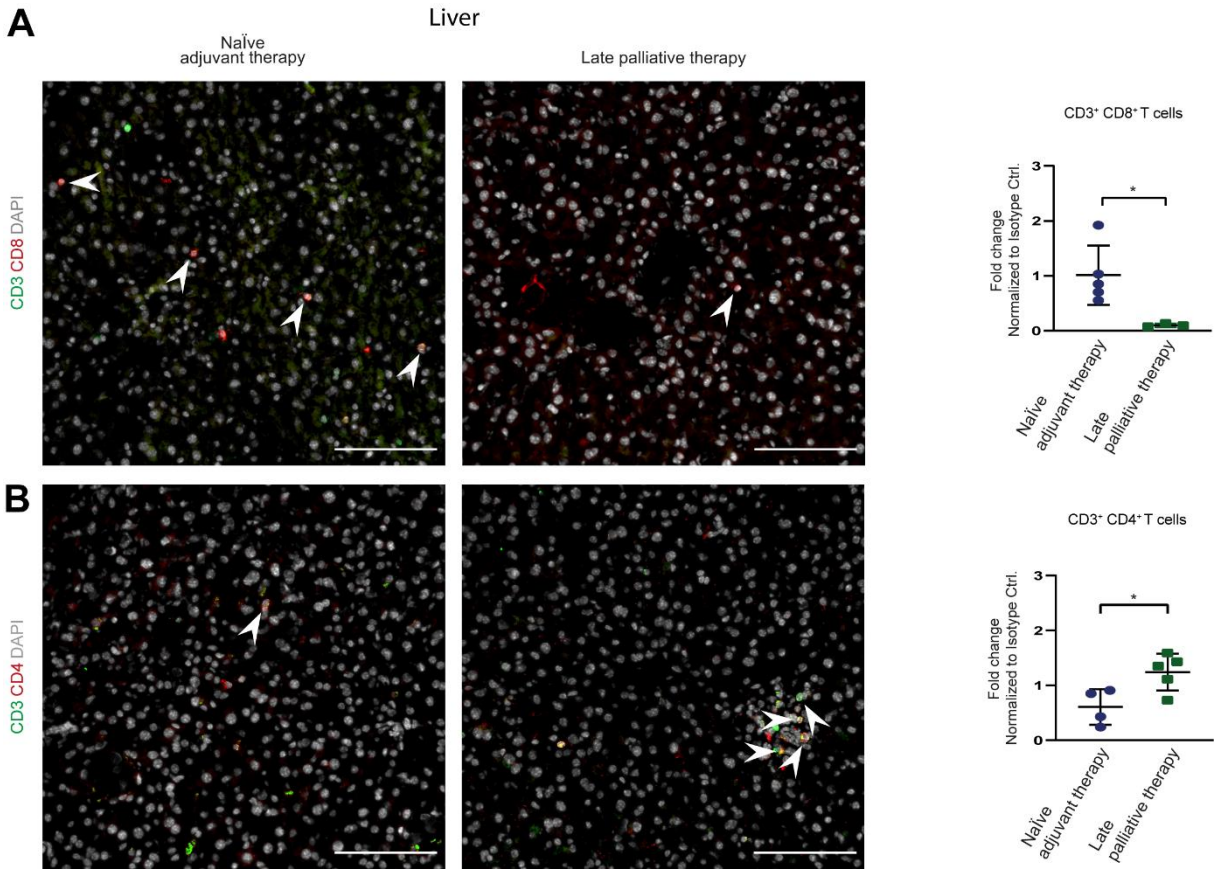

Figure 13: Analysis of T cell subsets in the liver after naïve adjuvant and late palliative therapy.

Different immune cell subsets in the liver of mice treated either with the naïve adjuvant or late palliative ICI were analysed by immunofluorescence staining. ***A:*** *Analysis of T cell subsets. Quantification of CD3⁺ CD8⁺ T cells in livers of mice treated in the naïve adjuvant group (n=5) and in the late palliative therapy group (n=3). Number of immune cells of the therapy groups were normalized to the mean of the corresponding isotype controls (Fold change); (P=0.0296). Representative pictures of both groups are shown. Scale bars: 100 µm.* ***B:*** *Analysis of T cell subsets. Quantification of CD3⁺ CD4⁺ T cells in livers of mice treated in the naïve adjuvant group (n=4) and in the late palliative therapy group (n=5). Number of immune cells of the therapy groups were normalized to the mean of the corresponding isotype controls (Fold change); (P=0.0243). Representative pictures of both groups are shown. Scale bars: 100 µm. P values < 0.05 were assumed as statistically significant when * < 0.05, ** < 0.01, *** < 0.0001; ns= not significant.*

Furthermore, hepatic macrophages were significantly increased in the late palliative as compared to the naïve adjuvant therapy (Figure 14).

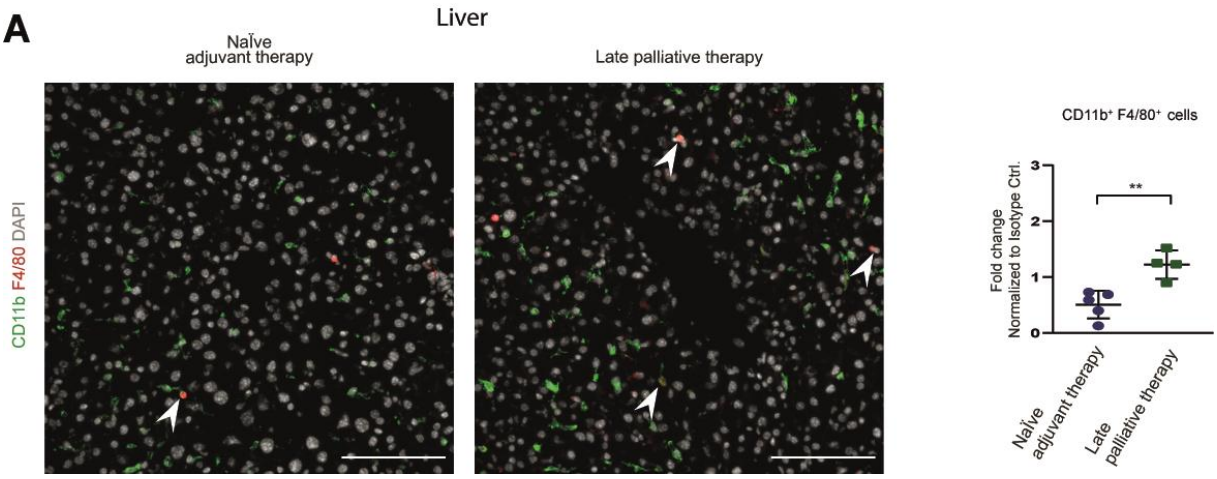

Figure 14: Analysis of macrophages in the liver after naïve adjuvant and late palliative therapy.

Different immune cell subsets in the liver of mice treated either with the naïve adjuvant or late palliative ICI were analysed by immunofluorescence staining. ***A:*** *Analysis of macrophages. Quantification of CD11b⁺ F4/80⁺cells in livers of mice treated in the naïve adjuvant group (n=5) and in the late palliative therapy group (n=4). Number of immune cells of the therapy groups were normalized to the mean of the corresponding isotype controls (Fold change); (P=0.0037). Representative pictures of both groups are shown. Scale bars: 100 µm. P values < 0.05 were assumed as statistically significant when * < 0.05, ** < 0.01, *** < 0.0001; ns= not significant.*

In order to investigate whether immunosuppressive immune cell populations conveyed the decreased therapeutic response in the late palliative therapy setting, the number of CD45$^+$ Ly6C$^+$ as well as CD45$^+$ Ly6G$^+$ in the livers of mice were analyzed. However, the numbers of CD45$^+$ Ly6C$^+$ cells (P = 0.8720) as well as CD45$^+$ Ly6G$^+$ cells (P= 0.5809) were unaltered (Figure 15A and B).

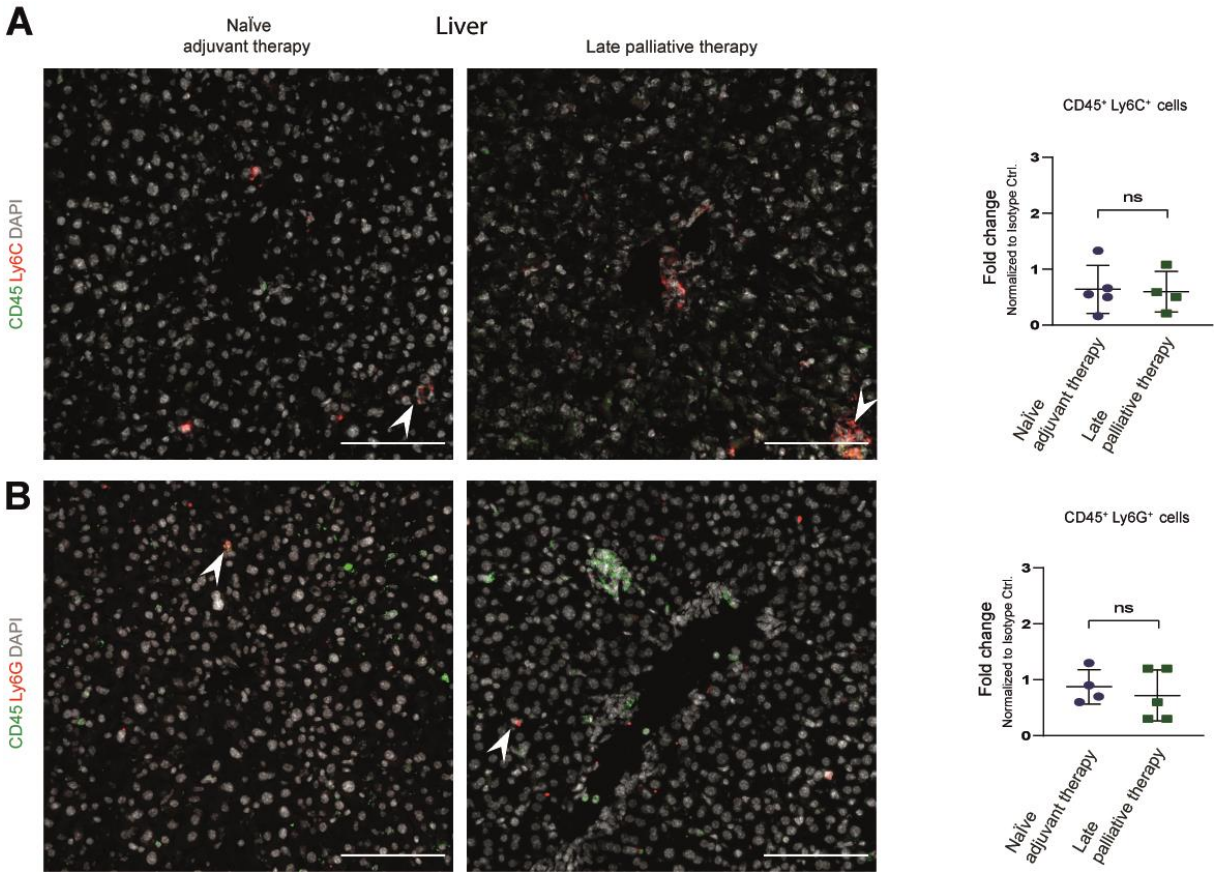

Figure 15: Analysis of myeloid cells in the liver after naïve adjuvant and late palliative therapy.

A: *Analysis of myeloid cell subsets. Quantification of CD45$^+$ Ly6C$^+$ cells in livers of mice. N=5 in the naïve adjuvant group and n=4 in the late palliative ICI group. Number of immune cells of the therapy groups were normalized to the mean of the corresponding isotype controls (Fold change); (P=0.8720).* ***B:*** *Analysis of myeloid cell subsets. Quantification of CD45$^+$ Ly6G$^+$ cells in livers of mice. N=4 in the naïve adjuvant group and n=5 in the late palliative ICI group. Number of immune cells of the therapy groups were normalized to the mean of the corresponding isotype controls (Fold change); (P=0.5809). Representative pictures of both groups are shown. Scale bars: 100 µm. P values < 0.05 were assumed as statistically significant when * < 0.05, ** < 0.01, *** < 0.0001; ns= not significant.*

4.3 Adjuvant and neoadjuvant ICI of liver metastases

Neoadjuvant ICI is a novel therapeutic concept applying ICI before surgical excision of the primary melanoma or lymph node metastases are still *in situ* (Figure 16A). Figure 16B illustrates our two mouse models including the neoadjuvant and adjuvant therapy model. In the neoadjuvant setting, the mice received the WT31 melanoma cells cutaneously on day 0 to mimic the primary melanoma, followed by the i.p. injections of the αPD-1/αCTLA-4 therapy or the corresponding isotype controls on day 12, 15 and 18. On day 18, the primary tumor was surgically resected, which was followed by the intrasplenic injection of the WT31 melanoma cell line. Mice were sacrificed after 21 days on day 39. This neoadjuvant therapy approach was compared to an adjuvant therapy approach with the resection of the primary tumor on day 18, i.p. injections of the αPD-1/αCTLA-4 therapy or the corresponding isotype controls on day 19, 22 and 25 and the intrasplenic injection of the WT31 melanoma cell line on day 25. Both neoadjuvant (P = 0.0003) and adjuvant ICI (P = 0.0009) led to a significant reduction of hepatic metastases as compared to their corresponding isotype controls (Figure 16C and D).

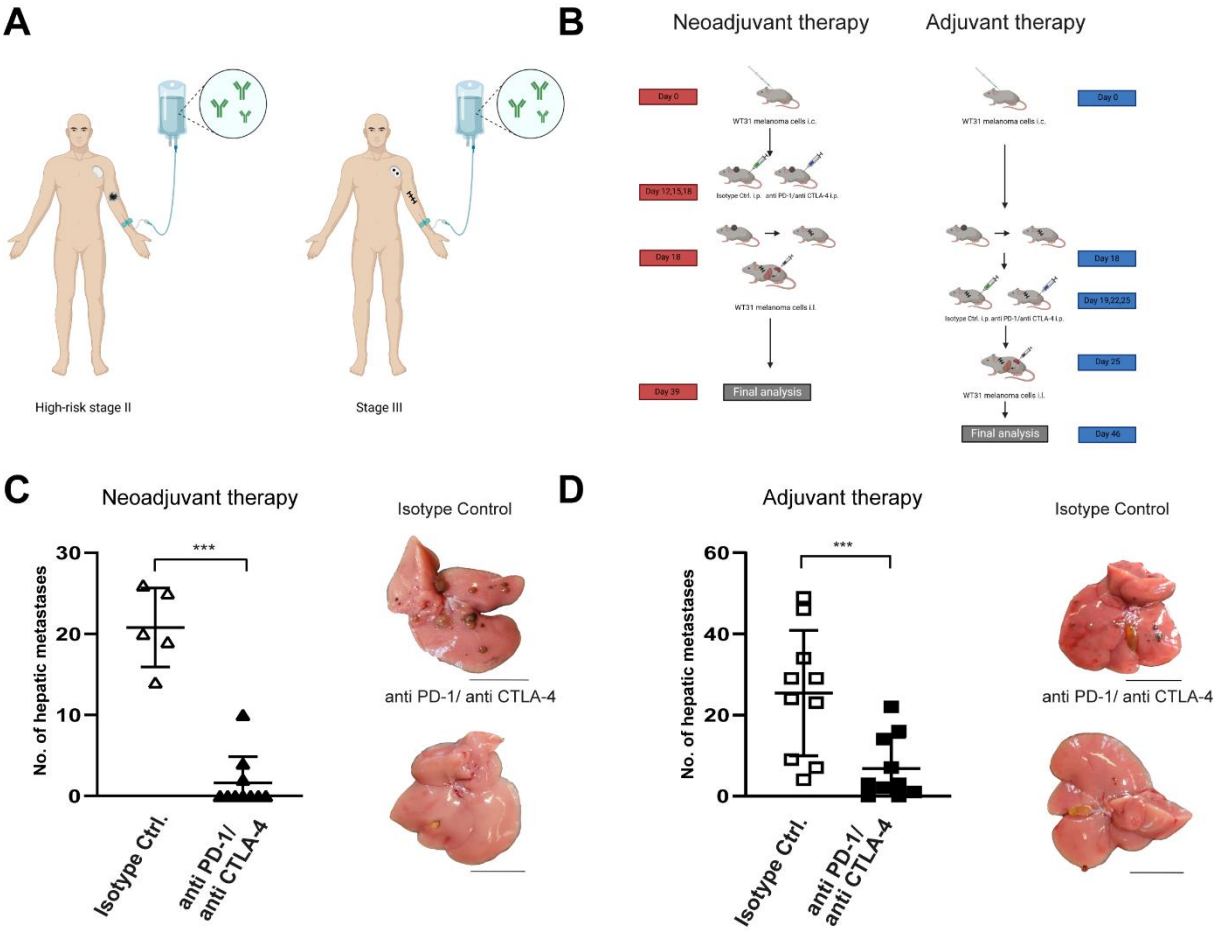

Figure 16: Adjuvant and neoadjuvant ICI protects from liver metastases.

A: *Illustration of a melanoma patient in stage II (High risk melanoma) or Stage III with a primary melanoma and lymph node involvement receiving ICI prior to the excision of the primary melanoma. Illustration was created using BioRender.com.* ***B: Neoadjuvant therapy:*** *On day -1*

blood samples were taken for flow cytometry. On day 0 WT31 melanoma cells were injected cutaneously. A primary dermal tumor developed. In the presence of the primary melanoma, αPD-1/αCTLA-4 or the corresponding isotype controls were injected i.p. on day 12, 15 and 18. In addition, on day 18 the primary dermal melanoma were resected and the WT31 melanoma cells were injected intrasplenically. Blood samples were taken on day -1, 16, 32 and 39. Mice were sacrificed on day 39. ***Adjuvant therapy:*** *On day -1 blood samples were taken for flow cytometry. On day 0, WT31 melanoma cells were injected cutaneously. A primary dermal tumor developed and was resected on day 18. The αPD-1/αCTLA-4 combination therapy or the corresponding isotype controls were injected i.p. on day 19, 22 and 25. On day 25, WT31 melanoma cells were injected intrasplenically. Blood samples were taken on day -1, 16, 32 and 39. Mice were sacrificed on day 46. Illustration was created using BioRender.com* ***C:*** *The number of macroscopic liver metastases were analysed for mice receiving αPD-1/αCTLA-4 (n=10) or the corresponding isotype controls (n=5) in the neoadjuvant therapy regimen (P=0.0003). Representative images of livers of each group are shown. Scale: 1 cm.* ***D:*** *The number of macroscopic liver metastases were analysed for mice receiving αPD-1/αCTLA-4 (n=10) or the corresponding isotype controls (n=10) in the adjuvant therapy regimen (P=0.0009). Representative images of livers of each group are shown. Scale: 1 cm. P values < 0.05 were assumed as statistically significant when * < 0.05, ** < 0.01, *** < 0.0001; ns= not significant. The WT31 melanoma cell line was used.*

Neoadjuvant ICI led to a significant reduction of the tumor burden as compared to the adjuvant therapy (P = 0.0494) (Figure 17B). Moreover, in the neoadjuvant setting about 72,5 % of the mice showed a complete response in comparison to 20 % in the adjuvant therapy regimen (P = 0.0270) (Figure 17A).

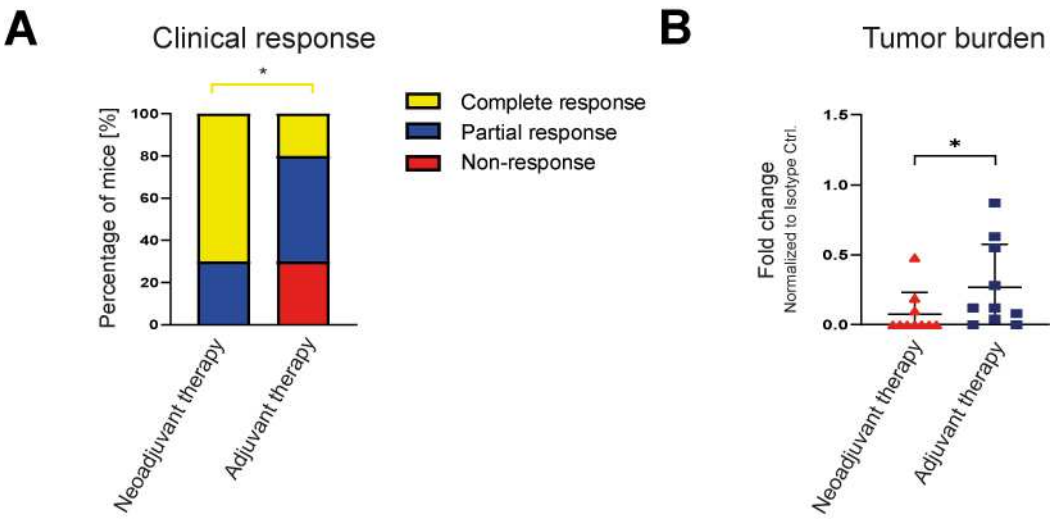

Figure 17: Neoadjuvant ICI most efficiently protects from liver metastases.

A: *The clinical response of the mice that received αPD-1/αCTLA-4 was divided into non-responders, partial responders and complete responders based on the corresponding isotype controls (P=0.0270).* ***B:*** *The tumor burden reduction of the mice treated with αPD-1/αCTLA-4 in the respective therapy regimen (neoadjuvant and adjuvant) was calculated in relation to the corresponding isotype controls. Number of hepatic metastases of the therapy group was normalized to the mean of the corresponding isotype controls (Fold change); (P=0.0494). P values*

*< 0.05 were assumed as statistically significant when * < 0.05, ** < 0.01, *** < 0.0001; ns= not significant.*

The morphology and the tumor growth of the primary melanomas were analyzed in both groups. No overt morphological differences were observed in H&E of the primary melanomas in both groups (Figure 18A). Furthermore, tumor growth seemed to be similar when both therapy groups were compared to their corresponding isotype controls (Neoadjuvant therapy: P = 0.0825; Adjuvant therapy P = 0.3070) (Figure 18B and C).

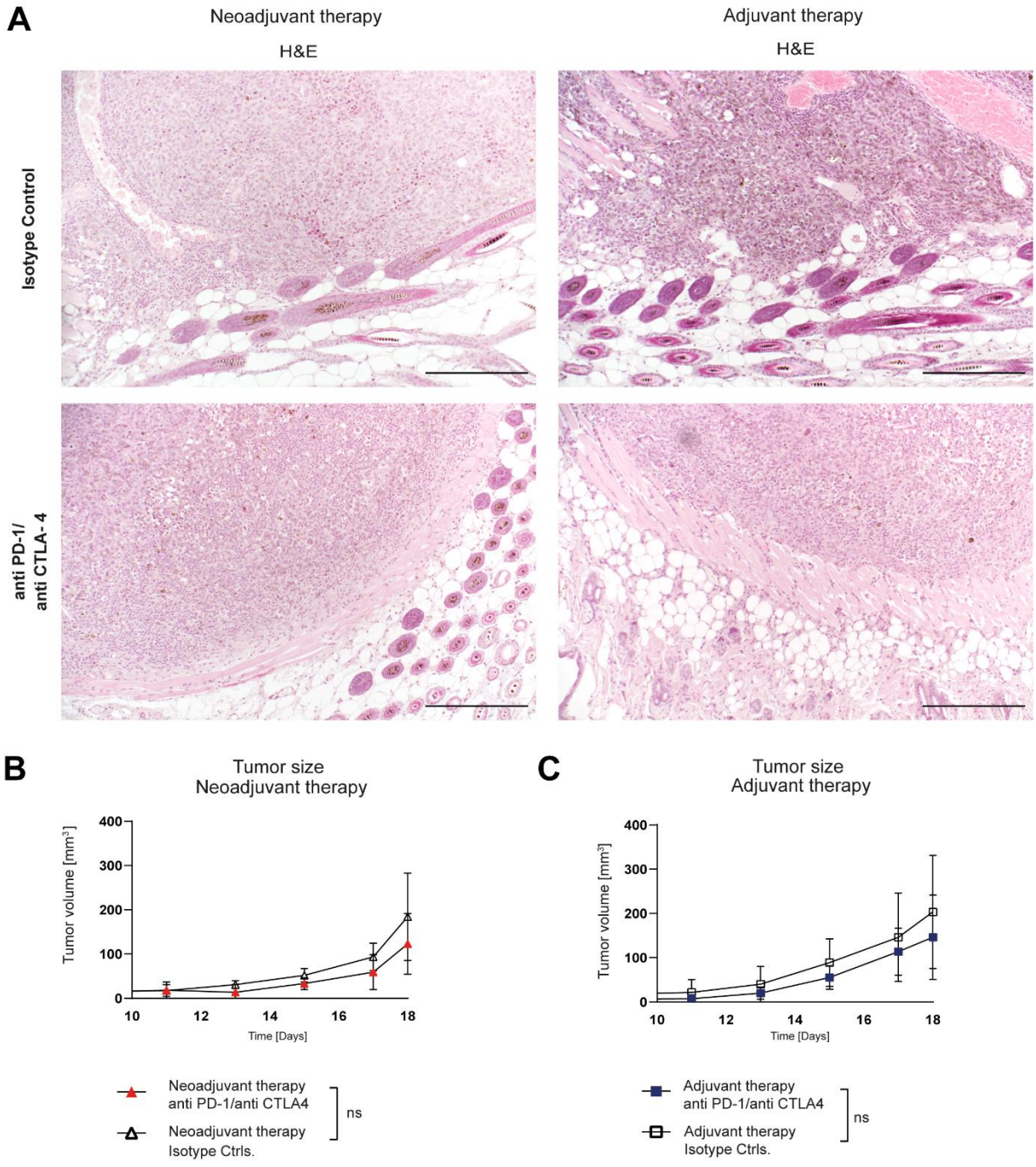

Figure 18: Neoadjuvant and adjuvant therapy have minor influences on the tumor size.

A: *Pictures of the primary cutaenous tumors stained by routine histochemical staining (H&E) of the respective therapy regimen (Neoadjuvant and adjuvant ICI) and the corresponding isotype*

controls are shown. Scale bars: 100 µm. ***B:*** *Comparison of the size of the primary dermal tumor from Isotype control and anti PD-1/anti CTLA-4 groups of the neoadjuvant therapy are shown over time [days] (P=0.0825).* ***C:*** *Comparison of the size of the primary dermal tumor from Isotype control and anti PD-1/anti CTLA-4 groups of the adjuvant therapy are shown over time [days] (P= 0.3070). P values < 0.05 were assumed as statistically significant when * < 0.05, ** < 0.01, *** < 0.0001; ns= not significant.*

Furthermore, the distribution of T cells was analyzed at the primary site by immunofluorescence staining. Within the primary cutaneous tumor, a significant increase in the number of $CD3^+$ $CD4^+$ T cells and a trend towards an increased number of $CD3^+$ $CD8^+$ T cells were observed by comparing the neoadjuvant to the adjuvant therapy regimen (Figure 19A and B). In line with this finding, we observed significantly increased numbers of either $CD3^+$ $CD4^+$ and $CD3^+$ $CD8^+$ T cells in the surrounding tissue of the adjuvant therapy regimen when compared to the neoadjuvant therapy regimen (Figure 19C and D).

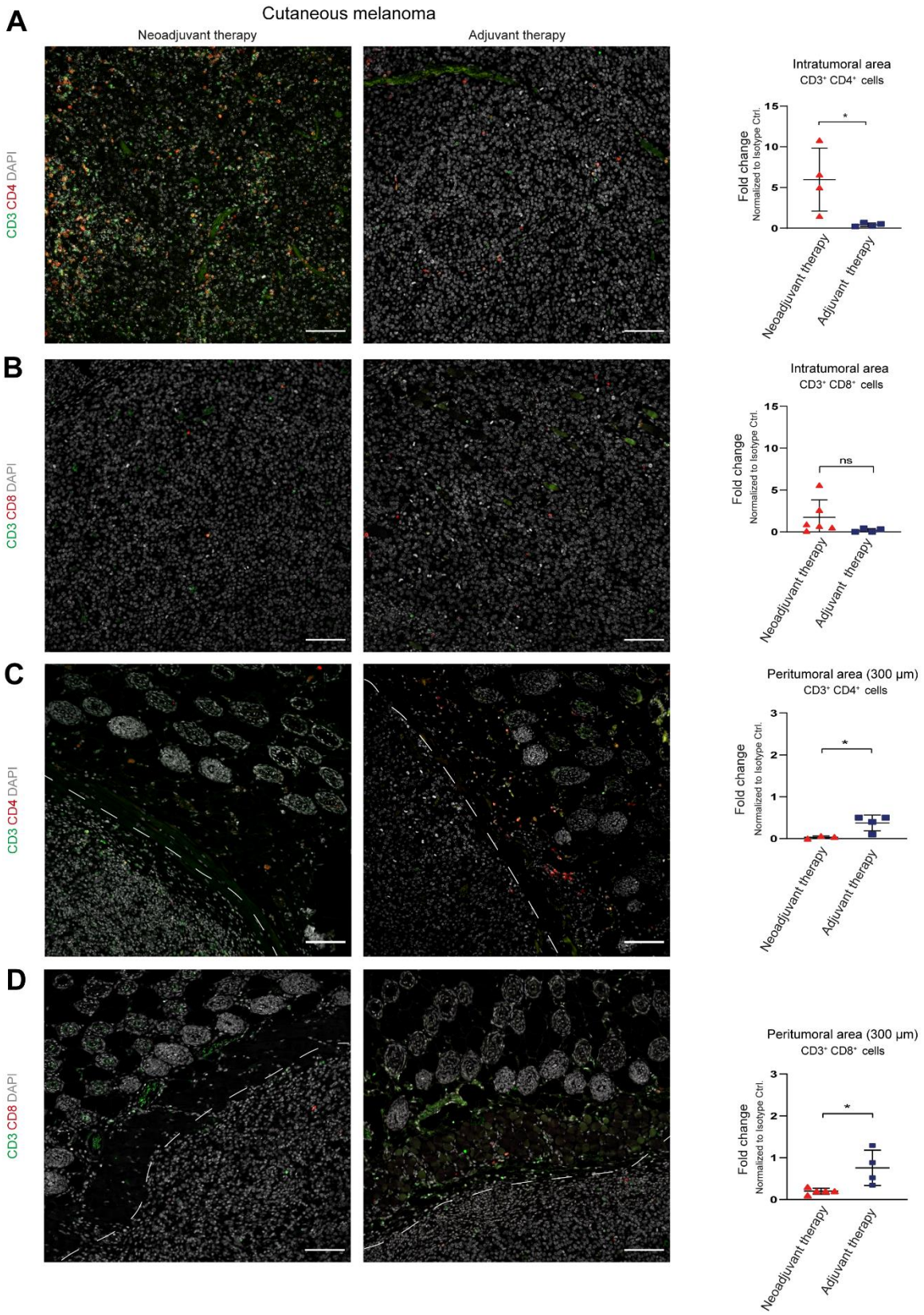
A
Cutaneous melanoma
Neoadjuvant therapy
Adjuvant therapy
CD3 CD4 DAPI
Intratumoral area
CD3+ CD4+ cells
Fold change
Normalized to Isotype Ctrl.
15
10
5
0
*
Neoadjuvant therapy
Adjuvant therapy
B
CD3 CD8 DAPI
Intratumoral area
CD3+ CD8+ cells
Fold change
Normalized to Isotype Ctrl.
15
10
5
0
ns
Neoadjuvant therapy
Adjuvant therapy
C
CD3 CD4 DAPI
Peritumoral area (300 µm)
CD3+ CD4+ cells
Fold change
Normalized to Isotype Ctrl.
3
2
1
0
*
Neoadjuvant therapy
Adjuvant therapy
D
CD3 CD8 DAPI
Peritumoral area (300 µm)
CD3+ CD8+ cells
Fold change
Normalized to Isotype Ctrl.
3
2
1
0
*
Neoadjuvant therapy
Adjuvant therapy

Figure 19: Neoadjuvant ICI increases the infiltration of T cell subsets into the primary tumor.

Different immune cell subsets in the primary dermal and the surrounding tissue of mice treated either with the neoadjuvant or adjuvant ICI were analysed by immunofluorescence stainings. ***A:*** *Analysis of T cell subsets. Quantification of CD3⁺ CD4⁺ T cells in the primary tumor of mice treated in the neoadjuvant ICI group (n=4) and in the adjuvant ICI group (n=4). Number of immune cells of the therapy groups was normalized to the mean of the corresponding isotype controls (Fold change); (P=0.0285). Representative pictures of both groups are shown. Scale bars: 100 µm.* ***B:*** *Analysis of T cell subsets. Quantification of CD3⁺ CD8⁺ T cells in in the primary tumor of mice treated in the neoadjuvant ICI group (n=6) and adjuvant ICI group (n=4). Number of immune cells of the therapy groups was normalized to the mean of the corresponding isotype controls (Fold change); (P=0.1816). Representative pictures of both groups are shown. Scale bars: 100 µm.* ***C:*** *Analysis of T cell subsets in the surrounding tissue of the primary tumor (Distance: 300 µm). Quantification of CD3⁺ CD4⁺cells in the surrounding tissue of the primary tumor of mice treated in the neoadjuvant ICI group (n=3) and in the adjuvant ICI group (n=4). Number of immune cells of the therapy groups was normalized to the mean of the corresponding isotype controls (Fold change); (P=0.0293). Representative pictures of both groups are shown. Scale bars: 100 µm.* ***D:*** *Analysis of T cell subsets in the surrounding tissue of the primary tumor (Distance: 300 µm). Quantification of CD3⁺ CD8⁺cells in the surrounding tissue of the primary tumor of mice treated in the neoadjuvant ICI group (n=5) and in the adjuvant ICI group (n=4). Number of immune cells of the therapy groups was normalized to the mean of the corresponding isotype controls (Fold change); (P=0.0209). Representative pictures of both groups are shown. Scale bars: 100 µm. P values < 0.05 were assumed as statistically significant when * < 0.05, ** < 0.01, *** < 0.0001; ns= not significant.*

Since the immune microenvironment is activated at the primary site, circulating T cells were analysed by flow cytometry of the peripheral blood. Indeed, a significant increase of $CD3^+$ $CD4^+$ and $CD3^+$ $CD8^+$ T cells was observed on day 32 in the peripheral blood of mice treated in the neoadjuvant therapy regimen (Figure 20A and B). In addition, common cytokines were examined through multiplex analysis in the plasma of mice that received either the neoadjuvant or the adjuvant ICI (Figure 20C).

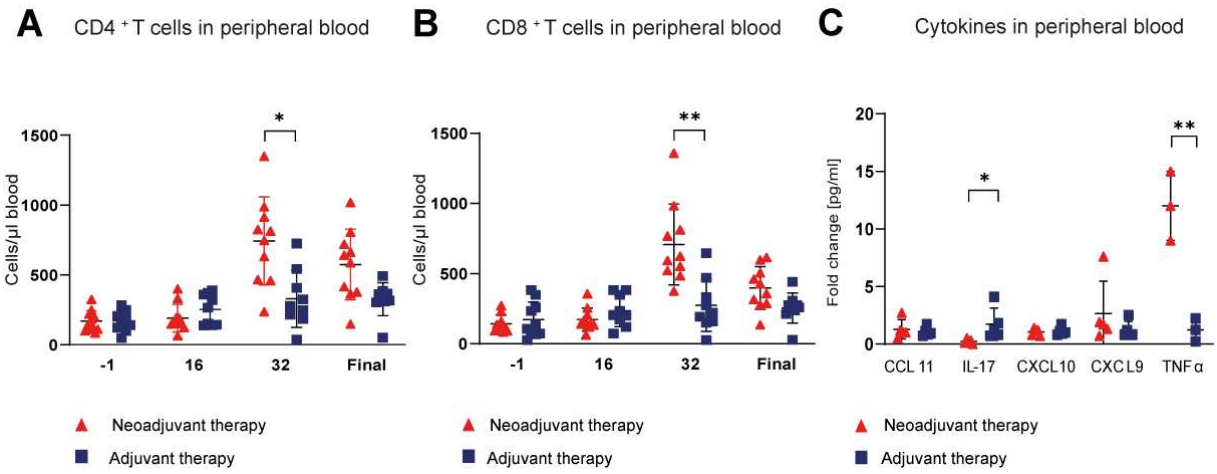

Figure 20: T cells are increased in the peripheral blood after neoadjuvant therapy.

A: *FACS analysis of $CD3^+$ $CD4^+$ T cells in the peripheral blood. Blood samples were taken at indicated time points.* ***B:*** *FACS analysis of $CD3^+$ $CD8^+$ T cells in the peripheral blood. Blood samples were taken and analyzed on day -1, day 16, day 32 and final day by flow cytometry. Day 32: $CD3^+$ $CD4^+$: P = 0.0141; $CD3^+$ $CD8^+$: P = 0.0051. Statistical analysis was performed by using a mixed effect model analysis. P values < 0.05 were assumed as statistically significant when * < 0.05, ** < 0.01, *** < 0.0001; ns= not significant.* ***C:*** *Multiplex analysis of plasma from mice treated in the neoadjuvant (n=5) and adjuvant therapy (n=5) regimen analyzed by Luminex. (P= 0.0449 (IL-17); P=0.0338 (TNFα)). P values < 0.05 were assumed as statistically significant when * < 0.05, ** < 0.01, *** < 0.0001; ns= not significant.*

To investigate, how the neoadjuvant therapy protected from hepatic metastasis, liver metastases were analyzed in detail. To investigate how neoadjuvant ICI mediates its enhanced protection against melanoma liver metastasis, H&E stainings were performed. No overt morphological differences were observed (Figure 21A). The analyses of the size of hepatic metastases demonstrated no differences when the therapy group was compared to their corresponding isotype controls (Neoadjuvant therapy: P = 0.9812); (Adjuvant therapy: P = 0.8092) (Figure 21B).

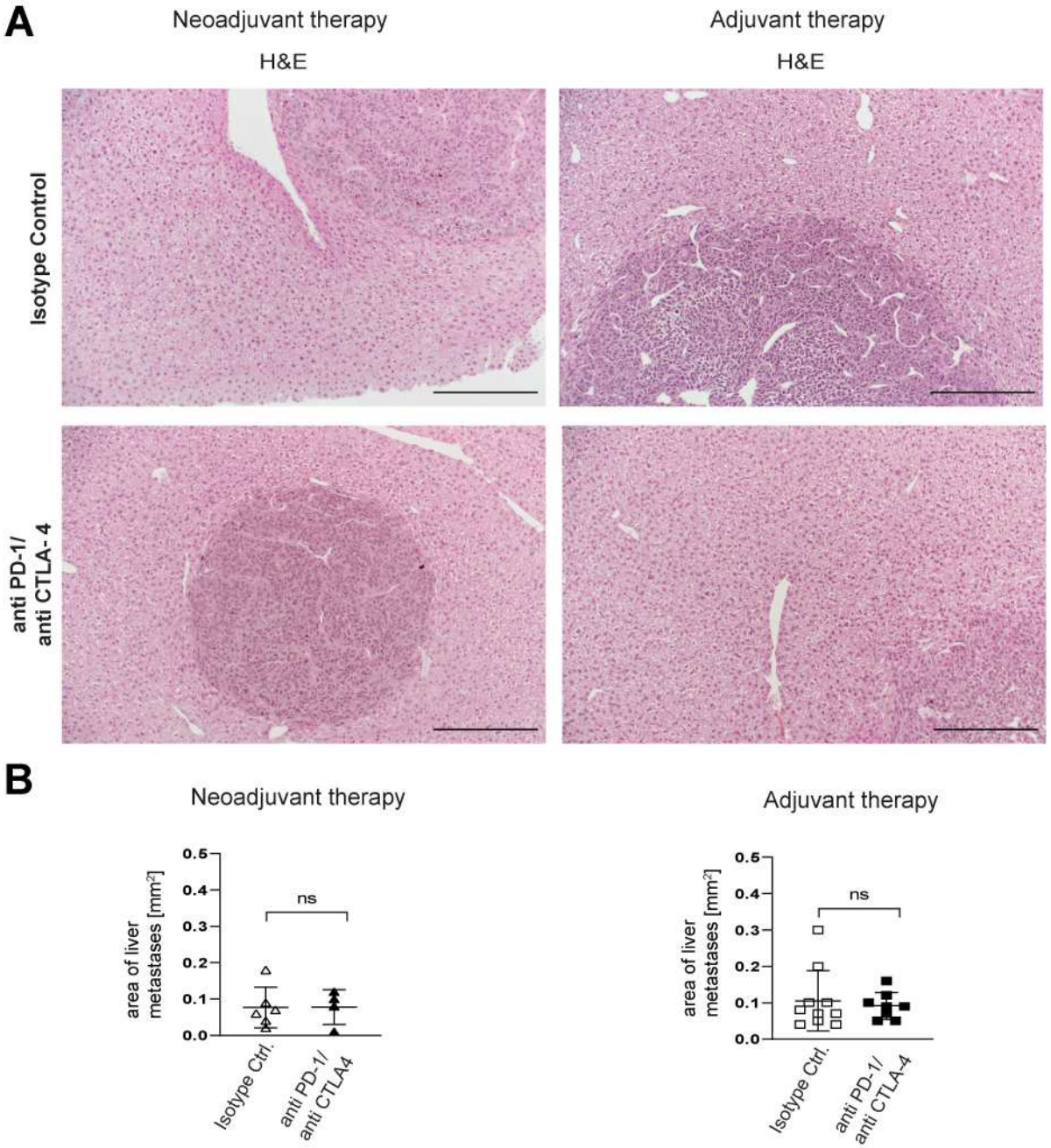

Figure 21: Neoadjuvant and adjuvant therapy does not change the morphology and size of liver metastases.

A: *Pictures of livers stained by routine histochemical staining (H&E) of the respective therapy regimen (Neoadjuvant and adjuvant ICI) are shown. Scale bars: 100 µm.* ***B: Neoadjuvant ICI:*** *Size of liver metastases are shown (Isotype: n=6 anti PD-1/anti CTLA-4: n=4; P=0.9812).* ***Adjuvant ICI:*** *Size of liver metastases are shown (Isotype: n=10; anti-PD-1/anti-CTLA-4: n=8; P=0.8092). P values < 0.05 were assumed as statistically significant when * < 0.05, ** < 0.01, *** < 0.0001; ns= not significant.*

The hepatic immune microenvironment was analyzed by immunofluorescence staining. A trend towards increased numbers of $CD3^+$ $CD4^+$ T cells was observed in the neoadjuvant compared to the adjuvant therapy (P = 0.0935). Furthermore, $CD3^+$ $CD8^+$ positive T cells significantly increased in the livers of mice treated with the neoadjuvant therapy regimen

(P = 0.0002) (Figure 22A and B). The numbers of macrophages (P = 0.1030) (Figure 23A), moncocytes (P = 0.8720) (Figure 23B) and neutrophils (P = 0.5809) (Figure 23C) were unaltered.

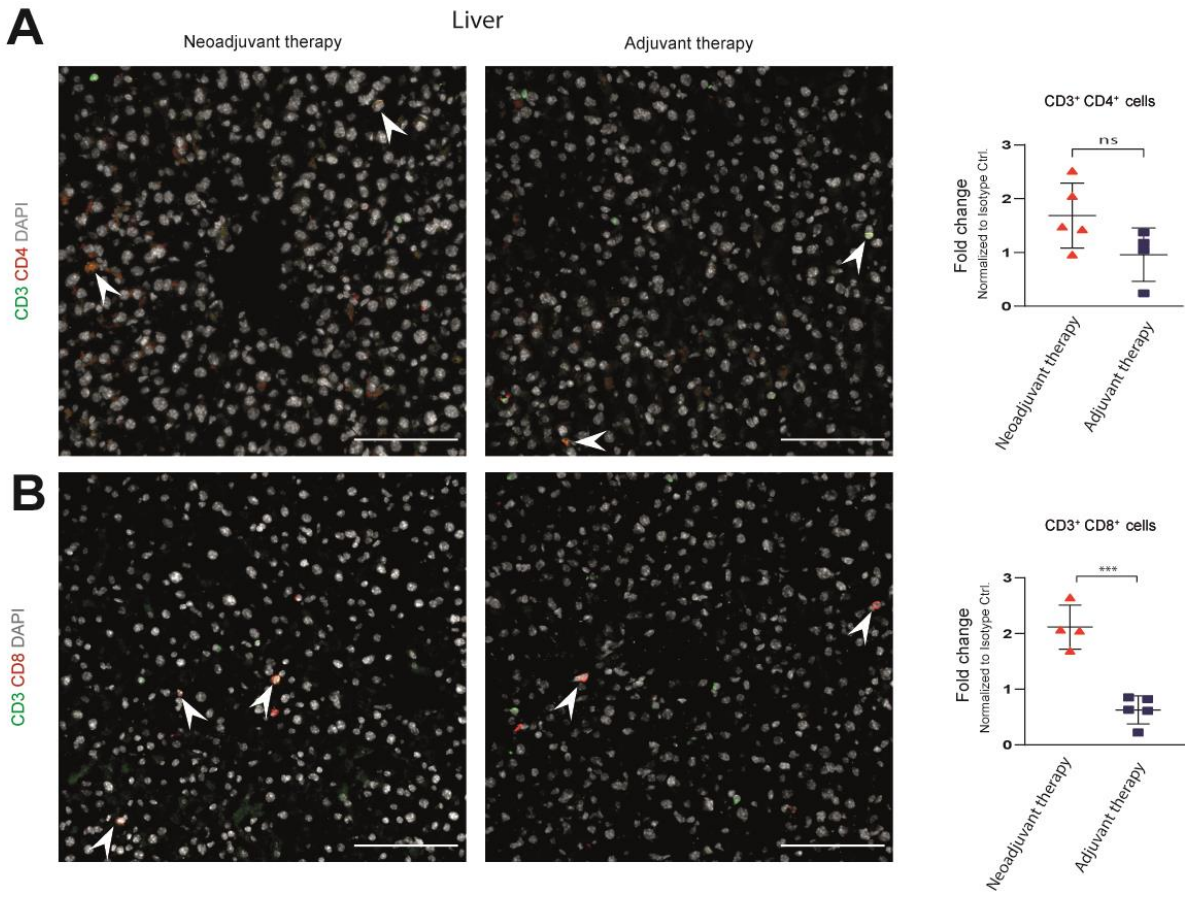

Figure 22: Analysis of T cell subsets in the liver after neoadjuvant and adjuvant ICI.

Different immune cell subsets in the liver of mice treated either with the neoadjuvant or adjuvant ICI were analysed by immunofluorescence staining. Analysis of T cell subsets. ***A:*** *Quantification of $CD3^+$ $CD4^+$ T cells in livers of mice treated in the neoadjuvant ICI group (n=5) and in the adjuvant ICI group (n=4). Number of immune cells of the therapy groups was normalized to the mean of the corresponding isotype controls (Fold change); (P=0.0935). Representative pictures of both groups are shown. Scale bars: 100 µm.* ***B:*** *Quantification of $CD3^+$ $CD8^+$ T cells in livers of mice treated in the neoadjuvant ICI group (n=4) and adjuvant ICI group (n=3). Number of immune cells of the therapy groups was normalized to the mean of the corresponding isotype controls (Fold change); (P=0.0002). Representative pictures of both groups are shown. Scale bars: 100 µm. P values < 0.05 were assumed as statistically significant when * < 0.05, ** < 0.01, *** < 0.0001; ns= not significant.*

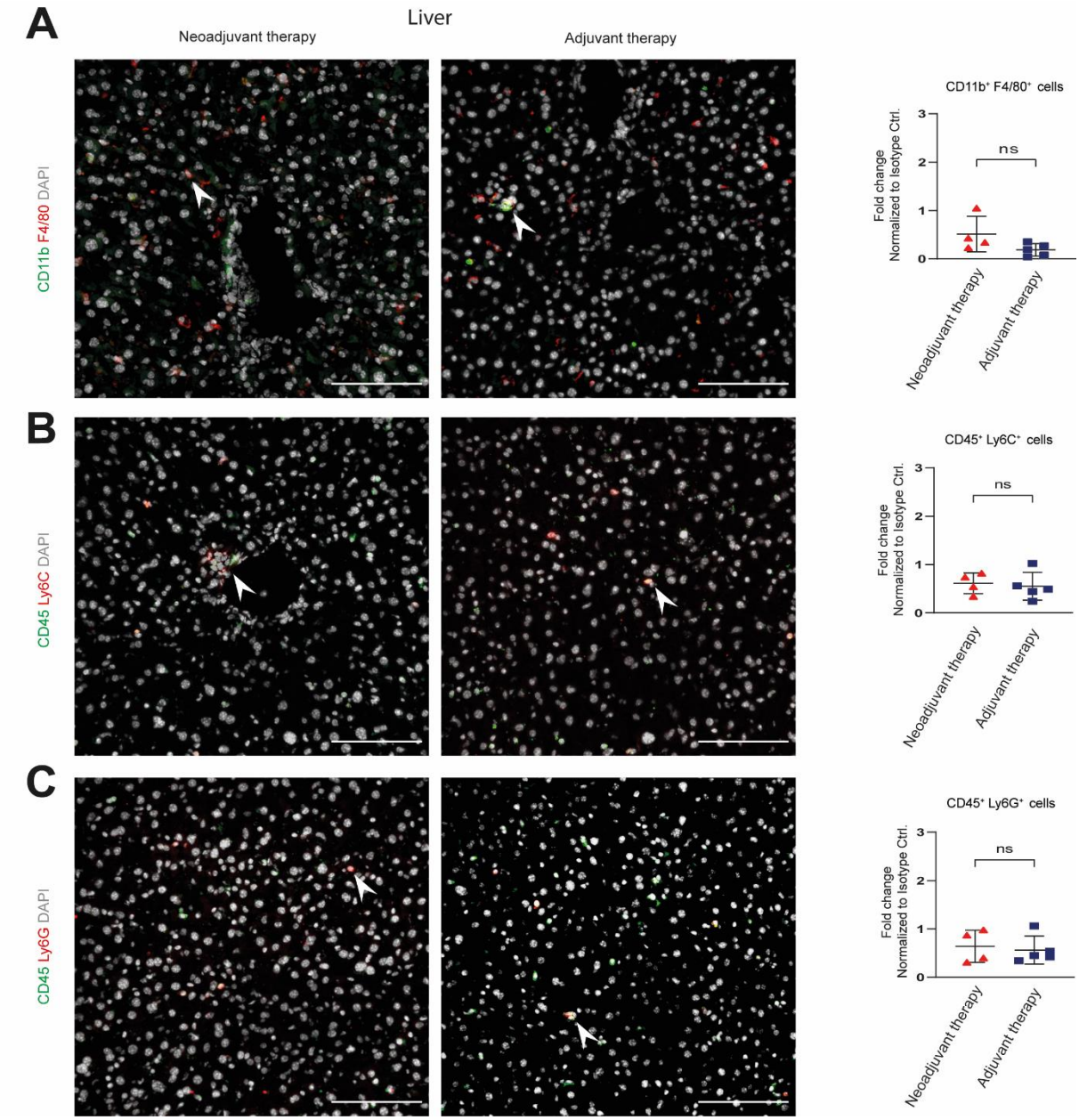

Figure 23: Analysis of macrophages, neutrophils and monocytes in the liver after neoadjuvant and adjuvant ICI.

Different immune cell subsets in the liver of mice treated either with the neoadjuvant or adjuvant ICI were analysed by immunofluorescence stainings. ***A:*** *Analysis of macrophages and myeloid cells. Quantification of CD11b⁺ F4/80⁺ cells in livers of mice treated in the neoadjuvant ICI group (n=4) and in the adjuvant ICI group (n=5). Number of immune cells of the therapy group was normalized to the mean of the corresponding isotype controls (Fold change); (P=0.1030). Representative pictures of both groups are shown. Scale bars: 100 µm.* ***B:*** *Analysis of macrophages and myeloid cells. Quantification of CD45⁺ Ly6C⁺ cells in livers of mice. N=4 in the neoadjuvant ICI group and n=5 in the adjuvant ICI group. Number of immune cells of the therapy group was normalized to the mean of the corresponding isotype controls (Fold change); (P=0.8720). Representative pictures of both groups are shown. Scale bars: 100 µm.* ***C:*** *Quantification of CD45⁺ Ly6G⁺ cells in livers of mice. N=4 in the neoadjuvant ICI group and n=5 in the adjuvant ICI group. Number of immune cells of the therapy group was normalized to*

*the mean of the corresponding isotype controls; (P=0.5809). Representative pictures of both groups are shown. Scale bars: 100 µm. P values < 0.05 were assumed as statistically significant when * < 0.05, ** < 0.01, *** < 0.0001; ns= not significant.*

In addition, important chemo- and cytokines were analyzed in livers of the naïve adjuvant and palliative therapy as well as in the neoadjuvant and adjuvant therapy regimens to understand what mediates the changes in the hepatic immune microenvironment. Levels of IFNγ were increased as assessed by multiplex analysis, while IL-4 significantly decreased in livers of mice treated with the naïve adjuvant therapy compared to livers of mice treated with the late palliative therapy (Figure 24A). IL-4 and IL-15 revealed significantly increased levels in livers of mice treated with the adjuvant therapy as compared to the neoadjuvant therapy setting (Figure 24B).

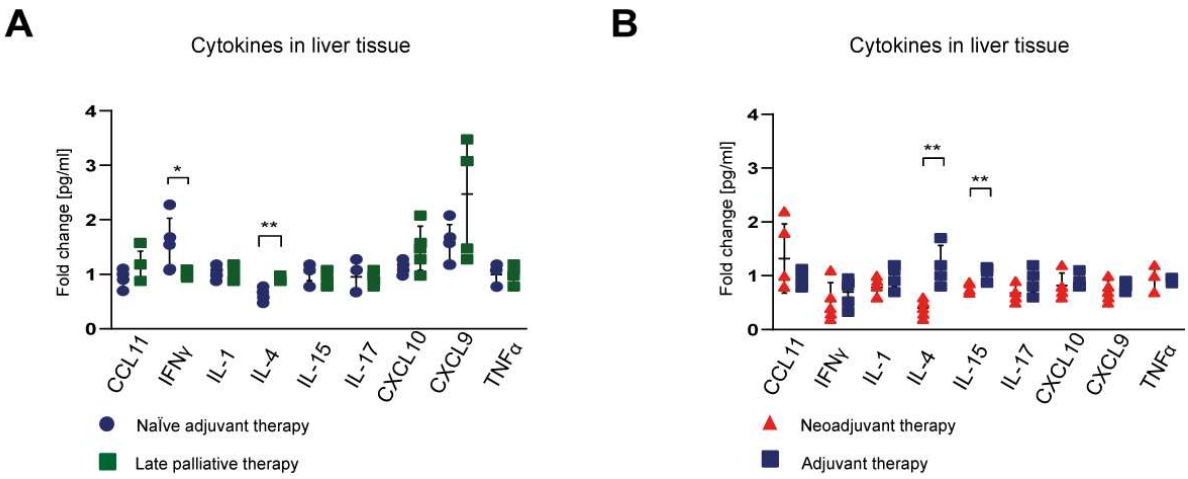

Figure 24: Cytokines specific for the Th1 to Th2 switch are changed in the different ICI therapy regimens.

A: *Multiplex analysis of cytokine and chemokine levels from livers of mice treated in the adjuvant (n=5) and late palliative ICI (n=5) regimen (P= (IFNγ=0.0407); P=0.0011 (IL-4)). Mutiplex assay was analyzed by Luminex. Amounts of cytokines/chemokines of the therapy group was normalized to the mean of the corresponding isotype control groups (Fold change).* ***B:*** *Multiplex analysis of cytokine and chemokine levels from livers of mice treated in the neoadjuvant (n=5) and adjuvant ICI (n=5) regimen (P=0.0044 (IL-4); P=0.0051 (IL-15)). Mutiplex assay was analyzed by Luminex. Amounts of cytokines/chemokines of the therapy group was normalized to the mean of the corresponding isotype control groups (Fold change); P values < 0.05 were assumed as statistically significant when * < 0.05, ** < 0.01, *** < 0.0001; ns= not significant.*

Due to the fact that IL-4 was significantly altered in all four therapy regimens and is a counterpart to IFNγ, both cytokines were analyzed in the livers of the different therapy regimens by immunofluorescence stainings or fluorescence *in situ* hybridization (*FISH*). Furthermore, we wanted to investigate which cell types produce the two cytokines IL-4 and IFNγ. IFNγ was significantly increased in $CD3^+$ T cells in livers of mice treated in the naïve adjuvant (P = 0.0381) and the neoadjuvant therapy setting (P = 0.0159) (Figure 25A and B).

However, no differences in the expression of IL-4 in $CD3^+$ T cells were observed between the different therapy regimens (Figure 25C (P = 0.5952) and Figure 25D (P = 0.4284)).

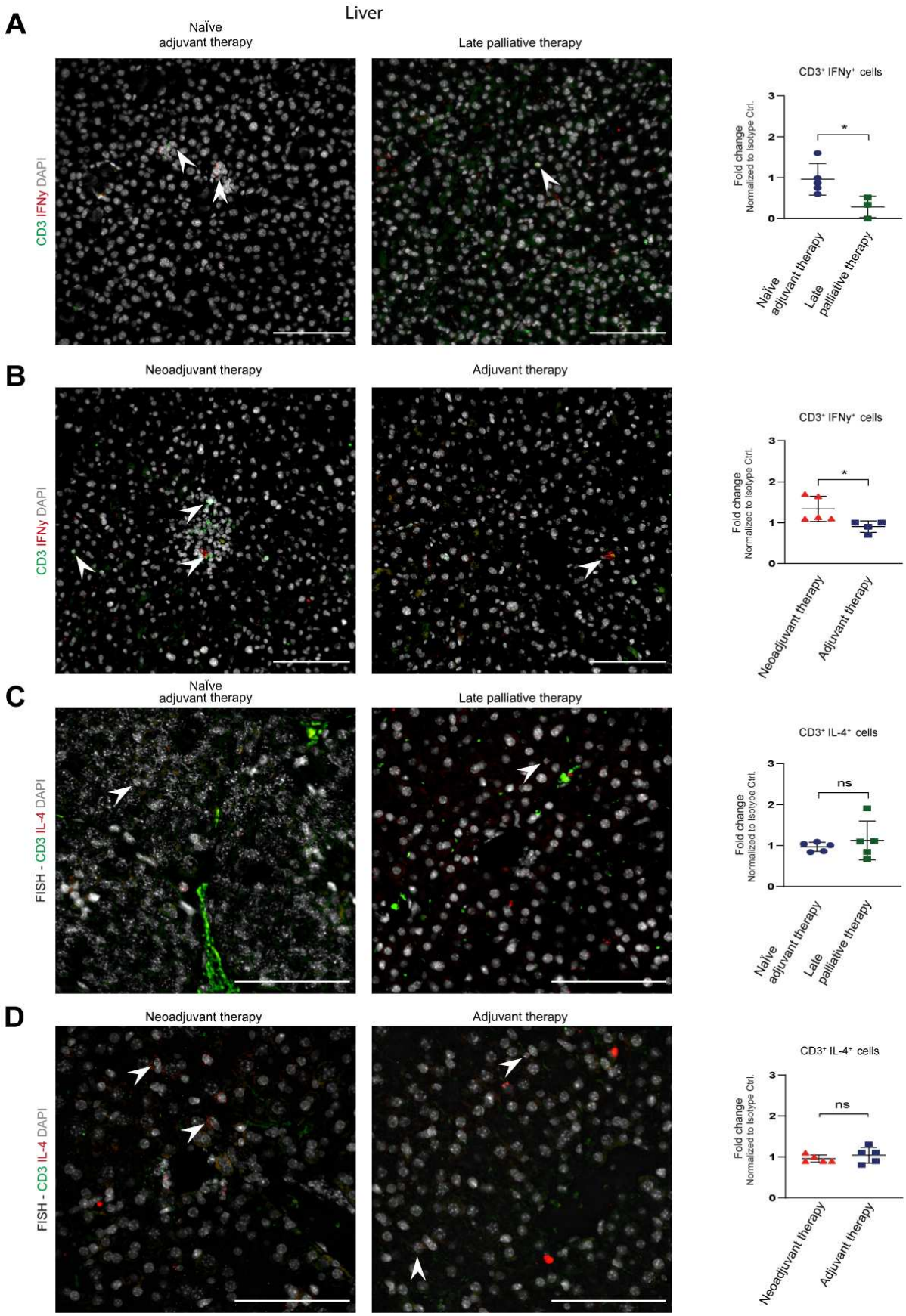
Liver
A
Naïve
adjuvant therapy
Late palliative therapy
CD3 IFNy DAPI
CD3⁺ IFNy⁺ cells
Fold change
Normalized to Isotype Ctrl.
*
Naïve
adjuvant therapy
Late
palliative therapy
B
Neoadjuvant therapy
Adjuvant therapy
CD3 IFNy DAPI
CD3⁺ IFNy⁺ cells
Fold change
Normalized to Isotype Ctrl.
*
Neoadjuvant therapy
Adjuvant therapy
C
Naïve
adjuvant therapy
Late palliative therapy
FISH - CD3 IL-4 DAPI
CD3⁺ IL-4⁺ cells
Fold change
Normalized to Isotype Ctrl.
ns
Naïve
adjuvant therapy
Late
palliative therapy
D
Neoadjuvant therapy
Adjuvant therapy
FISH - CD3 IL-4 DAPI
CD3⁺ IL-4⁺ cells
Fold change
Normalized to Isotype Ctrl.
ns
Neoadjuvant therapy
Adjuvant therapy

Figure 25: Naïve adjuvant and adjuvant therapy with ICI induced IFNγ positive T cells in the liver.

Different immune cell subsets in the liver of mice treated either the adjuvant or late palliative or neoadjuvant or adjuvant ICI were analysed by immunofluorescence staining or Fluorescence in situ hybridization. ***A:*** *Analysis of specific T cell subsets. Quantification of $CD3^+$ $IFN\gamma^+$ T cells in the liver of mice treated in the adjuvant ICI group (n=5) and in the late palliative ICI group (n=3). P=0.0381. Representative pictures of both groups are shown. Scale bar: 100 µm.* ***B:*** *Analysis of specific T cell subsets. Quantification of $CD3^+$ $IFN\gamma^+$ T cells in the liver of mice treated in the neoadjuvant ICI group (n=5) and adjuvant ICI group (n=4). Number of immune cells of the therapy group was normalized to the mean of the corresponding isotype controls (Fold change); (P=0.0159). Representative pictures of both groups are shown. Scale bars: 100 µm.* ***C:*** *Analysis of specific T cell subsets. Quantification of $CD3^+$ $IL4^+$cells in the liver of mice treated in the adjuvant ICI group (n=5) and in the late palliative ICI group (n=5). Number of immune cells of the therapy group was normalized to the mean of the corresponding isotype controls (Fold change); (P=0.5952). Representative pictures of both groups are shown. Scale bars: 100 µm.* ***D:*** *Analysis of specific T cell subsets. Quantification of $CD3^+$ $IL4^+$ cells in the liver of mice treated in the neoadjuvant ICI group (n=5) and in the adjuvant ICI group (n=5). Number of immune cells of the therapy group was normalized to the mean of the corresponding isotype controls (Fold change); (P=0.4284). Representative pictures of both groups are shown. Scale bars: 100 µm. P values < 0.05 were assumed as statistically significant when * < 0.05, ** < 0.01, *** < 0.0001; ns= not significant.*

Besides, we investigated the expression of IFNγ and IL-4 at the primary site by *FISH* (Figure 26). Cutaneous melanomas of mice treated in the neoadjuvant therapy setting showed a significantly increased expression of IFNγ in $CD4^+$ T cells compared to the cutaneous melanoma of the adjuvant setting (P = 0.0078) (Figure 26A). The analysis of the expression of IL-4 (P = 0.8303) and TNFα (P = 0.9338) revealed no differences (Figure 26B and C).

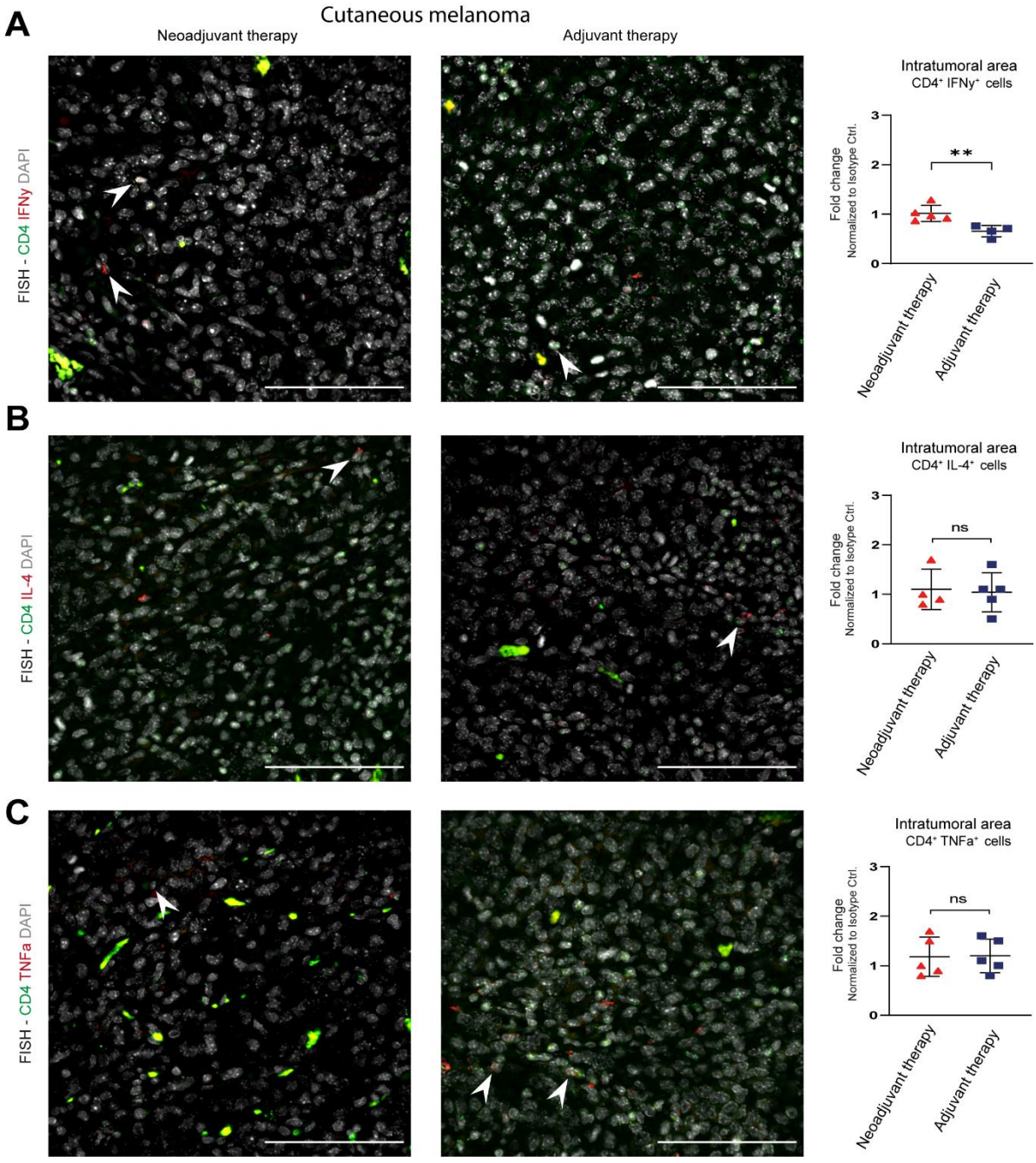

Figure 26: Neoadjuvant ICI increased the number of CD4 IFNγ positive T cells in the primary tumor.

Different immune cell subsets in the primary dermal and the surrounding tissue of mice treated either with the adjuvant or palliative or neoadjuvant or adjuvant ICI were analysed by immunofluorescence staining. Analysis of specific T cell subsets. ***A:*** *Quantification of CD4⁺ IFNγ⁺ T cells in the primary tumor of mice treated in the neoadjuvant ICI group (n=4) and in the adjuvant ICI group (n=5). Number of immune cells of the therapy group was normalized to the mean of the corresponding isotype controls (Fold change); (P=0.0078). Representative pictures of both groups are shown. Scale bars: 100 µm.* ***B:*** *Quantification of CD4⁺ IL4⁺ T cells in in the primary tumor of mice treated in the neoadjuvant ICI group (n=4) and adjuvant ICI group (n=5). Number of immune cells of the therapy group was normalized to the mean of the corresponding isotype controls (Fold change); (P = 0.8303). Representative pictures of both groups are shown. Scale bars: 100 µm.* ***C:*** *Quantification of CD4⁺ TNFα⁺ cells in the primary tumor of mice treated in the neoadjuvant*

*ICI group (n=5) and in the adjuvant ICI group (n=5). Number of immune cells of the therapy group was normalized to the mean of the corresponding isotype controls (Fold change); (P=0.9338). Representative pictures of both groups are shown. Scale bars: 100 µm. P values < 0.05 were assumed as statistically significant when * < 0.05, ** < 0.01, *** < 0.0001; ns= not significant.*

Since IFNγ and IL-4, two key cytokines for Th1 (IFNγ) to Th2 (IL-4) differentiation of T cells were significantly altered among the different therapy modalities, the Th1 and Th2 differentiation of T cells was further investigated in the livers of mice treated in the different therapy modalities. Therefore, Gata3 and T-bet, two important transcription factors for either the Th1 driven T cells (T-bet) or the Th2 driven T cells (Gata3) were analyzed by immunofluorescence stainings.

A trend towards an increased amount of $CD4^+$ $Gata3^+$ T cells was found in the livers of mice treated in the late palliative setting, indicating a Th2 immune response (P = 0.0862) (Figure 27A). In addition, neoadjuvant ICI led to significantly lower amount of $CD4^+$ $Gata3^+$ T cells when compared to the adjuvant ICI (P = 0.0103) (Figure 27B). The analysis of Th1 differentiation by immunofluorescence stainings for T-bet revealed no differences between the naïve and the late palliative ICI (P = 0.6069) (Figure 27C). However, the numbers of $CD4^+$ $T\text{-}bet^+$ T cells significantly rose in the neoadjuvant group compared to the adjuvant therapy group (P = 0.0013) (Figure 27D), indicating that a neoadjuvant application of ICI drives a Th1 immune response.

Altogether, I could show that the neoadjuvant therapy with ICI showed an improved therapeutic response in comparison to the adjuvant and late palliative therapy. In addition, my results show that the neoadjuvant therapy regimen supports the switch from an immune cell excluded to a more T cell inflamed cutaneous melanoma. The neoadjuvant ICI was also associated with increased numbers of T cells in the peripheral blood. Besides the increased systemic immune response, the data indicates that the adjuvant ICI promotes a more Th2-driven immune response, whereas the neoadjuvant therapy showed a more Th1-driven immune response in the liver.

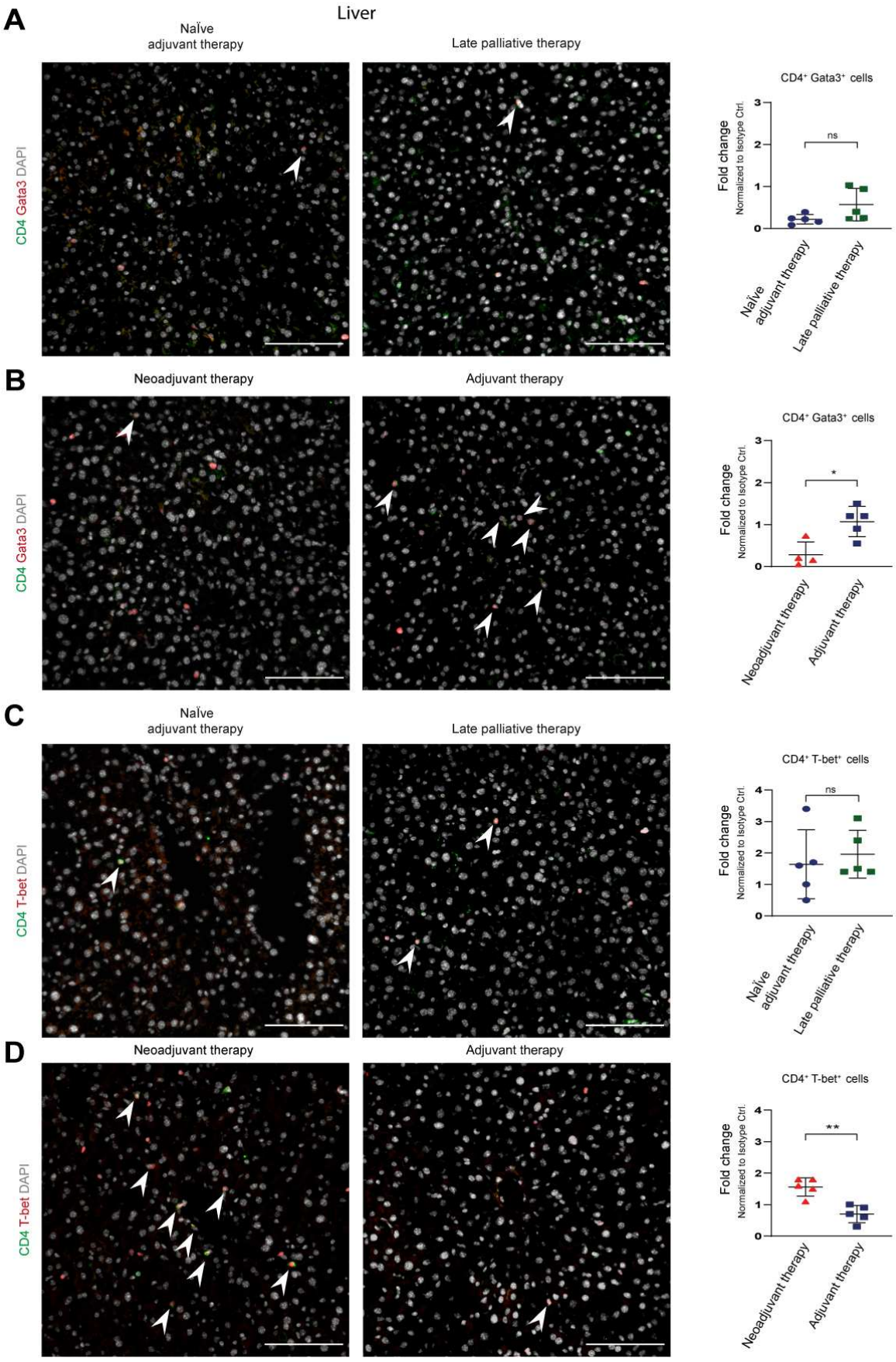
A
Liver
Naïve
adjuvant therapy
Late palliative therapy
CD4 Gata3 DAPI
CD4⁺ Gata3⁺ cells
Fold change
Normalized to Isotype Ctrl.
ns
Naïve adjuvant therapy
Late palliative therapy
B
Neoadjuvant therapy
Adjuvant therapy
CD4 Gata3 DAPI
CD4⁺ Gata3⁺ cells
Fold change
Normalized to Isotype Ctrl.
*
Neoadjuvant therapy
Adjuvant therapy
C
Naïve
adjuvant therapy
Late palliative therapy
CD4 T-bet DAPI
CD4⁺ T-bet⁺ cells
Fold change
Normalized to Isotype Ctrl.
ns
Naïve adjuvant therapy
Late palliative therapy
D
Neoadjuvant therapy
Adjuvant therapy
CD4 T-bet DAPI
CD4⁺ T-bet⁺ cells
Fold change
Normalized to Isotype Ctrl.
**
Neoadjuvant therapy
Adjuvant therapy

Figure 27: Anti tumoral Th1 T cell subsets are increased in livers of the neoadjuvant ICI regimen.

Th1 and Th2 T cell subsets in the liver of mice treated either the adjuvant or palliative or neoadjuvant or adjuvant ICI were analysed by immunofluorescence staining. ***A:*** *Quantification of $CD4^+$ $Gata3^+$ T cells in the liver of mice treated in the adjuvant ICI group (n=5) and in the late palliative ICI group (n=3). Number of immune cells of the therapy group was normalized to the mean of the corresponding isotype controls (Fold change); (P= 0.0862). Representative pictures of both groups are shown. Scale bars: 100 µm.* ***B:*** *Quantification of $CD4^+$ $Gata3^+$ T cells in the liver of mice treated in the neoadjuvant ICI group (n=5) and adjuvant ICI group (n=4). Number of immune cells of the therapy group was normalized to the mean of the corresponding isotype controls (Fold change); (P=0.0103). Representative pictures of both groups are shown. Scale bars: 100 µm.* ***C:*** *Quantification of $CD4^+$ $Tbet^+$ T cells in the liver of mice treated in the adjuvant ICI group (n=5) and in the late palliative ICI group (n=5). Number of immune cells of the therapy group was normalized to the mean of the corresponding isotype controls (Fold change); (P=0.6069). Representative pictures of both groups are shown. Scale bars: 100 µm.* ***D:*** *Quantification of $CD4^+$ $Tbet^+$ cells in the liver of mice treated in the neoadjuvant ICI group (n=5) and in the adjuvant ICI group (n=5). Number of immune cells of the therapy group was normalized to the mean of the corresponding isotype controls (Fold change); (P=0.0013). Representative pictures of both groups are shown. Scale bars: 100 µm. P values < 0.05 were assumed as statistically significant when * < 0.05, ** < 0.01, *** < 0.0001; ns= not significant.*

5 Discussion

5.1 Pre-metastatic activation of the hepatic niche

In my study, I investigated the influence of a primary cutaneous melanoma on the hepatic metastasie formation. To compare the different treatment regimens of ICI, it was important to study pre-metastatic activation of the hepatic niche by a primary tumor. In our model, the presence of a primary tumor for 18 days before the intralienal injection of tumor cells did not significantly alter the number of metastases, however the variability of metastatic numbers appeared to decrease (Figure 6B).

Since we wanted to investigate the influence of different therapy regimens (palliative, adjuvant and neoadjuvant treatment) on melanoma metastasis, this experiment was important. Based on this experiment, an increase in hepatic metastases based on the presence of a primary cutaneous melanoma could be excluded. The potential influence of a primary tumor on the formation of metastases at distant organ sites has been demonstrated for several organs. For example, Kaplan *et al*. showed that bone marrow derived haematopoetic progenitor cells expressing VEGFR1 form cellular clusters at the distant organ site allow the chemotactic attraction and attachment of circulating tumor cells (CTCs) to the lung in a Lewis lung carcinoma and B16 melanoma model (93). Furthermore, Peinado *et al.* found that exosomes from the B16F10 melanoma cell line express a specific repertoire of integrins mediating the adhesion of tumor cells to the extracellular matrix of specific cell types. For example, B16F10 exosomes which express Integrin$\alpha_v\beta_5$ bind specifically to Kupffer cells. The uptake of exosomes expressing Integrin$\alpha_v\beta_5$ by Kupffer cells leads to the upregulation of different genes including the S100 gene and thereby leads to the increased susceptibility to liver metastases (94) (Chapter 1.4.3).

Another important player of the formation of a pre-metastatic niche can be Liver sinusoidal endothelial cells (LSECs). For example, it was demonstrated by Yang *et al.* that the phenotype and function of microvascular endothelial cells (HLCECs) from human liver cancer tissue was different in comparison to LSECs from a healthy liver. The expression of the intracellular-adhesion molecule (ICAM-1) was reduced in comparison to healthy LSECs. Furthermore, the tumor-necrosis factor receptor (TNFR) p75 and the two integrins αvβ3 and αvβ3 were more abundant in HLCECs. This leads to the increased adherence of the human hepatocellular carcinoma BEL-7402 cells to endothelial cells resulting in cancer development (230). In addition, Yu *et al.* show that the reversion of the tolerogenic liver environment through α-mellitin nanoparticles targeting LSECs decreased the susceptibility to the formation of liver metastases. Here, the survival rates of mice were increased in about 80 % in a spontaneous liver metastatic mouse model (111) (Chapter 1.4.3). Therefore, LSECs can be an important player in the formation of a pre-metastatic niche and should be investigated in more detail

during the colonization of the liver by CTCs. However, in our melanoma model an increased susceptibility to the formation of hepatic metastases caused by the primary tumor could not be observed. This may be due to the fact that the primary cutaneous tumor was resected prior to the arrival of the tumor cells in the liver. In order to study, the pre-metastatic niche in our melanoma mouse model in more detail, we could perform the intrasplenic injection of the tumor cells in the presence of the primary cutaneous melanoma, e.g. the intracutaneous injection of tumor cells is performed one week prior to the intrasplenic injection of the tumor cells. With this additional mouse model, the influence of a primary cutaneous melanoma could be investigated in more detail and might influence the formation of hepatic melanoma metastases.

5.2 Immune checkpoint inhibition of liver metastases

5.2.1 Palliative and naïve adjuvant ICI of liver metastases

In 2017 Tumeh *et al.* showed that patients with cutaneous melanoma and liver metastases show a significantly reduced cumulative survival in comparison to patients without liver metastases after the treatment with Pembrolizumab (205). To investigate at which time point the therapeutic resistance to ICI originating from melanoma metastases is starting, ICI was initiated at different time points. The early ICI (starting on day 6) was able to significantly reduce the amount of hepatic metastases compared to their corresponding isotype controls (Figure 7C). The late ICI did not significantly alter the number of hepatic metastases when compared to their corresponding isotype controls (Figure 7D). In addition, the naïve adjuvant therapy with ICI was able to significantly reduce the amount of hepatic metastases when compared to the corresponding isotype controls (Figure 8A). This data suggests that the early ICI protected more efficiently against the colonization of the liver by circulating tumor cells than the late palliative ICI showed by the numeric reduction of hepatic metastases. Furthermore, the naïve adjuvant therapy protected even more against the hepatic metastases formation in the WT31 melanoma model showed by the trend towards a reduced tumor burden and significant differences in the clinical response rates (Figure 9). In the B16F10 *luc2* melanoma model a significant reduction of hepatic metastases could not be observed by comparing either the palliative or the adjuvant therapy group to their corresponding isotype controls (Figure 10). Since the performance of the late palliative therapy setting in the B16F0 *luc2* melanoma model is not possible due to the time points of the ICI, the naïve adjuvant therapy was compared to the palliative therapy regimen in the B16F10 mouse model and significant changes were observed regarding the tumor burden reduction and clinical response rates (Figure 11). That the adjuvant therapy with ICI and BRAFi and MEKi for stage III CM with locoregional metastasis significantly improves the PFS of patients was already shown by several clinical studies (202, 203). Likewise, the adjuvant therapy with Pembrolizumab for stage IIB and IIC high-risk CM shows a reduced recurrence free survival and was recently approved by the FDA (209).

As we had found these differences in treatment responses between the different regimens, we were interested to identify the underlying cellular and molecular mechanisms that may mediate reduced therapeutic responses in the late palliative therapy regimen.

Therefore, the livers of mice treated in the different therapy regimens were analyzed by immunofluorescence stainings. In livers of mice treated in the naïve adjuvant therapy setting in the WT31 model significantly increased numbers of $CD3^+$ $CD8^+$ T cells were observed (Figure 13A). This is in line with the finding of Tumeh *et al.* that patients with liver metastases showed significantly lower levels of $CD8^+$ T cells at the invasive tumor margin in comparison to patients without liver metastases (205). This might in part be explained by Yu *et al.* showing that $CD11b^+$ $F4/80^+$ macrophages led to the apoptosis of the hepatic cytotoxic $CD8^+$ T cells via the FasL FasR pathway (206). The mechanism described by Yu *et al.* is in line with another Hallmark of cancer, namely the avoidance of immune destructions where the tumor cells are able to circumvent attacks of the immune systems such as the preparation of a highly immunosuppressive microenvironment (Chapter 1.3) (17, 54, 55).

In the late palliative therapy setting, significantly increased numbers of $CD11b^+$ $F4/80^+$ macrophages were found (Figure 14). The early palliative ICI indicated a limited but significant reduction in the number of hepatic metastases, whereas the naïve adjuvant ICI in tumor naïve mice significantly reduced the number of liver metastases. This data indicates that in the late palliative therapy setting, increased $CD11b^+$ $F4/80^+$ macrophages which are associated with reduced therapy responses were already present, whereas in the naïve adjuvant therapy setting no significantly increased numbers of $CD11b^+$ $F4/80^+$ macrophages were found which might have been prevented by the adjuvant application of the ICIs. In addition, significantly increased numbers of $CD3^+$ $CD4^+$ T cells were found in the livers of mice treated in the late palliative therapy setting (Figure 13B). Naïve $CD4^+$ T cells can be differentiated as different T cell subsets such as Th1, Th2 and regulatory T cells (231). Lee *et al.* showed that liver metastases are associated with the coordinated activation of regulatory T cells (T_{regs}) which recruit and modulate intratumoral $CD11b^+$ monocytes leading to a systemic immunosuppression (207). In order to investigate if in our model T_{regs} are responsible for the reduced response to ICI, further IF staining including the transcription factor FoxP3 have to be performed (231). It is already known that T_{regs} show a high expression of CTLA-4 (232, 233) , which is in line with the finding of Lee *et al.* that the treatment with the anti CTLA-4 antibody led to a significant reduction of the intratumoral $CD11b^+$ monocytes recruited by T_{regs} and a tumor rejection when combined with the anti PD-1 therapy (207). Since the combination therapy anti PD-1/anti CTLA-4 was used in our mouse model, T_{regs} might not be the prime player leading to the reduced response in the late palliative therapy setting.

Taken together, this data indicates that earlier is better for the therapy response of liver metastases to ICI. As decreased therapy response in palliative therapy was associated with increased $CD11b^+$ $F4/80^+$ macrophages which were not induced in adjuvant treatment we propose that prevention of this mechanism of resistance is the mode of action in the adjuvant therapy. Macrophages are highly abundant within the tumor (234, 235). Already established liver metastases (late palliative) might recruit $CD11b^+$ $F4/80^+$ macrophages to the liver suggesting that these cells are already present when the ICI is applied, whereas in the naive adjuvant therapy the recruitment of $CD11b^+$ $F4/80^+$ macrophages is prevented early enough. In the clinical setting, the therapy with ICI must be started immediately after the detection of liver metastases or even earlier. In the clinical setting, the adjuvant therapy with anti PD-1 inhibitors shows an improved survival of patients but 20 % of cases suffer from melanoma recurrence in the liver and brain (210). About 40 - 60 % of patients diagnosed with advanced or metastatic melanoma respond to ICI but about one half of these patients show recurrence in the metastatic setting (236). The analysis of the Keynote-054 study using adjuvant Pembrolizumab revealed at a median follow-up of 42.3 months, a recurrence rate in the liver of 8 % in the treatment arm compared to 11 % in the placebo arm. The strongest reduction of the recurrence rates were found for distant organ sites including the lymph node and lung (203).

Regarding the high recurrence rate for the liver after the therapy with ICI, different therapy concepts need to be considered.

One therapeutic option which was already postulated by Yu *et al.* would be the combination of radiotherapy with ICI in order to destroy the $CD11b^+$ $F4/80^+$ macrophages within the liver (206). Another option might be the therapy with ICI in combination with Clodronate, an agent belonging to the drug family of bisphosphonates which is currently used for the treatment of bone metastases and osteoporosis (237). Furthermore, Clodronate is used for the specific depletion of macrophages (238) and already showed anti-tumor efficacy in a primary and metastatic melanoma mouse model (237). In order to overcome therapy resistance in the presence of liver metastases, a therapy with Clodronate prior to the ICI might be sufficient to increase the clinical response rate in the late palliative therapy setting. However, the combination therapy of Clodronate and ICI can have some limitations, since clodronate is also able to deplete all macrophages not only the TAMs. For example depletion of $CD169^+$ macrophages which are promoting an anti-tumoral microenvironment e.g. in glioblastoma might have a negative effect (239). Therefore, further investigation of approaches which specifically target hepatic and tumor-induced or associated macrophages is crucial in order to improve the therapeutic response to ICI in the late palliative therapy setting.

In addition, I found significantly increased levels of IL-4 whereas IFNy was significantly decreased in livers of mice treated in the late palliative therapy setting (Figure 24A). Further, a trend towards increased numbers of $CD4^+$ $Gata3^+$ T cells was found in the livers of mice treated in the late palliative therapy setting (Figure 27A), indicating a switch towards a Th2 immune response in this therapeutic regimen. Since Dupilumab, an anti IL-4 antibody is already used for the treatment of asthma (240), the combination of an anti IL-4 antibody and ICI might be an option to overcome the therapeutic resistance in the late palliative therapy setting. In a case review of 7 patients with a cutaneous T cell lymphoma, the application of Dupilumab has shown a short-term transient improvement before the progression of the disease (241).

Our naïve adjuvant therapy setting has some limitations as in the clinical setting no melanoma patient is tumor naïve. However, our naïve adjuvant therapy model might be a good option to further investigate the influence of the ICI on the liver.

However, new therapeutic strategies have to be considered to reduce the recurrence rate of melanoma to the liver and to improve the clinical outcome of patients with liver metastases.

5.2.2 Adjuvant and neoadjuvant ICI of liver metastases

Neoadjuvant ICI is a novel therapeutic concept for melanoma. Here, the patient receives the therapy with ICI in the presence of the primary tumor (High risk Stage II) and/or lymph node metastases (Stage III). This might have several advantages including the fact that patients with a detectable melanoma are treated before surgery in order to boost the therapy response (priming of T cells) or to achieve operability if this was not feasible in the first line (211, 242).

In order to directly compare the neoadjuvant and adjuvant therapy the ICI were applied at different time points either in the presence (neoadjuvant) or in the absence (adjuvant) of the primary cutaneous melanoma. Since spontaneously metastasizing mouse models are not available or only show an insufficient number of hepatic metastases, spleen injections were performed in order to investigate the protection of the different ICI therapy on hepatic melanoma colonization (243). Both therapeutic settings significantly reduced the number of hepatic metastases in comparison to their corresponding isotype controls. However, in the neoadjuvant therapy setting about 72.5 % of mice showed a complete response in comparison to 20 % in the adjuvant therapy setting (Figure 17A). Furthermore, the tumor burden of mice treated in the neoadjuvant therapy setting was two-fold reduced in comparison to the tumor burden of mice treated in the adjuvant therapy setting (Figure 17B). The difference in the percentage of complete responders between the naïve adjuvant therapy setting and the adjuvant therapy might be caused by effects of the pre- and pro-metastatic niche (244) (Section 1.4.3 and 1.4.4). However, as we have already shown in Section 4.1 a primary cutaneous melanoma has no influence on the number of hepatic metastases. Still, the primary cutaneous melanoma can have an influence on the colonization of melanoma cells in the liver as it was shown by Costa-Silva *et al*. in a pancreatic ductal adenocarcinoma (PDAC) mouse model. This publication pointed out that PDAC derived exosomes are taken up by KCs inducing the production of TGFβ and the increased fibronectin production by HPCs which in turn facilitates the recruitment of bone-marrow derived macrophages (96). Peinado *et al.* showed that specific integrins on tumor exosomes can determine organotropic metastases formation (95). Neither the neoadjuvant nor the adjuvant therapy with ICI has an influence on the size of the primary cutaneous melanoma (Figure 18B) or the liver metastases (Figure 21) in comparison to their corresponding isotype control groups. However, the neoadjuvant therapy with the ICI influences the composition of different T cells at the primary site, the peripheral blood and the liver as the investigated metastatic site.

The infiltration of different T cell subsets was analyzed in the primary cutaneous melanoma. The number of intratumoral $CD3^+$ $CD4^+$ T cells was significantly increased in the cutaneous melanomas of the neoadjuvant therapy setting in comparison to the adjuvant setting (Figure 19A). Moreover, a trend towards increased numbers of $CD3^+$ $CD8^+$ positive T cells was observed intratumoral (Figure 19B). On the other hand, the number of $CD3^+$ $CD4^+$ and $CD3^+$

$CD8^+$ T cells were significantly increased in the peritumoral area of the cutaneous melanoma of mice treated in the adjuvant therapy setting (Figure 19C and D). Primary melanomas are normally referred to be a T cell excluded tumor or “cold” tumor (245). However, the application of the neoadjuvant ICI turned the “cold” immune cell excluded primary melanomas into “hot” or T cell inflamed primary melanomas. The switch from a cold into a hot tumor is a promising result since it was shown that these tumors are more responsive to ICI. In addition, the antigen priming and T cell expansion seems to be increased (246). This data also correlates with clinical studies of the neoadjuvant therapy as it was shown in patients that clinical responders show higher amounts of TILs (218, 222, 247). Also, the abundance of $CD4^+$ $IFN\gamma^+$, $CD4^+$ $IL\text{-}4^+$ and CD4 $TNF\alpha^+$ were analyzed in the primary cutaneous melanoma of mice treated in the neoadjuvant and adjuvant therapy setting (Figure 26). The increased amounts of $CD4^+$ $IFN\gamma^+$ T cells were found in the primary cutaneous melanomas of the neoadjuvant therapy setting, which is in line with the finding that in the primary tumor of clinical responders increased amounts of IFNγ were found (219, 221). Then, the question was whether the increased immune cell activation present in the primary cutaneous melanoma is associated with a global immune cell activation and if this is also reflected in the blood and at the metastatic site.

Therefore, the peripheral blood of mice treated in the adjuvant and neoadjuvant therapy regimen was analyzed and revealed significantly increased numbers of $CD4^+$ and $CD8^+$ T cells in the peripheral blood of mice treated in the neoadjuvant therapy setting on day 32 (Figure 20A and B). The finding that the numbers of $CD4^+$ and $CD8^+$ T cells are increased in the primary tumor and the periphery is in line with clinical neoadjuvant studies (218, 219, 221, 222, 247). Amaria *et al.* (NCT02519322) showed that the neoadjuvant therapy in Stage III patients using the combination of Ipilimumab and Nivolumab yielded an overall response rate (ORR) of 73 % and pathological clinical response (pCR) of 45 % but showed in 73 % of patients grade 3 adverse events. The monotherapy with Nivolumab showed an ORR of 25 % and pCR of 25 % and was associated with a low toxicity (8 % grade 3). Furthermore, it was shown that clinical responders in both therapies show higher and more clonal and diverse lymphoid infiltrates (218). In addition, Blank *et al.* demonstrated that patients (Stage III) receiving the neoadjuvant therapy with Ipilimumab and Nivolumab show an increased expansion of tumor-resident T cell clones compared to patients receiving the adjuvant therapy. In the peripheral blood of each patients the 100 top tumor-resident T cell clones were tracked and analyzed beginning with the start of the ICI until week 6. The number of clones in the neoadjuvant arm was around two fold increased as compared to the adjuvant arm (219). The OpACIN-neo trial (Stage III melanoma patients) investigating the neoadjuvant therapy with Ipilimumab in combination with Nivolumab shows that a high rate of patients show a pathological response and that none of these patients have relapsed after a median follow up of 32 months (221).

In addition, Huang *et al.* observed in 2019 that 8 of 27 patients experienced a complete or major pathological response after a single dose of an anti PD-1 antibody and that these patients remained disease free. These observations were associated with an accumulation of exhausted $CD8^+$ T cells in the primary tumor and a reinvigoration in the blood (222). In addition, Amaria *et al.* investigated the combination therapy of Relatlimab and Nivolumab in a neoadjuvant setting. Patients received two doses of neoadjuvant Nivolumab and Relatlimab which was followed by the surgical resection and ten doses of the adjuvant combination therapy. The combination therapy of 30 patients resulted in 57 % of patients showing a pCR and 70 % of patients showing an overall pathological response (oPR). The 1-and 2-year recurrence-free survival was 100 % and 92 % and 88 % and 55 % in patients without a pathological response. The high therapeutic response was associated with an increased immune cell infiltration in the tumor and a decreased amount of M2 macrophages during treatment (247). Furthermore, it was shown by Fairfax *et al.* that the expansion of cytotoxic and effector memory $CD8^+$ T cells in Stage IV melanoma patients correlates with an improved PFS and OS (248). Multiplex analysis of plasma of mice treated in the different therapeutic settings revealed significantly increased levels of TNFα and IL-17 (Figure 20C). However, the role of these two cytokines in our therapeutic mouse model is unclear since both cytokines have different roles regarding tumor immunity. Both cytokines can act either anti-tumoral (249, 250) or pro-tumoral (251, 252).

Then, the immune cell infiltration at the metastatic side was analyzed. The livers of mice treated in the neoadjuvant therapy setting showed a trend towards increased numbers of $CD3^+$ $CD4^+$ T cells and cytotoxic $CD3^+$ $CD8^+$ T cells were significantly increased in the livers of these mice (Figure 22). The analysis of myeloid cells in the liver of mice treated in the different therapy settings revealed no significant differences. Both, the neoadjuvant and adjuvant therapy setting showed a trend towards reduced numbers of $CD11b^+$ $F4/80^+$ cells which indicates that no therapy resistance caused by hepatic macrophages has developed (206). In addition, no significant differences in the number of $CD45^+$ $Ly6C^+$ and $CD45^+$ $Ly6G^+$ cells were observed in the livers (Figure 23). Multiplex assays from whole liver protein of the different therapeutic settings were performed (Figure 24A and B) and revealed significant differences in the amount of IFNγ, IL-4 and IL-15. The role of IL-15 is described as an anti-tumoral cytokine because it is supposed to increase the priming and expansion of different immune cells such as CD8 T cells or NK cells (253, 254). Further, it was found that the serum of metastatic melanoma patients show high levels of sIL-15/IL-15Rα (255). The use of IL-15 is already tested in several Phase I clinical trials (NCT02395822, NCT01385423, NCT03388632, NCT01572493,NCT01021059, NCT01369888, NCT01875601) for the treatment of adult and pediatric solid tumors (256). Most of the studies investigate the use of single IL-15 for the treatment of Acute Myelogenous Leukemia

(AML) (NCT02395822, NCT01385423). IL-15 was also tested in a phase I clinical trial in combination with ICI for the treatment of metastatic solid tumors (NCT03388632). The NCT01021059 phase I clinical trial tested recombinant IL-15 for the treatment of cutaneous melanoma (256). However, the role of IL-15 in our therapeutic setting is unclear and has to be further investigated. To test which cells produce the different chemokines and cytokines different immunofluorescence stainings and FISHs were performed. In line with the results of the multiplex assay increased numbers of $CD3^+$ $IFN\gamma^+$ T cells were found in livers of mice treated in the naïve adjuvant and neoadjuvant therapy setting (Figure 25A and B). The FISH for $CD3^+$ $IL\text{-}4^+$ T cells revealed no significant differences (Figure 25C and D), which might be caused by the fact that by this method RNA levels are analysed instead of protein. Since IFNγ and IL-4 are two specific cytokines for Th1 and Th2 T cells, I suggested the hypothesis that the neoadjuvant therapy with ICI mediates the switch from a Th2 to a Th1 mediated immune response. Th1 and Th2 T cells are classified by different specific transcription factors such as T-bet and Gata3 (257) (Figure 28).

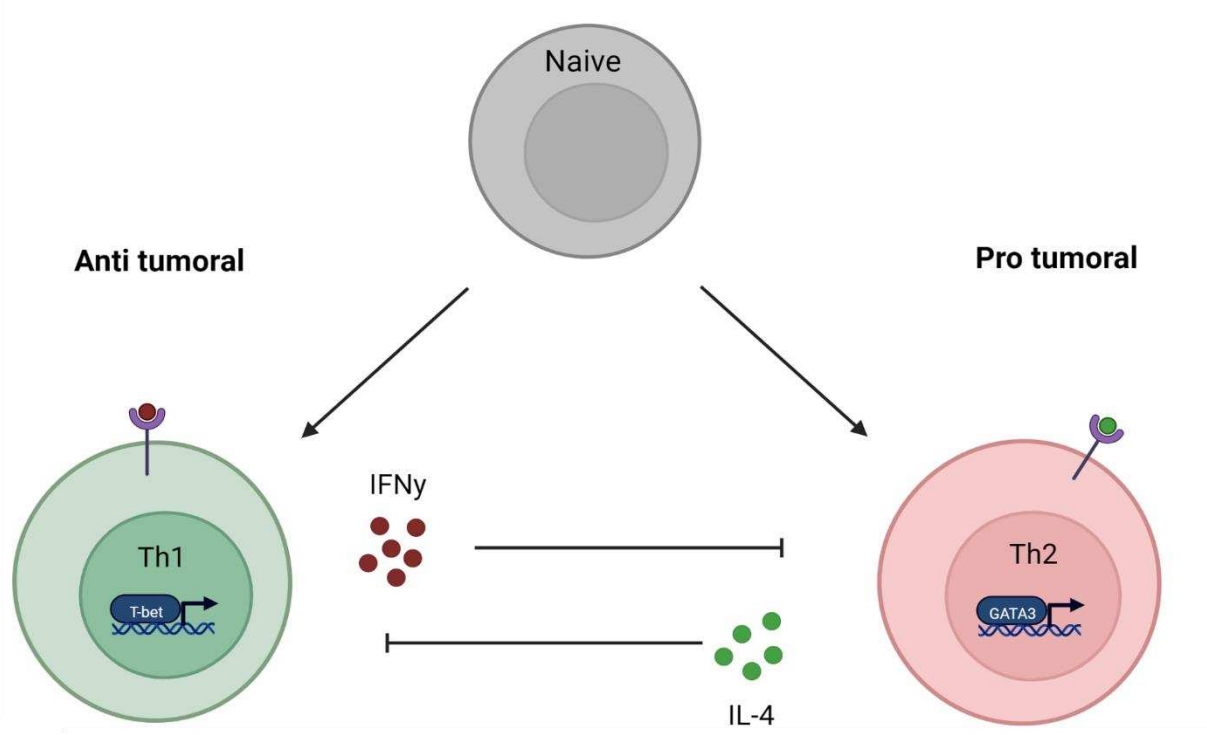

Figure 28: The different Th1 and Th2 T cell subsets.

Naive T cells can differentiate into different T cell subsets named Th1 and Th2 T cells. These two subsets are classified by the expression of different transcription factors such as T-bet (Th1) and Gata3 (Th2). Th1 T cells predominantly secrete IFNγ which inhibits the differentiation to Th2 T cells. Th2 T cells predominantly produce IL-4 (257). Illustration is adapted from (258) and created using BioRender.com.

The analysis and quantification of $CD4^+$ $Gata3^+$ and $CD4^+$ $T\text{-}bet^+$ T cells revealed significant differences in both therapeutic settings. On the one hand, the numbers of $CD4^+$ $Gata3^+$ positive T cells are significantly increased in the adjuvant setting whereas on the other hand, $CD4^+$ $T\text{-}bet^+$ positive T cells are significantly increased in the neoadjuvant therapy (Figure 27B and D). In summary, this data indicates that the neoadjuvant ICI can efficiently protect against the development of liver metastases. Furthermore, I could show that the neoadjuvant therapy with ICI induced a Th1 driven immune response with increased numbers of cytotoxic T cells and $CD4^+$ $T\text{-}bet^+$ T cells in the liver. If directly compared to the adjuvant therapy setting, the neoadjuvant ICI might promote the switch from a more Th2 driven immune response to a predominantly Th1 driven immune response. In order to proof, whether the switch towards the predominant Th1 immune response might rescue the therapeutic resistance in the presence of liver metastases, an IL-4 antibody or specific antibodies against Th2 T cells might be combined with the ICI in the late palliative therapy setting. In addition, the ICI could be combined with IL-2, a drug which has already been approved for the treatment of malignant melanoma. IL-2 could be used to stimulate T cell mediated activities and might help to overcome the therapeutic resistance caused by liver metastases. The NCT04562129 phase II clinical trial is testing the combination of IL-2 with Ipilimumab followed by Nivolumab for the treatment of stage III and IV melanoma patients, but no results have been published until now. Targeting different immunosuppressive cytokines was shown to be effective in different cancer entities (259, 260). Regarding the involvement of the T helper cells to overcome therapy resistance in the neoadjuvant setting, it might be interesting to further investigate novel ICIs. Since it was shown that LAG-3 is not expressed on naïve T cells but on exhausted $CD4^+$ and $CD8^+$ T cells and that LAG-3 expressing T_{regs} produce high amounts of immunoregulatory cytokines such as IL-10 and TGF-β, which are also involved in the differentiation of naïve T cells to Th2 T cells (258). Therefore, it might be interesting to investigate whether the inhibition of LAG-3 in the neoadjuvant therapy setting could be further increase the clinical response. The use of the TIM 3 antibody in our experimental setting is critical since TIM-3 is highly expressed on Th1 T cells (261) which are highly increased in the livers of mice treated in the neoadjuvant therapy setting. To specifically target antigens or markers expressed on tumor cells or immune cells might be a good option for the treatment of the malignant melanoma. The use of personalized vaccines targeting specific antigens on melanoma cells are currently under investigation and showed promising results in a phase I clinical trial (154). The use of personalized vaccines in the neoadjuvant therapeutic regimen might even enhance the clinical outcome of melanoma patients. Therefore, it is possible that the parallel vaccination with tumor antigens may be able to boost the ICI similarly to the presence of a primary tumor in the neoadjuvant therapy. However, this would need to be addressed in experimental models and clinical studies.

Besides the fact that our experimental model has a clinical and translational relevance for the treatment of patients diagnosed with high risk Stage II and Stage III melanoma, our experimental model also has some limitations. In our model, our focus was set on the investigation of the liver colonization since liver metastases are associated with a poor prognosis for the treatment with TT and ICI (205, 208). Therefore, my conclusions can only be transferred to the colonization of the liver. Furthermore, experimental mouse models for the investigation of spontaneously metastasizing melanomas are missing therefore the liver colonization was only investigated by using the intravenous and intrasplenic injection of the WT31 melanoma cell line (243). Therefore, it might be important to investigate the neoadjuvant ICI using a spontaneous metastasizing mouse model in order to more specifically mimic the clinical setting of CM patients. In addition, it would be interesting to investigate the influence of the neoadjuvant therapy with ICI on brain metastases since brain metastases are also described to be a poor prognostic factor (204). Moreover, almost all clinical trials of the neoadjuvant therapy approach are limited to the Stage III disease. It has to be considered that for the neoadjuvant therapy the primary tumor has to reside within the patient until the neoadjuvant therapy is finished. The surgical resection of the tumor can be performed only after immunotherapy. Two-thirds of patients receiving the diagnose of inoperable and hence incurable cancer showed significant distress and depressive symptoms (262). The residual tumor can therefore potentially cause mental health problems until its resection and this has to be considered when choosing this therapy modality. However, our data implicates that the neoadjuvant therapy should also be evaluated for the treatment of high-risk stage II melanoma patients since ICI in the presence of a primary cutaneous melanoma seems to boost the activation and expansion of T cells. The neoadjuvant therapy with Pembrolizumab for Stage II melanoma patients is currently under investigation in two clinical trials (NCT03757689 NCT03698019), however no results are available until now.

My data implicates that the neoadjuvant ICI might be a potential therapeutic option for the treatment of High risk Stage II and Stage III melanoma patients as it may prevent hepatic metastatic spread mediating treatment resistance and therefore should be further investigated in relation to the overall outcome of patients and also metastasis formation in other organs.

6 Conclusion and Outlook

My PhD project highlights the neoadjuvant ICI as a new therapeutic setting for the treatment of the cutaneous melanoma and to prevent the melanoma metastases formation.

First, I investigated whether the different timing of the ICI changed the therapeutic response of liver metastases. Our data showed that the naïve adjuvant ICI protects better against liver colonization compared to the late palliative therapy setting. The enhanced protection against liver colonization might be caused by the increased infiltration of cytotoxic T cells into the liver. In addition, I found more $CD11b^+$ $F4/80^+$ macrophages in the livers of mice treated in the palliative therapy setting compared to the naïve adjuvant setting. This data implicates that the timing of ICI might have an influence on the development of hepatic therapeutic resistance mechanisms.

Furthermore, I analyzed an additional therapeutic setting of the ICI. An experimental mouse model for the direct comparison of the neoadjuvant and adjuvant ICI was established. The neoadjuvant therapy revealed significantly reduced numbers of liver metastases when compared to the adjuvant therapy. Additionally, the data implicates that the neoadjuvant ICI in the presence of the primary tumor led to an increased infiltration of $CD8^+$ and $CD4^+$ T cells into the cutaneous melanoma (T cell inflamed melanoma). On the other hand, the adjuvant therapy setting showed a more immune excluded primary cutaneous melanoma.

Besides, the peripheral blood of mice showed increased numbers of $CD3^+$ $CD4^+$ and $CD3^+$ $CD8^+$ T cells when mice received the neoadjuvant ICI in comparison to the adjuvant ICI.

The livers of mice treated in the neoadjuvant therapy setting showed increased numbers of cytotoxic and $CD4^+$ T-bet^+ T cells. Livers of the adjuvant therapy setting showed increased numbers of $CD4^+$ $Gata3^+$ T cells indicating a switch towards a Th1 driven immune response in the neoadjuvant therapy setting.

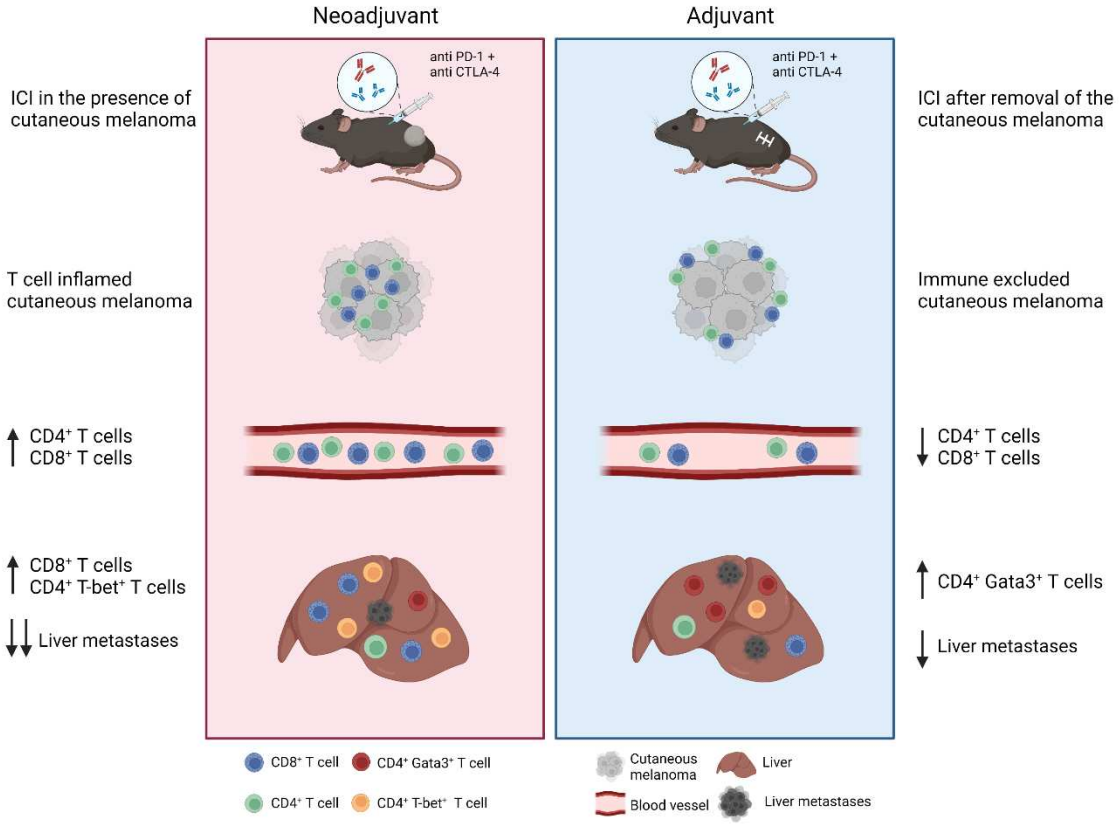

Figure 29: Comparison of the two therapeutic settings with ICI.

Neoadjuvant ICI: *Treatment with ICI in the presence of a cutaneous melanoma showed a more T cell inflamed melanoma with increased numbers of CD4 and CD8 positive T cells. Analysis of the peripheral blood showed an increased number of CD4⁺ and CD8⁺ T cells. In the liver increased numbers of cytotoxic and CD4⁺ T-bet⁺ T cells were found. Neoadjuvant therapy led to strong reduction of liver metastases.* ***Adjuvant ICI:*** *Treatment with ICI in the absence of a cutaneous melanoma showed a more immune cell excluded cutaneous melanoma and the number of CD4 and CD8 positive T cells was reduced compared to the neoadjuvant ICI. Livers of these mice showed increased numbers of CD4⁺ Gata3⁺ T cells. Illustration created by using BioRender.com.*

In summary, this project showed that the timing and type of ICI (adjuvant, palliative and neoadjuvant) significantly alters the therapeutic response and might be crucial to overcome treatment resistance of hepatic melanoma metastasis.

To further validate our data, the comparison of the neoadjuvant with the adjuvant therapy setting will be performed using a different melanoma cell line. Additionally, and in order to get a more detailed analysis of the different T cell subsets supporting the enhanced therapeutic response to the neoadjuvant ICI, Dennis Agardy from the AG Platten (DKFZ; Heidelberg) and I performed single cell RNA sequencing of different T cell subsets of the primary tumor, the blood and the liver of mice treated in the neoadjuvant and adjuvant therapy regimen. As the analysis is currently ongoing, it is not included in this PhD thesis. The scRNA Sequencing

Analysis will be used to get a deeper mechanistic insight regarding the difference between the neoadjuvant and adjuvant ICI. The experiment will be used to perform TCR trafficking analysis and analysis of the distribution of different T cell subsets in the primary cutaneous melanoma, the blood and the liver. Additionally, the expression of different genes or gene clusters of T cells will be analyzed in the different compartments (cutaneous melanoma, blood and liver).

This analysis will be used to further investigate the improved therapeutic response of liver metastases to the neoadjuvant therapy and eventually may contribute to the further improvement of the clinical outcome of CM patients.

7 References

1. Kanitakis J. Anatomy, histology and immunohistochemistry of normal human skin. Eur J Dermatol 2002;12:390-399; quiz 400-391.

2. Elder DE. Precursors to melanoma and their mimics: nevi of special sites. Mod Pathol 2006;19 Suppl 2:S4-20.

3. Eggermont AMM, Spatz A, Robert C. Cutaneous melanoma. The Lancet 2014;383:816-827.

4. Erdmann F, Spix C, Katalinic A, Christ M, Folkerts J, Hansmann J, Kranzhöfer K, et al. Krebs in Deutschland für 2017/2018. 2021.

5. de Vries E, van de Poll-Franse LV, Louwman WJ, de Gruijl FR, Coebergh JW. Predictions of skin cancer incidence in the Netherlands up to 2015. Br J Dermatol 2005;152:481-488.

6. Pflugfelder A, Kochs C, Blum A, Capellaro M, Czeschik C, Dettenborn T, Dill D, et al. S3-guideline "diagnosis, therapy and follow-up of melanoma" -- short version. J Dtsch Dermatol Ges 2013;11:563-602.

7. Friedman RJ, Rigel DS, Kopf AW. Early detection of malignant melanoma: the role of physician examination and self-examination of the skin. CA: a cancer journal for clinicians 1985;35:130-151.

8. Wang SQ, Hashemi P. Noninvasive imaging technologies in the diagnosis of melanoma. Semin Cutan Med Surg 2010;29:174-184.

9. Balch CM, Gershenwald JE, Soong SJ, Thompson JF, Atkins MB, Byrd DR, Buzaid AC, et al. Final version of 2009 AJCC melanoma staging and classification. J Clin Oncol 2009;27:6199-6206.

10. Mohr P, Eggermont AM, Hauschild A, Buzaid A. Staging of cutaneous melanoma. Ann Oncol 2009;20 Suppl 6:vi14-21.

11. Alexandrov LB, Nik-Zainal S, Wedge DC, Aparicio SA, Behjati S, Biankin AV, Bignell GR, et al. Signatures of mutational processes in human cancer. Nature 2013;500:415-421.

12. Akbani R, Akdemir KC, Aksoy BA, Albert M, Ally A, Amin SB, Arachchi H, et al. Genomic classification of cutaneous melanoma. Cell 2015;161:1681-1696.

13. Hayward NK, Wilmott JS, Waddell N, Johansson PA, Field MA, Nones K, Patch A-M, et al. Whole-genome landscapes of major melanoma subtypes. Nature 2017;545:175-180.

14. Jemal A, Siegel R, Xu J, Ward E. Cancer statistics, 2010. CA Cancer J Clin 2010;60:277-300.

15. Patel JK, Didolkar MS, Pickren JW, Moore RH. Metastatic pattern of malignant melanoma: A study of 216 autopsy cases. The American Journal of Surgery 1978;135:807-810.

16. Hanahan D, Weinberg RA. The hallmarks of cancer. Cell 2000;100:57-70.

17. Hanahan D, Weinberg RA. Hallmarks of cancer: the next generation. Cell 2011;144:646-674.

18. Blasco MA. Telomeres and human disease: ageing, cancer and beyond. Nature Reviews Genetics 2005;6:611-622.

19. Shay JW, Wright WE. Hayflick, his limit, and cellular ageing. Nature reviews Molecular cell biology 2000;1:72-76.

20. Stewart SA, Weinberg RA. Telomeres: cancer to human aging. Annu. Rev. Cell Dev. Biol. 2006;22:531-557.

21. Hahn WC, Counter CM, Lundberg AS, Beijersbergen RL, Brooks MW, Weinberg RA. Creation of human tumour cells with defined genetic elements. Nature 1999;400:464-468.

22. Barthel FP, Wei W, Tang M, Martinez-Ledesma E, Hu X, Amin SB, Akdemir KC, et al. Systematic analysis of telomere length and somatic alterations in 31 cancer types. Nat Genet 2017;49:349-357.

23. Nakamura TM, Morin GB, Chapman KB, Weinrich SL, Andrews WH, Lingner J, Harley CB, et al. Telomerase catalytic subunit homologs from fission yeast and human. Science 1997;277:955-959.

24. Counter CM, Meyerson M, Eaton EN, Ellisen LW, Caddle SD, Haber DA, Weinberg RA. Telomerase activity is restored in human cells by ectopic expression of hTERT (hEST2), the catalytic subunit of telomerase. Oncogene 1998;16:1217-1222.

25. Huang DS, Wang Z, He XJ, Diplas BH, Yang R, Killela PJ, Meng Q, et al. Recurrent TERT promoter mutations identified in a large-scale study of multiple tumour types are associated with increased TERT expression and telomerase activation. Eur J Cancer 2015;51:969-976.

26. Nagore E, Heidenreich B, Requena C, García-Casado Z, Martorell-Calatayud A, Pont-Sanjuan V, Jimenez-Sanchez AI, et al. TERT promoter mutations associate with fast-growing melanoma. Pigment Cell Melanoma Res 2016;29:236-238.

27. Zapata JM, Pawlowski K, Haas E, Ware CF, Godzik A, Reed JC. A diverse family of proteins containing tumor necrosis factor receptor-associated factor domains. J Biol Chem 2001;276:24242-24252.

28. Levine AJ. p53, the cellular gatekeeper for growth and division. cell 1997;88:323-331.

29. Friedman PN, Chen X, Bargonetti J, Prives C. The p53 protein is an unusually shaped tetramer that binds directly to DNA. Proceedings of the National Academy of Sciences 1993;90:3319-3323.

30. Mihara M, Erster S, Zaika A, Petrenko O, Chittenden T, Pancoska P, Moll UM. p53 has a direct apoptogenic role at the mitochondria. Molecular cell 2003;11:577-590.

31. Cooper G, Adams K. The cell: a molecular approach: Oxford University Press, 2022.

32. Tsao H, Chin L, Garraway LA, Fisher DE. Melanoma: from mutations to medicine. Genes & development 2012;26:1131-1155.

33. Burkhart DL, Sage J. Cellular mechanisms of tumour suppression by the retinoblastoma gene. Nat Rev Cancer 2008;8:671-682.

34. Deshpande A, Sicinski P, Hinds PW. Cyclins and cdks in development and cancer: a perspective. Oncogene 2005;24:2909-2915.

35. Sherr CJ, McCormick F. The RB and p53 pathways in cancer. Cancer Cell 2002;2:103-112.

36. Colombino M, Capone M, Lissia A, Cossu A, Rubino C, De Giorgi V, Massi D, et al. BRAF/NRAS mutation frequencies among primary tumors and metastases in patients with melanoma. J Clin Oncol 2012;30:2522-2529.

37. Talmadge JE, Fidler IJ. AACR centennial series: the biology of cancer metastasis: historical perspective. Cancer research 2010;70:5649-5669.

38. Fidler IJ. The pathogenesis of cancer metastasis: the'seed and soil'hypothesis revisited. Nature reviews cancer 2003;3:453-458.

39. Kim YH, Choi YW, Lee J, Soh EY, Kim J-H, Park TJ. Senescent tumor cells lead the collective invasion in thyroid cancer. Nature communications 2017;8:15208.

40. Lo HC, Xu Z, Kim IS, Pingel B, Aguirre S, Kodali S, Liu J, et al. Resistance to natural killer cell immunosurveillance confers a selective advantage to polyclonal metastasis. Nature Cancer 2020;1:709-722.

41. Géraud C, Koch PS, Damm F, Schledzewski K, Goerdt S. The metastatic cycle: metastatic niches and cancer cell dissemination. JDDG: Journal der Deutschen Dermatologischen Gesellschaft 2014;12:1012-1019.

42. Slominski A, Tobin DJ, Shibahara S, Wortsman J. Melanin pigmentation in mammalian skin and its hormonal regulation. Physiological reviews 2004;84:1155-1228.

43. Gray-Schopfer V, Wellbrock C, Marais R. Melanoma biology and new targeted therapy. Nature 2007;445:851-857.

44. Haass NK, Smalley KS, Herlyn M. The role of altered cell–cell communication in melanoma progression. Journal of molecular histology 2004;35:309-318.

45. Carmeliet P, Jain RK. Angiogenesis in cancer and other diseases. Nature 2000;407:249-257.

46. Hanahan D, Folkman J. Patterns and emerging mechanisms of the angiogenic switch during tumorigenesis. Cell 1996;86:353-364.

47. Gille J. Antiangiogenic cancer therapies get their act together: current developments and future prospects of growth factor- and growth factor receptor-targeted approaches. Exp Dermatol 2006;15:175-186.

48. Sparano JA, Gray R, Giantonio B, O'Dwyer P, Comis RL. Evaluating antiangiogenesis agents in the clinic: the Eastern Cooperative Oncology Group Portfolio of Clinical Trials. Clin Cancer Res 2004;10:1206-1211.

49. Motl S. Bevacizumab in combination chemotherapy for colorectal and other cancers. Am J Health Syst Pharm 2005;62:1021-1032.

50. Vacca A, Ria R, Ribatti D, Bruno M, Dammacco F. [Angiogenesis and tumor progression in melanoma]. Recenti Prog Med 2000;91:581-587.

51. Plum SM, Holaday JW, Ruiz A, Madsen JW, Fogler WE, Fortier AH. Administration of a liposomal FGF-2 peptide vaccine leads to abrogation of FGF-2-mediated angiogenesis and tumor development. Vaccine 2000;19:1294-1303.

52. Sessa C, Viganò L, Grasselli G, Trigo J, Marimon I, Lladò A, Locatelli A, et al. Phase I clinical and pharmacological evaluation of the multi-tyrosine kinase inhibitor SU006668 by chronic oral dosing. European Journal of Cancer 2006;42:171-178.

53. Ehrlich P. On the current state of cancer research. Ned Tijdschr Geneeskd 1909;5:273-290.

54. Dunn GP, Bruce AT, Ikeda H, Old LJ, Schreiber RD. Cancer immunoediting: from immunosurveillance to tumor escape. Nat Immunol 2002;3:991-998.

55. Dunn GP, Old LJ, Schreiber RD. The three Es of cancer immunoediting. Annu Rev Immunol 2004;22:329-360.

56. Stutman O. Immunodepression and malignancy. Adv Cancer Res 1975;22:261-422.

57. Street SE, Cretney E, Smyth MJ. Perforin and interferon-gamma activities independently control tumor initiation, growth, and metastasis. Blood 2001;97:192-197.

58. Smyth MJ, Thia KY, Street SE, Cretney E, Trapani JA, Taniguchi M, Kawano T, et al. Differential tumor surveillance by natural killer (NK) and NKT cells. J Exp Med 2000;191:661-668.

59. van den Broek ME, Kägi D, Ossendorp F, Toes R, Vamvakas S, Lutz WK, Melief CJ, et al. Decreased tumor surveillance in perforin-deficient mice. J Exp Med 1996;184:1781-1790.

60. Shinkai Y, Rathbun G, Lam KP, Oltz EM, Stewart V, Mendelsohn M, Charron J, et al. RAG-2-deficient mice lack mature lymphocytes owing to inability to initiate V(D)J rearrangement. Cell 1992;68:855-867.

61. Penn I. Malignant tumors in organ transplant recipients: Springer Science & Business Media, 2012.

62. Vesely MD, Kershaw MH, Schreiber RD, Smyth MJ. Natural innate and adaptive immunity to cancer. Annu Rev Immunol 2011;29:235-271.

63. Schreiber RD, Old LJ, Smyth MJ. Cancer Immunoediting: Integrating Immunity’s Roles in Cancer Suppression and Promotion. Science 2011;331:1565-1570.

64. Aguirre-Ghiso JA. Models, mechanisms and clinical evidence for cancer dormancy. Nat Rev Cancer 2007;7:834-846.

65. Khong HT, Restifo NP. Natural selection of tumor variants in the generation of "tumor escape" phenotypes. Nat Immunol 2002;3:999-1005.

66. Passarelli A, Mannavola F, Stucci LS, Tucci M, Silvestris F. Immune system and melanoma biology: a balance between immunosurveillance and immune escape. Oncotarget 2017;8:106132.

67. Jacobs JF, Nierkens S, Figdor CG, de Vries IJM, Adema GJ. Regulatory T cells in melanoma: the final hurdle towards effective immunotherapy? The lancet oncology 2012;13:e32-e42.

68. Pardoll DM. The blockade of immune checkpoints in cancer immunotherapy. Nature Reviews Cancer 2012;12:252-264.

69. Polak M, Borthwick N, Gabriel F, Johnson P, Higgins B, Hurren J, McCormick D, et al. Mechanisms of local immunosuppression in cutaneous melanoma. British journal of cancer 2007;96:1879-1887.

70. Munn DH, Mellor AL. IDO in the tumor microenvironment: inflammation, counter-regulation, and tolerance. Trends in immunology 2016;37:193-207.

71. Brochez L, Chevolet I, Kruse V. The rationale of indoleamine 2, 3-dioxygenase inhibition for cancer therapy. European journal of cancer 2017;76:167-182.

72. Warburg O. On the origin of cancer cells. Science 1956;123:309-314.

73. Warburg O, Wind F, Negelein E. The metabolism of tumors in the body. The Journal of general physiology 1927;8:519.

74. Jones RG, Thompson CB. Tumor suppressors and cell metabolism: a recipe for cancer growth. Genes & development 2009;23:537-548.

75. DeBerardinis RJ, Lum JJ, Hatzivassiliou G, Thompson CB. The biology of cancer: metabolic reprogramming fuels cell growth and proliferation. Cell metabolism 2008;7:11-20.

76. Scott DA, Richardson AD, Filipp FV, Knutzen CA, Chiang GG, Ze'ev AR, Osterman AL, et al. Comparative metabolic flux profiling of melanoma cell lines: beyond the Warburg effect. Journal of Biological Chemistry 2011;286:42626-42634.

77. Kuphal S, Winklmeier A, Warnecke C, Bosserhoff A-K. Constitutive HIF-1 activity in malignant melanoma. European Journal of Cancer 2010;46:1159-1169.

78. Mills CN, Joshi SS, Niles RM. Expression and function of hypoxia inducible factor-1 alpha in human melanoma under non-hypoxic conditions. Molecular cancer 2009;8:1-12.

79. Aprelikova O, Pandolfi S, Tackett S, Ferreira M, Salnikow K, Ward Y, Risinger JI, et al. Melanoma antigen-11 inhibits the hypoxia-inducible factor prolyl hydroxylase 2 and activates hypoxic response. Cancer research 2009;69:616-624.

80. Kumar SM, Yu H, Edwards R, Chen L, Kazianis S, Brafford P, Acs G, et al. Mutant V600E BRAF increases hypoxia inducible factor-1α expression in melanoma. Cancer research 2007;67:3177-3184.

81. Read AE. Clinical physiology of the liver. Br J Anaesth 1972;44:910-917.

82. Abdel-Misih SR, Bloomston M. Liver anatomy. Surg Clin North Am 2010;90:643-653.

83. Trefts E, Gannon M, Wasserman DH. The liver. Curr Biol 2017;27:R1147-r1151.

84. Moore KL, Dalley AF, Agur AM. Clinically oriented anatomy: Lippincott Williams & Wilkins, 2013.

85. Poisson J, Lemoinne S, Boulanger C, Durand F, Moreau R, Valla D, Rautou P-E. Liver sinusoidal endothelial cells: Physiology and role in liver diseases. Journal of hepatology 2017;66:212-227.

86. Augustin HG, Koh GY. Organotypic vasculature: from descriptive heterogeneity to functional pathophysiology. Science 2017;357:eaal2379.

87. PUESTOW CB. THE DISCHARGE OF BILE INTO THE DUODENUM: AN EXPERIMENTAL STUDY. Archives of Surgery 1931;23:1013-1029.

88. Wisse E. An electron microscopic study of the fenestrated endothelial lining of rat liver sinusoids. Journal of ultrastructure research 1970;31:125-150.

89. Koch P-S, Lee KH, Goerdt S, Augustin HG. Angiodiversity and organotypic functions of sinusoidal endothelial cells. Angiogenesis 2021;24:289-310.

90. Hautekeete ML, Geerts A. The hepatic stellate (Ito) cell: its role in human liver disease. Virchows Archiv 1997;430:195-207.

91. Tu T, Calabro SR, Lee A, Maczurek AE, Budzinska MA, Warner FJ, McLennan SV, et al. Hepatocytes in liver injury: Victim, bystander, or accomplice in progressive fibrosis? J Gastroenterol Hepatol 2015;30:1696-1704.

92. Dixon LJ, Barnes M, Tang H, Pritchard MT, Nagy LE. Kupffer cells in the liver. Compr Physiol 2013;3:785-797.

93. Kaplan RN, Riba RD, Zacharoulis S, Bramley AH, Vincent L, Costa C, MacDonald DD, et al. VEGFR1-positive haematopoietic bone marrow progenitors initiate the pre-metastatic niche. Nature 2005;438:820-827.

94. Peinado H, Alečković M, Lavotshkin S, Matei I, Costa-Silva B, Moreno-Bueno G, Hergueta-Redondo M, et al. Melanoma exosomes educate bone marrow progenitor cells toward a pro-metastatic phenotype through MET. Nat Med 2012;18:883-891.

95. Hoshino A, Costa-Silva B, Shen TL, Rodrigues G, Hashimoto A, Tesic Mark M, Molina H, et al. Tumour exosome integrins determine organotropic metastasis. Nature 2015;527:329-335.

96. Costa-Silva B, Aiello NM, Ocean AJ, Singh S, Zhang H, Thakur BK, Becker A, et al. Pancreatic cancer exosomes initiate pre-metastatic niche formation in the liver. Nat Cell Biol 2015;17:816-826.

97. Hess KR, Varadhachary GR, Taylor SH, Wei W, Raber MN, Lenzi R, Abbruzzese JL. Metastatic patterns in adenocarcinoma. Cancer 2006;106:1624-1633.

98. Ryu SW, Saw R, Scolyer RA, Crawford M, Thompson JF, Sandroussi C. Liver resection for metastatic melanoma: equivalent survival for cutaneous and ocular primaries. J Surg Oncol 2013;108:129-135.

99. Van den Eynden GG, Majeed AW, Illemann M, Vermeulen PB, Bird NC, Hoyer-Hansen G, Eefsen RL, et al. The multifaceted role of the microenvironment in liver metastasis: biology and clinical implications. Cancer Res 2013;73:2031-2043.

100. Enns A, Gassmann P, Schluter K, Korb T, Spiegel HU, Senninger N, Haier J. Integrins can directly mediate metastatic tumor cell adhesion within the liver sinusoids. J Gastrointest Surg 2004;8:1049-1059; discussion 1060.

101. Vollmar B, Menger MD. The hepatic microcirculation: mechanistic contributions and therapeutic targets in liver injury and repair. Physiol Rev 2009;89:1269-1339.

102. Benedicto A, Romayor I, Arteta B. Role of liver ICAM-1 in metastasis. Oncology letters 2017;14:3883-3892.

103. Zuo Y, Ren S, Wang M, Liu B, Yang J, Kuai X, Lin C, et al. Novel roles of liver sinusoidal endothelial cell lectin in colon carcinoma cell adhesion, migration and in-vivo metastasis to the liver. Gut 2013;62:1169-1178.

104. Arteta B, Lasuen N, Lopategi A, Sveinbjörnsson B, Smedsrød B, Vidal-Vanaclocha F. Colon carcinoma cell interaction with liver sinusoidal endothelium inhibits organ-specific antitumor immunity through interleukin-1-induced mannose receptor in mice. Hepatology 2010;51:2172-2182.

105. Mendt M, Cardier JE. Activation of the CXCR4 chemokine receptor enhances biological functions associated with B16 melanoma liver metastasis. Melanoma Res 2017;27:300-308.

106. Wohlfeil SA, Häfele V, Dietsch B, Schledzewski K, Winkler M, Zierow J, Leibing T, et al. Hepatic Endothelial Notch Activation Protects against Liver Metastasis by Regulating Endothelial-Tumor Cell Adhesion Independent of Angiocrine Signaling. Cancer Research 2019;79:598-610.

107. Thomson AW, Knolle PA. Antigen-presenting cell function in the tolerogenic liver environment. Nat Rev Immunol 2010;10:753-766.

108. Doherty DG. Immunity, tolerance and autoimmunity in the liver: A comprehensive review. J Autoimmun 2016;66:60-75.

109. Diehl L, Schurich A, Grochtmann R, Hegenbarth S, Chen L, Knolle PA. Tolerogenic maturation of liver sinusoidal endothelial cells promotes B7-homolog 1-dependent CD8+ T cell tolerance. Hepatology 2008;47:296-305.

110. Höchst B, Schildberg FA, Böttcher J, Metzger C, Huss S, Türler A, Overhaus M, et al. Liver sinusoidal endothelial cells contribute to CD8 T cell tolerance toward circulating carcinoembryonic antigen in mice. Hepatology 2012;56:1924-1933.

111. Yu X, Chen L, Liu J, Dai B, Xu G, Shen G, Luo Q, et al. Immune modulation of liver sinusoidal endothelial cells by melittin nanoparticles suppresses liver metastasis. Nat Commun 2019;10:574.

112. Domingues B, Lopes JM, Soares P, Pópulo H. Melanoma treatment in review. Immunotargets Ther 2018;7:35-49.

113. Garbe C, Eigentler TK. Diagnosis and treatment of cutaneous melanoma: state of the art 2006*. Melanoma Research 2007;17:117-127.

114. Hauschild A, Eiling S, Lischner S, Haacke TC, Christophers E. Sicherheitsabstände bei der Exzision des primären malignen MelanomsDiskussionsvorschläge aufgrund von Ergebnissen aus kontrollierten klinischen Studien. Der Hautarzt 2001;52:1003-1010.

115. Ringborg U, Andersson R, Eldh J, Glaumann B, Hafström L, Jacobsson S, Jönsson PE, et al. Resection margins of 2 versus 5 cm for cutaneous malignant melanoma with a tumor thickness of 0.8 to 2.0 mm: a randomized study by the Swedish Melanoma Study Group. Cancer: Interdisciplinary International Journal of the American Cancer Society 1996;77:1809-1814.

116. Thomas JM, Newton-Bishop J, A'Hern R, Coombes G, Timmons M, Evans J, Cook M, et al. Excision margins in high-risk malignant melanoma. N Engl J Med 2004;350:757-766.

117. Bongers V, Borel Rinkes IH, Barneveld PC, Canninga-van Dijk MR, van Rijk PP, van Vloten WA. Towards quality assurance of the sentinel node procedure in malignant melanoma patients: a single institution evaluation and a European survey. European journal of nuclear medicine 1999;26:84-90.

118. Nieweg OE, Jansen L, Kroon BB. Technique of lymphatic mapping and sentinel node biopsy for melanoma. European Journal of Surgical Oncology (EJSO) 1998;24:520-524.

119. Morton DL, Thompson JF, Essner R, Elashoff R, Stern SL, Nieweg OE, Roses DF, et al. Validation of the accuracy of intraoperative lymphatic mapping and sentinel

lymphadenectomy for early-stage melanoma: a multicenter trial. Annals of surgery 1999;230:453.

120. Lenisa L, Santinami M, Belli F, Clemente C, Mascheroni L, Patuzzo R, Gallino G, et al. Sentinel node biopsy and selective lymph node dissection in cutaneous melanoma patients. Journal of Experimental & Clinical Cancer Research: CR 1999;18:69-74.

121. Gershenwald JE, Thompson W, Mansfield PF, Lee JE, Colome MI, Tseng C-h, Lee JJ, et al. Multi-institutional melanoma lymphatic mapping experience: the prognostic value of sentinel lymph node status in 612 stage I or II melanoma patients. Journal of Clinical Oncology 1999;17:976-976.

122. Kim C, Lee CW, Kovacic L, Shah A, Klasa R, Savage KJ. Long-term survival in patients with metastatic melanoma treated with DTIC or temozolomide. Oncologist 2010;15:765-771.

123. Ahmann DL, Creagan ET, Hahn RG, Edmonson JH, Bisel HF, Schaid DJ. Complete responses and long-term survivals after systemic chemotherapy for patients with advanced malignant melanoma. Cancer 1989;63:224-227.

124. Hill GJ, 2nd, Krementz ET, Hill HZ. Dimethyl triazeno imidazole carboxamide and combination therapy for melanoma. IV. Late results after complete response to chemotherapy (Central Oncology Group protocols 7130, 7131, and 7131A). Cancer 1984;53:1299-1305.

125. Bajetta E, Del Vecchio M, Bernard-Marty C, Vitali M, Buzzoni R, Rixe O, Nova P, et al. Metastatic melanoma: Chemotherapy. Seminars in Oncology 2002;29:427-445.

126. Samlowski WE, Moon J, Witter M, Atkins MB, Kirkwood JM, Othus M, Ribas A, et al. High frequency of brain metastases after adjuvant therapy for high-risk melanoma. Cancer Med 2017;6:2576-2585.

127. Shariati M, Meric-Bernstam F. Targeting AKT for cancer therapy. Expert Opin Investig Drugs 2019;28:977-988.

128. Flaherty KT. Targeting Metastatic Melanoma. Annual Review of Medicine 2012;63:171-183.

129. Brose MS, Volpe P, Feldman M, Kumar M, Rishi I, Gerrero R, Einhorn E, et al. BRAF and RAS mutations in human lung cancer and melanoma. Cancer research 2002;62:6997-7000.

130. Ballantyne AD, Garnock-Jones KP. Dabrafenib: first global approval. Drugs 2013;73:1367-1376.

131. Ascierto PA, Kirkwood JM, Grob J-J, Simeone E, Grimaldi AM, Maio M, Palmieri G, et al. The role of BRAF V600 mutation in melanoma. Journal of Translational Medicine 2012;10:85.

132. Davies H, Bignell GR, Cox C, Stephens P, Edkins S, Clegg S, Teague J, et al. Mutations of the BRAF gene in human cancer. Nature 2002;417:949-954.

133. Maurer G, Tarkowski B, Baccarini M. Raf kinases in cancer-roles and therapeutic opportunities. Oncogene 2011;30:3477-3488.

134. Chapman PB, Hauschild A, Robert C, Haanen JB, Ascierto P, Larkin J, Dummer R, et al. Improved survival with vemurafenib in melanoma with BRAF V600E mutation. N Engl J Med 2011;364:2507-2516.

135. Livingstone E, Zimmer L, Vaubel J, Schadendorf D. BRAF, MEK and KIT inhibitors for melanoma: adverse events and their management. Chin Clin Oncol 2014;3:29.

136. Skudalski L, Waldman R, Kerr PE, Grant-Kels JM. Melanoma: An update on systemic therapies. Journal of the American Academy of Dermatology 2022;86:515-524.

137. Wright CJ, McCormack PL. Trametinib: first global approval. Drugs 2013;73:1245-1254.

138. Ascierto PA, Schadendorf D, Berking C, Agarwala SS, van Herpen CM, Queirolo P, Blank CU, et al. MEK162 for patients with advanced melanoma harbouring NRAS or Val600 BRAF mutations: a non-randomised, open-label phase 2 study. Lancet Oncol 2013;14:249-256.

139. Schilling B, Sondermann W, Zhao F, Griewank KG, Livingstone E, Sucker A, Zelba H, et al. Differential influence of vemurafenib and dabrafenib on patients' lymphocytes despite similar clinical efficacy in melanoma. Annals of Oncology 2014;25:747-753.

140. Livingstone E, Zimmer L, Vaubel J, Schadendorf D. Current advances and perspectives in the treatment of advanced melanoma. J Dtsch Dermatol Ges 2012;10:319-325.

141. Robert C, Grob JJ, Stroyakovskiy D, Karaszewska B, Hauschild A, Levchenko E, Chiarion Sileni V, et al. Five-Year Outcomes with Dabrafenib plus Trametinib in Metastatic Melanoma. New England Journal of Medicine 2019;381:626-636.

142. Tefany FJ, Barnetson RS, Halliday GM, McCarthy SW, McCarthy WH. Immunocytochemical Analysis of the Cellular Infiltrate in Primary Regressing and Non-Regressing Malignant Melanoma. Journal of Investigative Dermatology 1991;97:197-202.

143. Rossen RD, Crane MM, Morgan AC, Giannini EH, Giovanella BC, Stehlin JS, Twomey JJ, et al. Circulating immune complexes and tumor cell cytotoxins as prognostic indicators in malignant melanoma: a prospective study of 53 patients. Cancer Res 1983;43:422-429.

144. Michels J, Becker N, Suciu S, Kaiser I, Benner A, Kosaloglu-Yalcin Z, Agoussi S, et al. Multiplex bead-based measurement of humoral immune responses against tumor-associated antigens in stage II melanoma patients of the EORTC18961 trial. Oncoimmunology 2018;7:e1428157.

145. Finn OJ. The dawn of vaccines for cancer prevention. Nat Rev Immunol 2018;18:183-194.

146. Sabel MS, Sondak VK. Tumor vaccines: a role in preventing recurrence in melanoma? Am J Clin Dermatol 2002;3:609-616.

147. Lens M. The role of vaccine therapy in the treatment of melanoma. Expert Opin Biol Ther 2008;8:315-323.

148. Morton DL, Foshag LJ, Hoon DS, Nizze JA, Famatiga E, Wanek LA, Chang C, et al. Prolongation of survival in metastatic melanoma after active specific immunotherapy with a new polyvalent melanoma vaccine. Ann Surg 1992;216:463-482.

149. Morton DL, Barth A. Vaccine therapy for malignant melanoma. CA Cancer J Clin 1996;46:225-244.

150. Chan AD, Morton DL. Active immunotherapy with allogeneic tumor cell vaccines: present status. Semin Oncol 1998;25:611-622.

151. Hsueh EC, Nathanson L, Foshag LJ, Essner R, Nizze JA, Stern SL, Morton DL. Active specific immunotherapy with polyvalent melanoma cell vaccine for patients with in-transit melanoma metastases. Cancer 1999;85:2160-2169.

152. Sosman JA, Sondak VK. Melacine®: an allogeneic melanoma tumor cell lysate vaccine. Expert Review of Vaccines 2003;2:353-368.

153. Hollingsworth RE, Jansen K. Turning the corner on therapeutic cancer vaccines. npj Vaccines 2019;4:7.

154. Sahin U, Oehm P, Derhovanessian E, Jabulowsky RA, Vormehr M, Gold M, Maurus D, et al. An RNA vaccine drives immunity in checkpoint-inhibitor-treated melanoma. Nature 2020;585:107-112.

155. Blass E, Ott PA. Advances in the development of personalized neoantigen-based therapeutic cancer vaccines. Nature Reviews Clinical Oncology 2021;18:215-229.

156. Meisel A, Pascolo S. mRNA vaccines against infectious diseases and cancer. healthbook TIMES Oncol Hematol 2021;9:24-31.

157. mRNA Vaccine Slows Melanoma Recurrence. Cancer Discovery 2023:OF1-OF1.

158. Poh A. First Oncolytic Viral Therapy for Melanoma. Cancer Discov 2016;6:6.

159. Pol J, Kroemer G, Galluzzi L. First oncolytic virus approved for melanoma immunotherapy. Oncoimmunology 2016;5:e1115641.

160. Andtbacka RH, Kaufman HL, Collichio F, Amatruda T, Senzer N, Chesney J, Delman KA, et al. Talimogene Laherparepvec Improves Durable Response Rate in Patients With Advanced Melanoma. J Clin Oncol 2015;33:2780-2788.

161. Andtbacka RHI, Curti B, Daniels GA, Hallmeyer S, Whitman ED, Lutzky J, Spitler LE, et al. Clinical Responses of Oncolytic Coxsackievirus A21 (V937) in Patients With Unresectable Melanoma. J Clin Oncol 2021;39:3829-3838.

162. Curti BD, Richards J, Hyngstrom JR, Daniels GA, Faries M, Feun L, Margolin KA, et al. Intratumoral oncolytic virus V937 plus ipilimumab in patients with advanced melanoma: the phase 1b MITCI study. J Immunother Cancer 2022;10.

163. Rohaan MW, Zijlker LP, Stahlie EHA, Franke V, Wilgenhof S, Noort Vvd, Akkooi ACJV, et al. Neo-adjuvant T-VEC plus nivolumab combination therapy for resectable early-stage or metastatic (IIIB-IVM1a) melanoma with injectable disease: The NIVEC trial. Journal of Clinical Oncology 2022;40:TPS9607-TPS9607.

164. Briukhovetska D, Dörr J, Endres S, Libby P, Dinarello CA, Kobold S. Interleukins in cancer: from biology to therapy. Nature Reviews Cancer 2021;21:481-499.

165. Bright R, Coventry BJ, Eardley-Harris N, Briggs N. Clinical Response Rates From Interleukin-2 Therapy for Metastatic Melanoma Over 30 Years' Experience: A Meta-Analysis of 3312 Patients. J Immunother 2017;40:21-30.

166. Marabondo S, Kaufman HL. High-dose interleukin-2 (IL-2) for the treatment of melanoma: safety considerations and future directions. Expert Opin Drug Saf 2017;16:1347-1357.

167. Charych DH, Hoch U, Langowski JL, Lee SR, Addepalli MK, Kirk PB, Sheng D, et al. NKTR-214, an engineered cytokine with biased IL2 receptor binding, increased tumor exposure, and marked efficacy in mouse tumor models. Clinical Cancer Research 2016;22:680-690.

168. Weide B, Derhovanessian E, Pflugfelder A, Eigentler TK, Radny P, Zelba H, Pföhler C, et al. High response rate after intratumoral treatment with interleukin-2. Cancer 2010;116:4139-4146.

169. Castro F, Cardoso AP, Gonçalves RM, Serre K, Oliveira MJ. Interferon-Gamma at the Crossroads of Tumor Immune Surveillance or Evasion. Front Immunol 2018;9:847.

170. Roh MR, Zheng Z, Kim HS, Jeung HC, Rha SY, Chung KY. Difference of interferon-α and interferon-β on melanoma growth and lymph node metastasis in mice. Melanoma Res 2013;23:114-124.

171. Ives NJ, Suciu S, Eggermont AMM, Kirkwood J, Lorigan P, Markovic SN, Garbe C, et al. Adjuvant interferon-α for the treatment of high-risk melanoma: An individual patient data meta-analysis. European Journal of Cancer 2017;82:171-183.

172. Eggermont AM, Suciu S, Testori A, Kruit WH, Marsden J, Punt CJ, Santinami M, et al. Ulceration and stage are predictive of interferon efficacy in melanoma: results of the phase III adjuvant trials EORTC 18952 and EORTC 18991. Eur J Cancer 2012;48:218-225.

173. Rosenberg SA, Restifo NP, Yang JC, Morgan RA, Dudley ME. Adoptive cell transfer: a clinical path to effective cancer immunotherapy. Nat Rev Cancer 2008;8:299-308.

174. Merhavi-Shoham E, Itzhaki O, Markel G, Schachter J, Besser MJ. Adoptive Cell Therapy for Metastatic Melanoma. Cancer J 2017;23:48-53.

175. Besser MJ, Shapira-Frommer R, Treves AJ, Zippel D, Itzhaki O, Hershkovitz L, Levy D, et al. Clinical Responses in a Phase II Study Using Adoptive Transfer of Short-term Cultured Tumor Infiltration Lymphocytes in Metastatic Melanoma Patients. Clinical Cancer Research 2010;16:2646-2655.

176. Pilon-Thomas S, Kuhn L, Ellwanger S, Janssen W, Royster E, Marzban S, Kudchadkar R, et al. Efficacy of adoptive cell transfer of tumor-infiltrating lymphocytes after lymphopenia induction for metastatic melanoma. J Immunother 2012;35:615-620.

177. Radvanyi LG, Bernatchez C, Zhang M, Fox PS, Miller P, Chacon J, Wu R, et al. Specific lymphocyte subsets predict response to adoptive cell therapy using expanded autologous tumor-infiltrating lymphocytes in metastatic melanoma patients. Clin Cancer Res 2012;18:6758-6770.

178. Neelapu SS, Locke FL, Bartlett NL, Lekakis LJ, Miklos DB, Jacobson CA, Braunschweig I, et al. Axicabtagene Ciloleucel CAR T-Cell Therapy in Refractory Large B-Cell Lymphoma. New England Journal of Medicine 2017;377:2531-2544.

179. Maude SL, Laetsch TW, Buechner J, Rives S, Boyer M, Bittencourt H, Bader P, et al. Tisagenlecleucel in Children and Young Adults with B-Cell Lymphoblastic Leukemia. New England Journal of Medicine 2018;378:439-448.

180. Park JH, Rivière I, Gonen M, Wang X, Sénéchal B, Curran KJ, Sauter C, et al. Long-Term Follow-up of CD19 CAR Therapy in Acute Lymphoblastic Leukemia. New England Journal of Medicine 2018;378:449-459.

181. June CH, Sadelain M. Chimeric Antigen Receptor Therapy. N Engl J Med 2018;379:64-73.

182. Wilkins O, Keeler AM, Flotte TR. CAR T-Cell Therapy: Progress and Prospects. Hum Gene Ther Methods 2017;28:61-66.

183. Farhood B, Najafi M, Mortezaee K. CD8(+) cytotoxic T lymphocytes in cancer immunotherapy: A review. J Cell Physiol 2019;234:8509-8521.

184. Murphy K, Weaver C. Janeway's immunobiology: Garland science, 2016.

185. Kandel S, Adhikary P, Li G, Cheng K. The TIM3/Gal9 signaling pathway: An emerging target for cancer immunotherapy. Cancer Letters 2021;510:67-78.

186. Tawbi HA, Schadendorf D, Lipson EJ, Ascierto PA, Matamala L, Castillo Gutiérrez E, Rutkowski P, et al. Relatlimab and Nivolumab versus Nivolumab in Untreated Advanced Melanoma. N Engl J Med 2022;386:24-34.

187. Maruhashi T, Sugiura D, Okazaki I-m, Okazaki T. LAG-3: from molecular functions to clinical applications. Journal for ImmunoTherapy of Cancer 2020;8:e001014.

188. Carlino MS, Larkin J, Long GV. Immune checkpoint inhibitors in melanoma. Lancet 2021;398:1002-1014.

189. Xin Yu J, Hubbard-Lucey VM, Tang J. Immuno-oncology drug development goes global. Nat Rev Drug Discov 2019;18:899-900.

190. Robert C. A decade of immune-checkpoint inhibitors in cancer therapy. Nat Commun 2020;11:3801.

191. Graziani G, Tentori L, Navarra P. Ipilimumab: A novel immunostimulatory monoclonal antibody for the treatment of cancer. Pharmacological Research 2012;65:9-22.

192. Robert C, Thomas L, Bondarenko I, O'Day S, Weber J, Garbe C, Lebbe C, et al. Ipilimumab plus dacarbazine for previously untreated metastatic melanoma. N Engl J Med 2011;364:2517-2526.

193. Hodi FS, O'Day SJ, McDermott DF, Weber RW, Sosman JA, Haanen JB, Gonzalez R, et al. Improved survival with ipilimumab in patients with metastatic melanoma. N Engl J Med 2010;363:711-723.

194. Robert C, Ribas A, Schachter J, Arance A, Grob JJ, Mortier L, Daud A, et al. Pembrolizumab versus ipilimumab in advanced melanoma (KEYNOTE-006): post-hoc 5-year results from an open-label, multicentre, randomised, controlled, phase 3 study. Lancet Oncol 2019;20:1239-1251.

195. Larkin J, Chiarion-Sileni V, Gonzalez R, Grob JJ, Rutkowski P, Lao CD, Cowey CL, et al. Five-Year Survival with Combined Nivolumab and Ipilimumab in Advanced Melanoma. N Engl J Med 2019;381:1535-1546.

196. Robert C, Schachter J, Long GV, Arance A, Grob JJ, Mortier L, Daud A, et al. Pembrolizumab versus Ipilimumab in Advanced Melanoma. N Engl J Med 2015;372:2521-2532.

197. Wolchok JD, Kluger H, Callahan MK, Postow MA, Rizvi NA, Lesokhin AM, Segal NH, et al. Nivolumab plus ipilimumab in advanced melanoma. N Engl J Med 2013;369:122-133.

198. Larkin J, Chiarion-Sileni V, Gonzalez R, Grob JJ, Cowey CL, Lao CD, Schadendorf D, et al. Combined Nivolumab and Ipilimumab or Monotherapy in Untreated Melanoma. N Engl J Med 2015;373:23-34.

199. Eggermont AM, Chiarion-Sileni V, Grob J-J, Dummer R, Wolchok JD, Schmidt H, Hamid O, et al. Prolonged survival in stage III melanoma with ipilimumab adjuvant therapy. New England Journal of Medicine 2016;375:1845-1855.

200. Weber J, Mandala M, Del Vecchio M, Gogas HJ, Arance AM, Cowey CL, Dalle S, et al. Adjuvant nivolumab versus ipilimumab in resected stage III or IV melanoma. New England Journal of Medicine 2017;377:1824-1835.

201. Eggermont AMM, Kicinski M, Blank CU, Mandala M, Long GV, Atkinson V, Dalle S, et al. Five-Year Analysis of Adjuvant Pembrolizumab or Placebo in Stage III Melanoma. NEJM Evidence 2022;1:EVIDoa2200214.

202. Long GV, Hauschild A, Santinami M, Atkinson V, Mandalà M, Chiarion-Sileni V, Larkin J, et al. Adjuvant Dabrafenib plus Trametinib in Stage III BRAF-Mutated Melanoma. N Engl J Med 2017;377:1813-1823.

203. Eggermont AMM, Blank CU, Mandala M, Long GV, Atkinson V, Dalle S, Haydon A, et al. Adjuvant Pembrolizumab versus Placebo in Resected Stage III Melanoma. N Engl J Med 2018;378:1789-1801.

204. Davies MA, Saiag P, Robert C, Grob JJ, Flaherty KT, Arance A, Chiarion-Sileni V, et al. Dabrafenib plus trametinib in patients with BRAF(V600)-mutant melanoma brain metastases (COMBI-MB): a multicentre, multicohort, open-label, phase 2 trial. Lancet Oncol 2017;18:863-873.

205. Tumeh PC, Hellmann MD, Hamid O, Tsai KK, Loo KL, Gubens MA, Rosenblum M, et al. Liver Metastasis and Treatment Outcome with Anti-PD-1 Monoclonal Antibody in Patients with Melanoma and NSCLC. Cancer Immunol Res 2017;5:417-424.

206. Yu J, Green MD, Li S, Sun Y, Journey SN, Choi JE, Rizvi SM, et al. Liver metastasis restrains immunotherapy efficacy via macrophage-mediated T cell elimination. Nature Medicine 2021;27:152-164.

207. Lee JC, Mehdizadeh S, Smith J, Young A, Mufazalov IA, Mowery CT, Daud A, et al. Regulatory T cell control of systemic immunity and immunotherapy response in liver metastasis. Sci Immunol 2020;5.

208. Hauschild A, Larkin J, Ribas A, Dréno B, Flaherty KT, Ascierto PA, Lewis KD, et al. Modeled Prognostic Subgroups for Survival and Treatment Outcomes in BRAF V600-Mutated Metastatic Melanoma: Pooled Analysis of 4 Randomized Clinical Trials. JAMA Oncol 2018;4:1382-1388.

209. Luke JJ, Rutkowski P, Queirolo P, Del Vecchio M, Mackiewicz J, Chiarion-Sileni V, de la Cruz Merino L, et al. Pembrolizumab versus placebo as adjuvant therapy in completely resected stage IIB or IIC melanoma (KEYNOTE-716): a randomised, double-blind, phase 3 trial. Lancet 2022;399:1718-1729.

210. Owen CN, Shoushtari AN, Chauhan D, Palmieri DJ, Lee B, Rohaan MW, Mangana J, et al. Management of early melanoma recurrence despite adjuvant anti-PD-1 antibody therapy(☆). Ann Oncol 2020;31:1075-1082.

211. Versluis JM, Long GV, Blank CU. Learning from clinical trials of neoadjuvant checkpoint blockade. Nat Med 2020;26:475-484.

212. Liu J, Blake SJ, Yong MC, Harjunpää H, Ngiow SF, Takeda K, Young A, et al. Improved Efficacy of Neoadjuvant Compared to Adjuvant Immunotherapy to Eradicate Metastatic Disease. Cancer Discov 2016;6:1382-1399.

213. Bahadoer RR, Dijkstra EA, van Etten B, Marijnen CAM, Putter H, Kranenbarg EM, Roodvoets AGH, et al. Short-course radiotherapy followed by chemotherapy before total mesorectal excision (TME) versus preoperative chemoradiotherapy, TME, and optional

adjuvant chemotherapy in locally advanced rectal cancer (RAPIDO): a randomised, open-label, phase 3 trial. Lancet Oncol 2021;22:29-42.

214. Conroy T, Bosset JF, Etienne PL, Rio E, François É, Mesgouez-Nebout N, Vendrely V, et al. Neoadjuvant chemotherapy with FOLFIRINOX and preoperative chemoradiotherapy for patients with locally advanced rectal cancer (UNICANCER-PRODIGE 23): a multicentre, randomised, open-label, phase 3 trial. Lancet Oncol 2021;22:702-715.

215. Kanani A, Veen T, Søreide K. Neoadjuvant immunotherapy in primary and metastatic colorectal cancer. British Journal of Surgery 2021;108:1417-1425.

216. Chalabi M, Fanchi LF, Dijkstra KK, Van den Berg JG, Aalbers AG, Sikorska K, Lopez-Yurda M, et al. Neoadjuvant immunotherapy leads to pathological responses in MMR-proficient and MMR-deficient early-stage colon cancers. Nature medicine 2020;26:566-576.

217. Schmid P, Cortes J, Pusztai L, McArthur H, Kümmel S, Bergh J, Denkert C, et al. Pembrolizumab for Early Triple-Negative Breast Cancer. New England Journal of Medicine 2020;382:810-821.

218. Amaria RN, Reddy SM, Tawbi HA, Davies MA, Ross MI, Glitza IC, Cormier JN, et al. Neoadjuvant immune checkpoint blockade in high-risk resectable melanoma. Nat Med 2018;24:1649-1654.

219. Blank CU, Rozeman EA, Fanchi LF, Sikorska K, van de Wiel B, Kvistborg P, Krijgsman O, et al. Neoadjuvant versus adjuvant ipilimumab plus nivolumab in macroscopic stage III melanoma. Nat Med 2018;24:1655-1661.

220. van Akkooi ACJ, Hieken TJ, Burton EM, Ariyan C, Ascierto PA, Asero S, Blank CU, et al. Neoadjuvant Systemic Therapy (NAST) in Patients with Melanoma: Surgical Considerations by the International Neoadjuvant Melanoma Consortium (INMC). Ann Surg Oncol 2022;29:3694-3708.

221. Rozeman EA, Menzies AM, van Akkooi ACJ, Adhikari C, Bierman C, van de Wiel BA, Scolyer RA, et al. Identification of the optimal combination dosing schedule of neoadjuvant ipilimumab plus nivolumab in macroscopic stage III melanoma (OpACIN-neo): a multicentre, phase 2, randomised, controlled trial. Lancet Oncol 2019;20:948-960.

222. Huang AC, Orlowski RJ, Xu X, Mick R, George SM, Yan PK, Manne S, et al. A single dose of neoadjuvant PD-1 blockade predicts clinical outcomes in resectable melanoma. Nat Med 2019;25:454-461.

223. Blank CU, Reijers ILM, Pennington T, Versluis JM, Saw RP, Rozeman EA, Kapiteijn E, et al. First safety and efficacy results of PRADO: A phase II study of personalized response-

driven surgery and adjuvant therapy after neoadjuvant ipilimumab (IPI) and nivolumab (NIVO) in resectable stage III melanoma. Journal of Clinical Oncology 2020;38:10002-10002.

224. Amaria RN, Postow MA, Tetzlaff MT, Ross MI, Glitza IC, McQuade JL, Wong MKK, et al. Neoadjuvant and adjuvant nivolumab (nivo) with anti-LAG3 antibody relatlimab (rela) for patients (pts) with resectable clinical stage III melanoma. Journal of Clinical Oncology 2021;39:9502-9502.

225. Lucas MW, Lijnsvelt J, Pulleman S, Scolyer RA, Menzies AM, Akkooi ACJV, Houdt WJv, et al. The NADINA trial: A multicenter, randomised, phase 3 trial comparing the efficacy of neoadjuvant ipilimumab plus nivolumab with standard adjuvant nivolumab in macroscopic resectable stage III melanoma. Journal of Clinical Oncology 2022;40:TPS9605-TPS9605.

226. Coit DG, Thompson JA, Albertini MR, Barker C, Carson WE, Contreras C, Daniels GA, et al. Cutaneous melanoma, version 2.2019, NCCN clinical practice guidelines in oncology. Journal of the National Comprehensive Cancer Network 2019;17:367-402.

227. Lindsay CR, Lawn S, Campbell AD, Faller WJ, Rambow F, Mort RL, Timpson P, et al. P-Rex1 is required for efficient melanoblast migration and melanoma metastasis. Nat Commun 2011;2:555.

228. Wohlfeil SA, Häfele V, Dietsch B, Weller C, Sticht C, Jauch AS, Winkler M, et al. Angiogenic and molecular diversity determine hepatic melanoma metastasis and response to anti-angiogenic treatment. In: Journal of translational medicine; 2022. p. 62.

229. Basiji DA, Ortyn WE, Liang L, Venkatachalam V, Morrissey P. Cellular image analysis and imaging by flow cytometry. Clin Lab Med 2007;27:653-670, viii.

230. Yang M, Zhang C. The role of liver sinusoidal endothelial cells in cancer liver metastasis. Am J Cancer Res 2021;11:1845-1860.

231. Golubovskaya V, Wu L. Different Subsets of T Cells, Memory, Effector Functions, and CAR-T Immunotherapy. Cancers 2016;8:36.

232. Simpson TR, Li F, Montalvo-Ortiz W, Sepulveda MA, Bergerhoff K, Arce F, Roddie C, et al. Fc-dependent depletion of tumor-infiltrating regulatory T cells co-defines the efficacy of anti-CTLA-4 therapy against melanoma. J Exp Med 2013;210:1695-1710.

233. Wang D, Quiros J, Mahuron K, Pai CC, Ranzani V, Young A, Silveria S, et al. Targeting EZH2 Reprograms Intratumoral Regulatory T Cells to Enhance Cancer Immunity. Cell Rep 2018;23:3262-3274.

234. Mantovani A, Allavena P. The interaction of anticancer therapies with tumor-associated macrophages. Journal of Experimental Medicine 2015;212:435-445.

235. Mantovani A, Marchesi F, Malesci A, Laghi L, Allavena P. Tumour-associated macrophages as treatment targets in oncology. Nature reviews Clinical oncology 2017;14:399-416.

236. Zaremba A, Eggermont AMM, Robert C, Dummer R, Ugurel S, Livingstone E, Ascierto PA, et al. The concepts of rechallenge and retreatment with immune checkpoint blockade in melanoma patients. European Journal of Cancer 2021;155:268-280.

237. Piaggio F, Kondylis V, Pastorino F, Di Paolo D, Perri P, Cossu I, Schorn F, et al. A novel liposomal Clodronate depletes tumor-associated macrophages in primary and metastatic melanoma: Anti-angiogenic and anti-tumor effects. Journal of Controlled Release 2016;223:165-177.

238. van Rooijen N, Hendrikx E: Liposomes for Specific Depletion of Macrophages from Organs and Tissues. In: Weissig V, ed. Liposomes: Methods and Protocols, Volume 1: Pharmaceutical Nanocarriers. Totowa, NJ: Humana Press, 2010; 189-203.

239. Kim HJ, Park JH, Kim HC, Kim CW, Kang I, Lee HK. Blood monocyte-derived CD169(+) macrophages contribute to antitumor immunity against glioblastoma. Nat Commun 2022;13:6211.

240. Moran A, Pavord ID. Anti-IL-4/IL-13 for the treatment of asthma: the story so far. Expert Opinion on Biological Therapy 2020;20:283-294.

241. Espinosa ML, Nguyen MT, Aguirre AS, Martinez-Escala ME, Kim J, Walker CJ, Pontes DS, et al. Progression of cutaneous T-cell lymphoma after dupilumab: Case review of 7 patients. Journal of the American Academy of Dermatology 2020;83:197-199.

242. Amaria RN, Menzies AM, Burton EM, Scolyer RA, Tetzlaff MT, Antdbacka R, Ariyan C, et al. Neoadjuvant systemic therapy in melanoma: recommendations of the International Neoadjuvant Melanoma Consortium. Lancet Oncol 2019;20:e378-e389.

243. Patton EE, Mueller KL, Adams DJ, Anandasabapathy N, Aplin AE, Bertolotto C, Bosenberg M, et al. Melanoma models for the next generation of therapies. Cancer Cell 2021;39:610-631.

244. Brodt P. Role of the Microenvironment in Liver Metastasis: From Pre- to Prometastatic Niches. Clin Cancer Res 2016;22:5971-5982.

245. Liu YT, Sun ZJ. Turning cold tumors into hot tumors by improving T-cell infiltration. Theranostics 2021;11:5365-5386.

246. Bonaventura P, Shekarian T, Alcazer V, Valladeau-Guilemond J, Valsesia-Wittmann S, Amigorena S, Caux C, et al. Cold Tumors: A Therapeutic Challenge for Immunotherapy. Front Immunol 2019;10:168.

247. Amaria RN, Postow M, Burton EM, Tezlaff MT, Ross MI, Torres-Cabala C, Glitza IC, et al. Neoadjuvant relatlimab and nivolumab in resectable melanoma. Nature 2022:1-6.

248. Fairfax BP, Taylor CA, Watson RA, Nassiri I, Danielli S, Fang H, Mahé EA, et al. Peripheral CD8(+) T cell characteristics associated with durable responses to immune checkpoint blockade in patients with metastatic melanoma. Nat Med 2020;26:193-199.

249. Ratner A, Clark WR. Role of TNF-alpha in CD8+ cytotoxic T lymphocyte-mediated lysis. J Immunol 1993;150:4303-4314.

250. Muranski P, Boni A, Antony PA, Cassard L, Irvine KR, Kaiser A, Paulos CM, et al. Tumor-specific Th17-polarized cells eradicate large established melanoma. Blood 2008;112:362-373.

251. Bertrand F, Rochotte J, Colacios C, Montfort A, Tilkin-Mariamé AF, Touriol C, Rochaix P, et al. Blocking Tumor Necrosis Factor α Enhances CD8 T-cell-Dependent Immunity in Experimental Melanoma. Cancer Res 2015;75:2619-2628.

252. Wang L, Yi T, Kortylewski M, Pardoll DM, Zeng D, Yu H. IL-17 can promote tumor growth through an IL-6-Stat3 signaling pathway. J Exp Med 2009;206:1457-1464.

253. Romee R, Cooley S, Berrien-Elliott MM, Westervelt P, Verneris MR, Wagner JE, Weisdorf DJ, et al. First-in-human phase 1 clinical study of the IL-15 superagonist complex ALT-803 to treat relapse after transplantation. Blood, The Journal of the American Society of Hematology 2018;131:2515-2527.

254. Margolin K, Morishima C, Velcheti V, Miller JS, Lee SM, Silk AW, Holtan SG, et al. Phase I Trial of ALT-803, A Novel Recombinant IL15 Complex, in Patients with Advanced Solid TumorsPhase I Trial of ALT-803 in Advanced Solid Tumors. Clinical Cancer Research 2018;24:5552-5561.

255. Bergamaschi C, Bear J, Rosati M, Beach RK, Alicea C, Sowder R, Chertova E, et al. Circulating IL-15 exists as heterodimeric complex with soluble IL-15Rα in human and mouse serum. Blood 2012;120:e1-8.

256. Piera Filomena F, Sabina Di M, Nicola T, Francesca Romana M, Gabriella P, Selene O, Simone N, et al. Interleukin-15 and cancer: some solved and many unsolved questions. Journal for ImmunoTherapy of Cancer 2020;8:e001428.

257. Luckheeram RV, Zhou R, Verma AD, Xia B. $CD4^+$T cells: differentiation and functions. Clin Dev Immunol 2012;2012:925135.

258. Lin C-N, Chien C-Y, Chung H-C. Are Friends or Foes? New Strategy for Head and Neck Squamous Cell Carcinoma Treatment via Immune Regulation. 2017;1:105-113.

259. Principe DR, DeCant B, Mascariñas E, Wayne EA, Diaz AM, Akagi N, Hwang R, et al. TGFβ Signaling in the Pancreatic Tumor Microenvironment Promotes Fibrosis and Immune Evasion to Facilitate Tumorigenesis. Cancer Research 2016;76:2525-2539.

260. Le DT, Lutz E, Uram JN, Sugar EA, Onners B, Solt S, Zheng L, et al. Evaluation of ipilimumab in combination with allogeneic pancreatic tumor cells transfected with a GM-CSF gene in previously treated pancreatic cancer. Journal of immunotherapy (Hagerstown, Md.: 1997) 2013;36:382.

261. Zhao L, Cheng S, Fan L, Zhang B, Xu S. TIM-3: An update on immunotherapy. Int Immunopharmacol 2021;99:107933.

262. de Boer AZ, Derks MGM, de Glas NA, Bastiaannet E, Liefers GJ, Stiggelbout AM, van Dijk MA, et al. Metastatic breast cancer in older patients: A longitudinal assessment of geriatric outcomes. J Geriatr Oncol 2020;11:969-975.

8 Appendix

8.1 List of figures

8.2 List of tables

8.3 List of abbrevations

ACT = Adoptive cell transfer

AEs = Adverse events

APCs = Antigen presenting cells

BLI = bioluminescence imaging

CAR = Chimeric antigen receptor

CD = Cluster of differentiation

CM = Cutaneous melanoma

CRC = colorectal cancer

CTCs = Circulating tumor cells

CTLA-4 = Cytotoxic T Lymphocyte-Associated Protein 4

Ctrl = Control

DAPI = 4’,6-Diamidino-2-phenylindol

DNA = desoxyribonucleic acid

DTCs = Disseminating tumor cells

EC = Endothelial cell

ECM = Extracellular matrix

EVs =Extracellular vesicles

FBS = Fetal bovine serum

FDA = Food and Drug Administration

H&E = Hematoxylin & Eosin

HD = High dose

HSCs = Hepatic stellate cells

i.p. = intraperitoneal

i.v. = intravenous

ICI = Immune checkpoint inhibition

IF = Immunofluorescence

IFN = Interferon

IL = Interleukin

LSEC = Liver sinusoidal endothelial cells

MCA = Methylcholanthrene

MDSCs = Myeloid derived suppressor cells

OCT = Optimum cutting temperature

OS = Overall survival

PBS = Phosphate buffered saline

pCR = Pathological clinical response

PD-1 = Programmed Cell Death Protein 1

PDAC = Pancreatic ductal adenocarcinoma

PD-L1 = Programmed Cell Death Ligand 1

PFA = Paraformaldehyde

PFS = Progression free survival

qRT-PCR = quantitative real-time Polymerase Chain Reaction

RAG = Recombination activating gene

RNA = Ribonucleic acid

RT = Room temperature

SD = Standard deviation

TAMs = Tumor associated macrophages

T-bet = T box expressed in T cells

TCR = T cell receptor

TILs = Tumor infiltrating lymphocytes

TNBC = Triple negative breast cancer

TNF = Tumor necrosis factor

T_{regs} = regulatory T cells

TT = Targeted therapies

Danksagung

Ein herzliches Dankeschön geht an Prof. Dr. Cyrill Géraud für die Überlassung des interessanten Themas und die Ermöglichung dieses Projektes, für die hilfreichen Anregungen und Begutachtung dieser Dissertation.

Des Weiteren danke ich Dr. Sebastian Wohlfeil für die Betreuung dieses Projektes. Bedanken möchte ich mich für die investierte Zeit, für das Korrekturlesen meiner Arbeit, für die Beantwortung all meiner Fragen und für die äußerst lehrreiche Zeit.

Bei Prof. Dr. Viktor Umansky und Prof. Dr. Dr. Georg Stöcklin möchte ich mich für die Übernahme des Erstgutachtens bzw. des Prüfungsvorsitzes herzlich bedanken. Außerdem danke ich Prof. Dr. Peter Angel für die Bereitschaft als Prüfer zu fungieren.

Dem Graduiertenkolleg RTG2099 danke ich für die finanzielle Unterstützung und den vielseitigen Möglichkeiten der interdisziplinären Fortbildung. Ein besonderer Dank geht hierbei an Martina Nolte-Bohres!

Ein ganz besonderer Dank geht an Bianca Dietsch für das Mitwirken bei diesem Projekt. Bianca, ich danke dir für die tolle Zusammenarbeit, deine Hilfe bei all meinen *in vivo* Versuchen und für die immer wiederkehrende seelische und moralische Unterstützung. Danke Bianca!

Ein großes Dankeschön geht an Verena Häfele für die Unterstützung bei den Immunzellquantifizierungen, das Korrekturlesen dieser Arbeit, dein offenes Ohr und deine immer hilfreichen Tipps. Danke auch dir, Verena!

Außerdem möchte ich mich ganz herzlich bei meiner Arbeitsgruppe und der AG Goerdt/Reiners-Koch bedanken. Danke für die unglaublich tolle Zeit mit Euch, den Spaß im und außerhalb des Labors und danke für Eure Unterstützung. Danke auch an unsere Medizinstudenten Anna, Ana, Anna Lena und Niklas die ich mit betreuen durfte und die auch einen großen Teil zu dieser Arbeit beigetragen haben.

Ein herzliches Dankeschön geht an Anna Lena, Bianca, Verena, Sina, Theresa, Tinja und Loreen, die für mich nicht nur Kollegen waren, sondern gute Freunden geworden sind.

Sarahli, dir danke ich für das Korrekturlesen dieser Arbeit, die wunderbaren Reiturlaube und dafür, dass du mir solch eine gute Freundin geworden bist!

Meinen Eltern, Rolf und Ulrike danke ich für die uneingeschränkte Unterstützung, fürs immer an mich glauben und dafür, dass sie immer für mich da sind! Alex, dir danke ich für dein Verständnis und deine Unterstützung vor allem in den letzten Wochen!

Danke